University of Reading

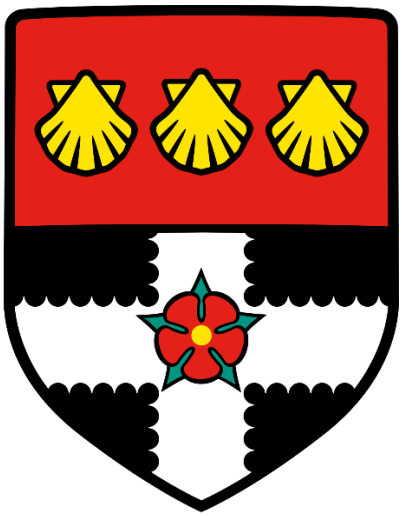

Combining Physiology and Genetics to dissect source-sink relationships in wheat

Peter Jackson

A thesis submitted to the School of Agriculture, Policy and Development

University of Reading

For the degree of Doctor of Philosophy
February 2019

Declaration of original authorship

I confirm that this is my own work and the use of all material from other sources has been properly and fully acknowledged

…… ……

Abstract

The growth and yield of wheat is subject to constant attempts at improvement. Recent technology has allowed us to speed this process up by utilising genetic markers. Previous work has had to concentrate on small groups of traits at any one time due to the limited allelic representation in bi-parental populations. The aim of this project was to identify and study the genetic underpinnings of source and sink related traits in field conditions. The crop was measured throughout the full season to observe how these traits interact with each other continuously. To this end, the National Institute of Agricultural Botany (NIAB) eight-parent population was studied in two field seasons. The allelic diversity and high level of recombination present in this population gives us an unprecedented opportunity to identify novel Quantitative Trait Loci (QTL) that control varying aspects that impact the final yield.

All traits measured exhibited a much greater range of diversity in the progeny compared to that of the founder lines. Using that diversity, we were able to identify QTL on every chromosome, with multiple major effect, stable, QTL occurring on 1B, 4B, 4D, 5A and 6A. Some of these have been described in previous literature, while others such as 1B appear to be novel. Further to this, there were two noteworthy QTL for yield that were not co-locating with any of the other measured traits. One of these QTL was stably located on 7B and explains on average 1.6% of the total phenotypic variation, while the other is located on 5B, explaining 6.02% of the total variation in a single environment.

Acknowledgements

Firstly, I would like to thank my supervisors Donal O'Sullivan and Elizabete Carmo-Silva for all of their support and guidance throughout this process. The knowledge and experience they have provided made this work possible and I'm extremely grateful for the time and effort that they have given to me. I owe gratitude and more to the technician team within the University's School of Agriculture, specifically Caroline Hadley, Liam Doherty, David McLay and Richard Casebow. Without them this thesis could never have happened, taking on the largest experiment done at Sonning Farm, harvesting until midnight and always being willing to help. Their dedication helped to keep me motivated throughout the last four years.

I'm indebted to all of my placement students: Claire Micklethwaite, Franca Lucia Corraine, Matteo Donnini, Simone Camazzola, Joel Potts and Samith Adhikari you all helped me with what was a daunting task with enthusiasm.

I owe thanks to everyone in my research group and office for creating an excellent working environment. I especially thank Samer Amer, who is always willing to help, whether it was discussing ideas or collecting samples from the field at 1am. You've always made difficult times more bearable.

I would like to thank my family and friends for providing emotional and moral support, especially my parents and Elle, believing in me when I wanted to give up. Finally, I would like to thank anyone that assisted with experiments, advice, or just listened when I needed it. Without everyone mentioned here, I could never have done this thesis.

This project was funded by the BBSRC Food Security DTP.

Contents

List of Figures

List of Tables

List of Abbreviations

Agc: Accumulated green cover

AM: Association Mapping

BLUP: *Best Linear Unbiased Prediction*

Br: Brittle rachis

Cdu: Canopy Duration

CIM: Composite Interval Mapping

CIMMYT: International Maize and Wheat Improvement Centre

cM: centiMorgan

Da: Date of Anthesis

DH: Double Haploid

Eht: Early Height

FAO: Food and Agriculture Organization of the United Nations

Fht: Final Height

GA: Grain Area

GAI: Green Area Index

GL: Grain Length

GS: Growth Stage

GW: Grain Width

GWAS: Genome- Wide Association Studies

GY: Grain Yield

H^2: Broad Sense Heritability

Ha: Hectare

IBD: Identity By Descent

Kg: Kilogram

LD: Linkage Disequilibrium

LOD: Logarithm of Odds score

MAGIC: Multiparent Advanced Generation InterCross

Mgv: Maximum Green Value

NABIM: The National Association of British & Irish Millers

NDVI: Normalized Difference Vegetation Index

NIAB: National Institute of Agricultural Botany

NIL: Near Isogenic Line

NIRS: Near-Infrared Reflectance Spectroscopy

PCC: Pearson's Correlation Coefficient

Ppd: Photoperiod alleles

QTL: Quantitative Trait Locus

RGB: Red Green Blue

Rht: Reduced Height gene

RIL: Recombinant Inbred Lines

SNP: Single Nucleotide Polymorphism

Snr: Senescence Rate

t/ha: Tonnes per hectare

TGW: Thousand Grain Weight

UoR: University of Reading

Yld: Yield

1. Introduction

1.1 Background

The global population is rising by around 1.7% a year (Rosegrant and Agcaoili, 2010), which equates to approximately an extra 110 million people. During the twentieth century alone, the world population increased from 1.65 billion to 6 billion. While cereal production has continued to increase in this time, so has demand, creating a yield gap (Fischer *et al*., 2009). Global production is actually higher than required solely for direct human consumption, however the rising affluence in developing nations and the climate change policies of developed nations add further strain to global systems by requiring increased production of meat and biofuel respectively (Godfray *et al*., 2010). In this context, it has been predicted that cereal production will need to increase by at least 50% by 2050 in order to feed an estimated 9 billion people. Global production of cereals stands at 2,980 million tonnes a year (FAOSTAT, 2019) (Figure 1.1), 90% of which is from just three main crops: Wheat, Maize and Rice - all of which are grass species with edible grains and share a common ancestor from around 50-70 million years ago (Kellogg, 2001). Wheat provides approximately 20% of the calories consumed globally, including a similar percentage of the dietary protein for about 2.5 billion people in less developed countries (Dixon *et al*., 2009). Some estimates suggest that, in Europe alone, wheat production will need to double to keep pace with demands and maintain stable prices. Increasing demand for cereal crops is challenged by a shortage of high-quality agricultural land, diseases, resource limitations, increased input costs and environmental issues that can drastically reduce optimum yields. The yield potential of wheat has been gradually increasing by around 1.1% per annum (Dixon *et al*., 2009), due

to introduction of new cultivars - but this is currently insufficient. There is evidence that on as much as 27% of the global area on which wheat is grown, wheat yields may have plateaued (Grassini *et al*., 2013), further increasing pressure on limited productive areas.

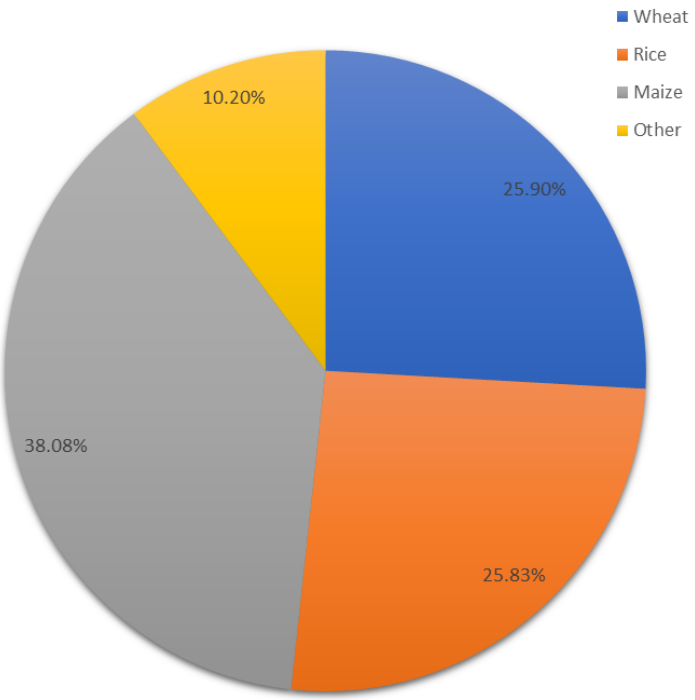

Figure 1-1 Global cereal production 2017

1.2 Economic importance of wheat

Average global yields are highly varied between countries and regions, ranging from 0.5t/ha in some areas of North Africa, to 15.6t/ha in New Zealand. The average global yield is around 3.0t/ha, largely due to limited soil resources, water shortages and susceptibility to disease and pests (FAO, 2016).

In 2015, 156 million tonnes of wheat were traded on the international markets, making it the most widely traded cereal crop in the world. This international trade represents

almost 20% of annual global production, with six main areas accounting for approximately 90% of exported wheat. Exact numbers vary year on year, but overall the largest wheat exporters in the world are: the USA; the EU; Australia; Canada; the Former Soviet Union; and Argentina (Figure 1.2). The wide geographical distribution of these exporters produces a generally stable wheat supply, with decreases in production from adverse conditions in one area being balanced by better conditions in other areas. However, this is not always the case, which has previously led to export restrictions and large price increases globally, with net importing nations bearing the brunt of these increases (FAO, 2016).

Figure 1-2 Major wheat exporters and importers 2016 (FAO Food Outlook 2016)

The top importers of wheat are concentrated in developing countries, particularly in North and Sub-Saharan Africa, Latin America and South-East Asia. These regions have had a greatly increased demand over the past few decades, due to rapidly expanding populations combined with an increasing economic wealth.

In addition to its economic nutritional importance, wheat is culturally important in many areas, and has uses in both food and non-food products. The gluten protein content of

wheat imparts elastic properties to doughs necessary for products such as bread, pasta and noodles (Shewry, 2009), and variants of these are staple foods in many cultures around the world. Wheat flour is also used as a thickening agent in sauces and soups, or the whole crop harvested green as silage for livestock, in addition to the uses of wheat in non-food items such as adhesives, paper and livestock bedding (Kersting *et al*., 1994).

1.3 Adaptability

Wheat is a highly adaptable crop, with a vast global distribution in a wide range of locations and climates that is unrivalled by any other cereal. It is cultivated at every latitude between 67°N and 45°S, from Northern Europe to New Zealand (Trethowan *et al*., 2005), thriving throughout Mediterranean, temperate and sub-tropical areas, and able to tolerate many variations in altitude, soil type and weather conditions (Figure 1.3)

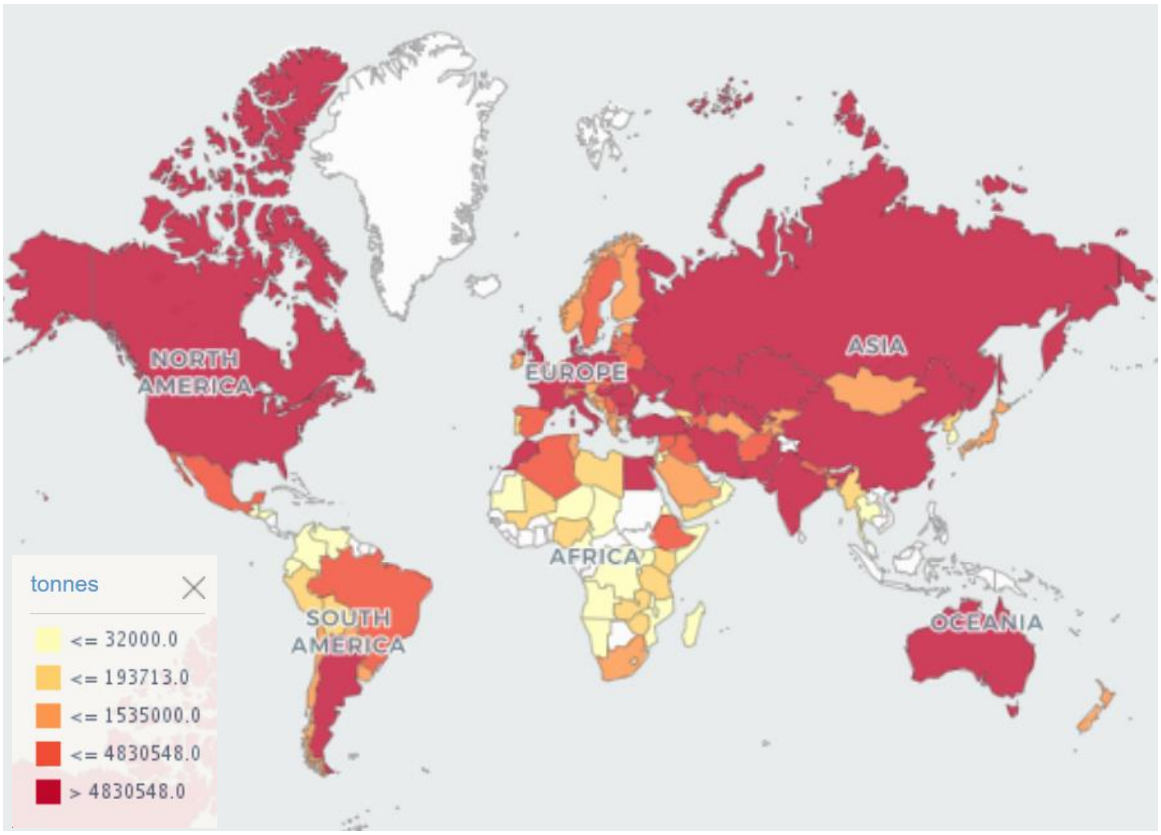

Figure 1-3 Global Wheat Production 2017 (http://www.fao.org/faostat/en/#data/QC/visualize)

Modern bread wheat cultivars can be categorised in two broad seasonal types - spring and winter. Winter wheat is sown in the autumn, which allows it to develop its initial vegetative stage before winter, then resuming its growth in spring. Already being established at the start of spring allows winter wheat to gain a head-start in light interception and biomass accumulation, while being in a better position to exploit the higher moisture levels in the environment. Spring wheat, as the name suggests, is sown in spring, has no "holding" phase, and does not need vernalisation (Snape *et al*., 2001). Both types are harvested around the same time in late summer. Both spring and winter wheat have their own advantages depending on the priorities of the farmers and the climate in which it is grown.

In the UK, winter wheat is favoured as the yield is typically higher than in spring varieties, and it allows more time in spring for other activities. Spring wheat is favoured in countries such as Egypt, where the climate allows multiple crops to be grown in rotation throughout the year.

1.4 Classification and grading

Within cultivated wheat varieties, two main groups appear: 'Bread' wheat and 'Durum' wheat, which are hexaploid and tetraploid respectively. Bread wheat (*Triticum aestivum*) is the most widely utilised, accounting for around 95% of global wheat production. Durum wheat (*Triticum turgidum*) accounts for around 5% of global production (Bushuk and Rasper, 1994; Carver, 2009), mainly for use in pasta production.

Wheat is divided into categories based on quality and end-use. In the UK, these are split into four quality groups as defined by the National Association of British and Irish Flour Millers (NABIM) (http://www.nabim.org.uk/). Group 1 is the highest quality class,

defined by hard endosperm and a high protein/gluten content and is used for bread-making. Group 2 varieties exhibit bread-making potential but not to the same extent as Group 1. Group 3 contains soft endosperm varieties, with low protein, and is typically used in production of cakes and biscuits, or distilling. Group 4 varieties lack bread- or biscuit-making qualities and generally exhibit the highest yields and lowest protein contents - this group is mainly grown for animal feed. Each wheat exporting country has their own grading systems that meet specific standards in moisture content, protein content, grain weight and foreign material content (Bushuk and Rasper, 1994; Carver, 2009).

1.5 The origin and domestication of wheat

Archaeological evidence suggests that wheat originated in an area of the Middle East known as the fertile crescent (Brown *et al*., 2009; Heun *et al*., 1997) (Figure 1.4). This area contains the basins of the Tigris, Euphrates and Jordan rivers, and is the site where it is thought that human civilisation first emerged from hunter-gatherer lifestyles into an agricultural-based existence (Preece *et al*., 2015). This change from the hunter-gatherer lifestyle caused a shift from a previously rich, diverse diet of small grains, pulses, wild fruits and any meats they could successfully hunt, to around eight plants recognised as Neolithic founder crops (Zohary *et al*., 2015). It was these crops that allowed individuals to specialise, create trade and form the basis of civilisation as we know it (Whittle and Cummings, 2007).

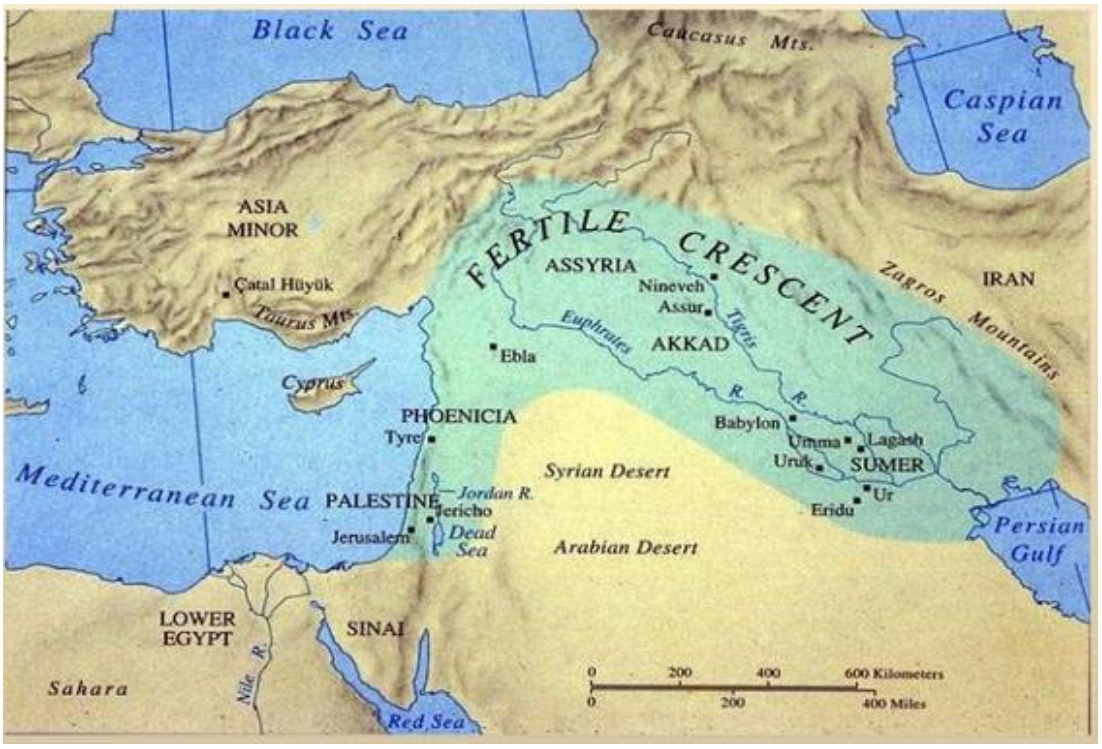

Figure 1-4 The Fertile Crescent (Image taken from https://www.sophia.org/tutorials/the-fertile-crescent, 2019)

1.5.1 Hybridization Events

Modern hexaploid and teraploid wheat are the result of two distinct hybridisation events (Figure 1.5), the first involving progenitors of the AA and BB genomes between 200,000 and 500,000 years ago (Dvořák *et al*., 1993; Huang *et al*., 2002). The AA genome has been traced back to a close relative of *Triticum urartu,* a diploid einkorn wheat (Huang *et al*., 2002). The BB genome donor is less certain, although previous studies have suggested potential candidates, including *Aegilops speltoides* (Maestra and Naranjo, 1998), and 5 species of *Sitopsis* - none of which are deemed to have sufficient homology to the BB genome to be considered the true ancestor (Blake *et al*., 1999).

The result of this hybrid was wild emmer (*Triticum dicoccoides*), an AABB tetraploid, which was later domesticated, giving rise to modern durum wheat (*Triticum turgidum*), which accounts for around 5% of global wheat production. More recently, around

10,000 years ago, *Aegilops tauschii* (DD) hybridised with the *T. dicoccoides* tetraploid to create modern, hexaploid *T. aestivum,* or bread wheat, which has become one of the most important crops in the world. Each hybridization event was followed by chromosome doubling in the new hybrid, allowing the production of fertile plants. The resulting hexaploid bread wheat carries 6 genomes, each with 7 chromosomes, and thus contains 42 chromosomes in total (Winfield, 2011).

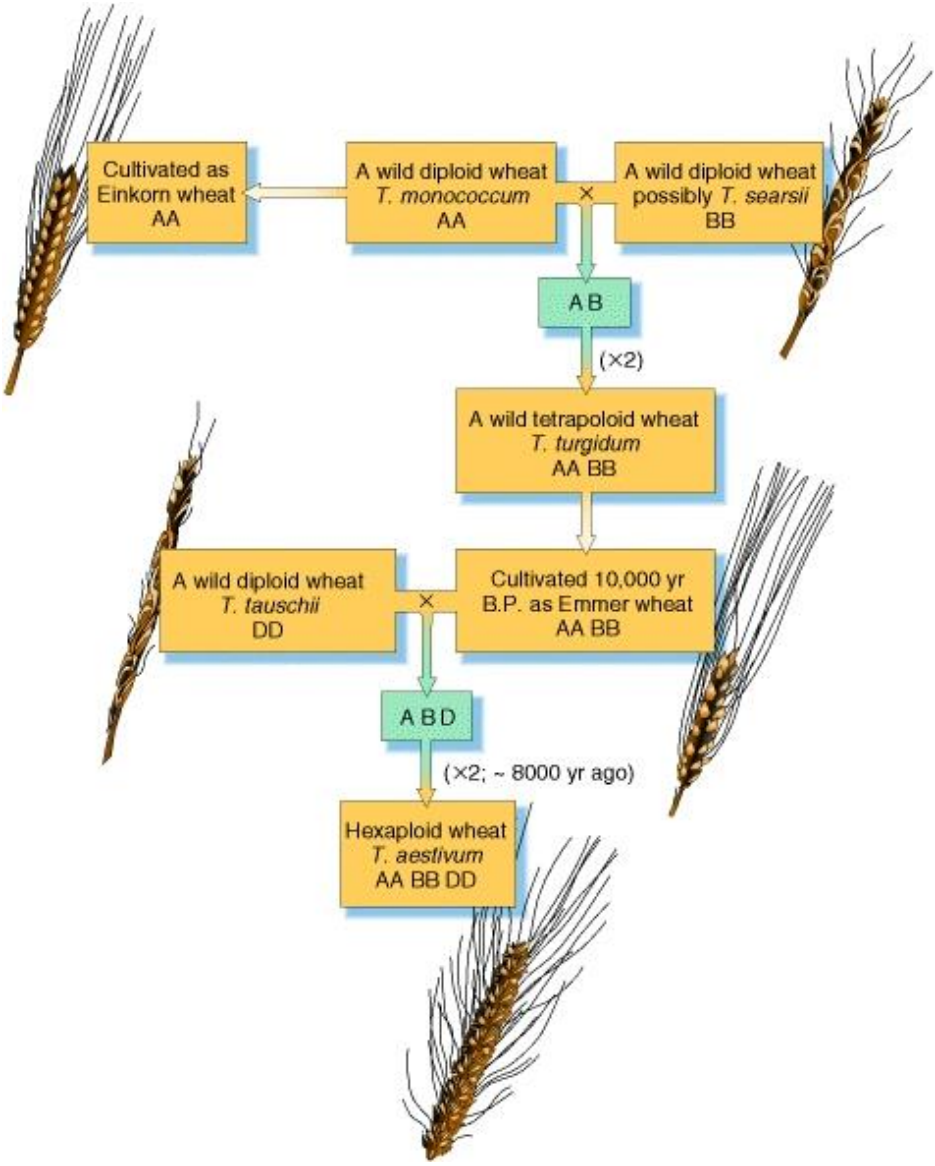

Figure 1-5 Evolution of hexaploid bread wheat - detailing the 2 separate hybridization events that allowed the evolution of bread wheat Triticum aestivum. 'X2' refers to the doubling of the chromosomes. (Figure taken from www.cerealsdb.uk.net)

1.5.2 Domestication syndrome

The domestication of crops from their wild progenitors has created genetic bottlenecks, limiting the genetic diversity in modern crops (Dubcovsky and Dvorak, 2007; Haudry *et al*., 2007). Grain crops were selected for larger grains and higher grain: chaff ratios, which reduced the amount of labour needed to extract the greatest amount of food (Harlan, 1967).

One of the most important changes that occurred to wheat during domestication was the mutation of the brittle rachis (*Br*) locus. In wild plants, the *Br* locus ensured that mature seeds would be dispersed, but in a domesticated crop is agriculturally deleterious. The mutation to non-*Br* supressed the formation of fractures in the rachis, leaving spikes intact until harvest, reducing pre-harvest losses (Nalam *et al*., 2006; Peng *et al*., 2011). A second major mutation occurred at the *Q* locus, changing the glumes from tenacious to soft, requiring less energy to be expended in threshing the grains from the chaff. Simons *et al.* (2006) shows that the *Q* locus also has an effect on spike characteristics and rachis fragility. Between these traits, domesticated wheat has lost its seed-dispersal mechanism, rendering it unable to survive without human intervention.

1.5.3 The Green Revolution

The Green Revolution has been the greatest change to crop production since domestication 10,000 years ago. The term Green Revolution was coined to describe a 20-year period from 1960s to 1980s marked by a radical stepping up of the pace of technology transfer, market development, crop research and infrastructure improvements in response to continually increasing population and food demand

(Hardin, 2008). During this period, effective fertilisers and pesticides became more widely available, improved irrigation techniques were adopted, and high-yielding cereal varieties were developed (Pingali, 2012).

In wheat, a major step-change in yield potential was obtained through the development and distribution of semi-dwarf varieties. These short varieties would be able to withstand higher nitrogen applications that might have caused lodging in taller varieties (Peng *et al*., 1999). The introduction of *R*educed *h*eight genes (*Rht*) was the main cause of the reduction in plant height. The *Rht* genes are a homoeologous set on the group 4 chromosomes, coding for DELLA proteins (Peng *et al*., 1999), transcriptional growth repressors which interact with gibberellic acid (GA) (Ellis *et al*., 2002; Peng *et al*., 1999). Normally, the repressive action of the DELLA gene products would be suppressed by GA, however the DELLA variants encoded by the *Rht* genes are insensitive to GA and maintain constitutive growth repression under conditions where endogenous GA levels would normally have promoted growth (Peter, 2003).

The *Rht* genes were introduced to UK germplasm by cross breeding with the Japanese variety Norin-10. Norin-10 possesses both *Rht-B1* and *Rht-D1*, B and D genome copies of the *Rht* genes (Gale and Youssefian, 1985). These dwarfing genes were selected because they cause a significant reduction in height without dwarfing the ears as well (Peng *et al*., 1999), therefore increasing the Harvest Index (Borlaug, 1983). The first commercial UK variety to possess a *Rht* gene was Gaines, which was characterised by stiffer, shorter straw that reduced lodging, and increased biomass in the ears (Gale and Youssefian, 1985). Other successes include Lerma Rojo-64 and Sonora-64, wheat varieties released in 1964 and grown in South-East Asia, helping to end famine in the

region by boosting yields by 3.6% per year (Borlaug, 1983; Peter, 2003; Shiferaw *et al*., 2013). In 1965, India and Pakistan imported a combined total of 450 tonnes of semi-dwarf seed, developed by the International Maize and Wheat Improvement Centre (CIMMYT), Mexico. By 1970, India was producing 20.1 million tonnes of wheat, and Pakistan harvested 7.3 million tonnes - an increase of over 60% on 1965 yields in each country. In 1972, Indian wheat production rose further to 27 million tonnes, although Pakistan's production dropped slightly in this timeframe, likely due to a smaller area being cultivated during the Indo-Pakistani war.

In addition to dwarfism, intensive breeding programmes at CIMMYT had the unintended consequence of favouring photoperiod insensitive varieties (Borlaug, 1983). This occurred because the breeding program was designed for two growing seasons a year for accelerated varietal development, with growing sites situated 10^{o} in latitude and over 2600m in altitude apart. As a result of this insensitivity, there was less need to tailor varieties to individual regions, and the new Green Revolution varieties could be distributed and grown around the world (Beales *et al*., 2007; Kato and Yokoyama, 1992).

Today the world is in need of a new Green Revolution. Yield plateaus, increasing populations and climate change demand a second Green Revolution that is sustainable and minimises damage to the environment and ecosystems. The previous revolution was concentrated on favourable areas with high levels of rainfall or irrigation (Pingali, 2012). The next revolution must encompass the entire world, especially in marginal areas that were overlooked in the first one.

These challenges can be met by re-establishing production systems and agricultural innovations with modern technological innovations and scientific knowledge (Pingali,

2012). This must happen, despite investments in agriculture having steadily and significantly dropped since the end of the Green Revolution (Pingali, 2012).

1.6 Genetic dissection of yield

Yield is the final outcome of the crop growth and development processes occurring throughout the growing season. However, yield is formed continually from sowing to harvest, with virtually all genes contributing directly or indirectly (Slafer, 2003). Although some processes governing yield are inherited in a qualitative manner, most yield related traits are inherited quantitatively, with a full range of potential variation. Yield itself may be considered to be the result of the actions and interactions of all other traits, rather than a trait in itself (Slafer, 2003). The Agriculture and Horticulture Development Board (AHDB) Wheat Growth Guide (Figure 1.6), though written from an agronomist and grower's perspective, provides a useful integrative picture of how the different stages of the life cycle are connected and together determine final yield. It demarcates three major phases of the winter wheat crop cycle - Foundation, Construction and Production.

The Foundation stage starts with seed germination and establishment of a vegetative canopy above ground and the root system below ground. Growth slows down as autumn progresses and reaches a minimum in the colder winter months, and the vernalization requirement, where present due to the possession of winter alleles at the *VRN-A1* locus, blocks the transition to reproductive development until sufficient chill units have been accumulated. The number and spatial organisation of leaves forming the vegetative canopy is established through tillering (branching) and the transition to

the Construction phase is marked genetically by the satisfaction of the vernalization requirement and the activation of floral pathways (Snape *et al*., 2001).

The Construction phase combines rapid vegetative growth from already established tillers with rapid development of the floral organs from the apical meristems of each tiller. The timespan from initiation of stem extension to anthesis is mainly a function of thermal time, subject to a genetically variable photoperiod sensitivity. Most UK winter wheats are photoperiod sensitive; that is, they repress floral development until daylength exceeds a certain threshold. This serves the purpose of avoiding exposure of delicate floral organs to late frosts.

The Production phase spans the remainder of the crop cycle from fertilization through grain filling to senescence and ripening. Although this phase starts with a set maximum number of grain sites per unit area, continued photosynthetic activity and an adequate supply of water and nutrients are needed to avoid seed abortion and lower than maximum potential grain filling.

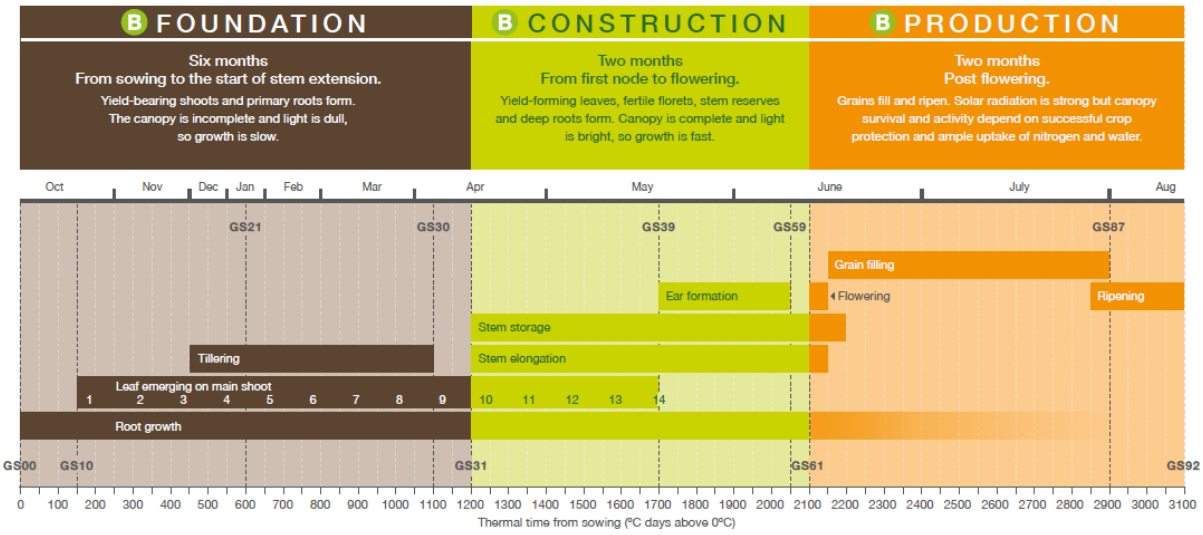

Figure 1-6 Wheat development phases reproduced from the AHDB Wheat Growth Guide

Figure 1.7, also reproduced from the Wheat Growth Guide, illustrates how yield potential derives from the ability to capture appropriate amounts of water and nutrients from the soil, light energy and carbon dioxide from the atmosphere and to channel the fixed carbon and nitrogen to the grain.

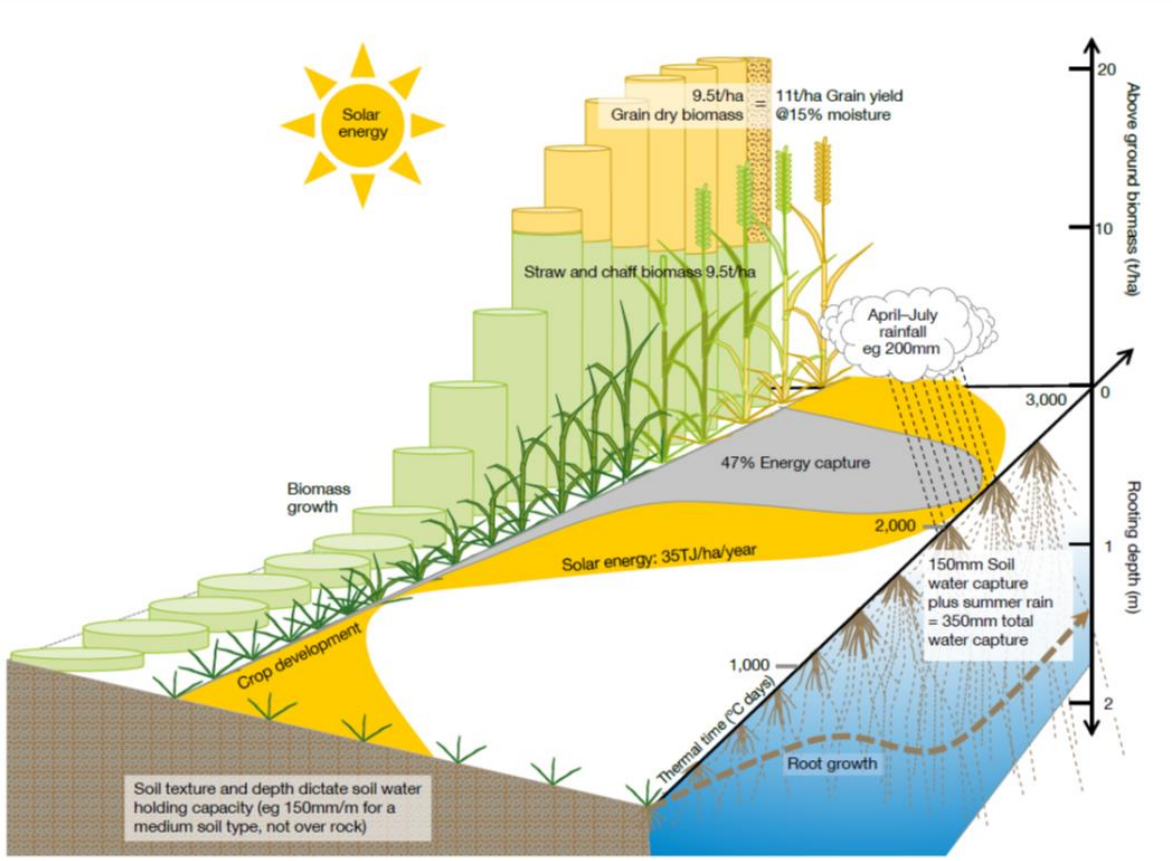

Figure 1-7 Summary of the capture and utilisation of natural resources, particularly solar energy, water and carbon dioxide. It illustrates how these resources convert into grain and non-grain energy (expressed here in t/ha biomass or grain). (reproduced from the AHDB Wheat Growth Guide)

1.6.1 The reductionist approach to yield

The traditional genetic approach to yield is essentially reductionist, based on defining a nested hierarchy of component traits that can be tackled one at a time.

At the top level, Grain Yield (per unit area) is of course the direct product of the number of grains per unit area and the average grain weight, usually expressed as the Thousand Grain Weight (TGW). Attempts to understand why grain size varies have focussed on the principal grain morphometric traits such as length and width, which determine the grain volume and Specific Weight, a measure of grain density per unit volume. These first order yield component traits are quite heritable, and their genetic underpinnings have been studied with some success. Further detail of specific loci governing GW, GL and TGW will be given in Chapter 3.

However, grains are found on ears, and therefore the number of grains found per unit area is itself the product of the number of plants per unit area (which is influenced by the number of seeds planted per unit area), the number of tillers per plant, and the average number of grains per ear. The tillering ability of the plant and number of grains per ear are partly genetically determined but are not independent of each other and of course respond dynamically to resource availability/capture and environmental stress. The plant's ability to establish fertile spikelets are fixed early in development - between Zadok's Stage 30 and 60 (Zadoks *et al*., 1974) - and is reliant on early vigour and water use efficiency (López-Castañeda and Richards, 1994).

Most previous studies focusing in depth at sink-related traits have limited scope in the sizes of the studied populations and are highly variable in the physical areas used for

measuring grain yield. Simmonds *et al* (2014), Brinton *et al* (2017) and Snape *et al* (2007), all used plots around 1 x 6m, Verma *et al* (2004) used 1.4 x 5m plots, while Griffiths *et al* (2015) used plots between $1m^2$ and $6m^2$ depending on the location. All of these studies used populations of varying sizes from 34 lines (Verma *et al*., 2004) to 202 lines (Snape *et al*., 2007).

1.6.2 Yield – the integrative approach

All of the above field studies involved collecting data from ear emergence or flowering onwards, with little in the way of data capture before this. Any source-related traits are usually confined to looking at the time around grain filling and senescence, rather than taking into account the gradual accumulation of source capacity over the full lifecycle. Some research, exemplified by Camargo *et al* (2018, 2016) and Pennacchi *et al* (2018) have begun to take a more integrative approach, measuring growth parameters throughout the season, with a view to understanding some of the complexity of how multiple traits together explain the final yield. Camargo *et al* used a fully automated glasshouse phenomics facility to capture detailed data on growth and development over a full crop cycle, concluding that there were benefits to the genetic mapping of growth curve parameters as well as single time point data to help develop a better understanding of developmental plasticity in wheat. The limitations of this study were the use of single pot-grown plants in a glasshouse environment, which means that the relevance of the findings to field-grown crops is somewhat uncertain, and a lack of genetic power imposed by the low number of genotypes (208) and two replicates catered for by the capacity of the facility. Pennacchi *et al* (2018) used a combination of

controlled environment and field trials, using 12 and 119 lines respectively, but has not yet published a genetic analysis.

With the exception of Camargo *et al* (2018, 2016), all other studies mentioned here were based on double-haploid lines in bi-parental populations. Simmonds *et al* (2014) and Brinton *et al* (2017) took these further, creating NILs for examining specific loci. The predominant use of bi-parental populations is potentially limiting on the detection of novel QTLs due to the limited genetic diversity represented from just two parents, and there is a lower mapping resolution for QTLs because of fewer opportunities for recombination events to occur. Camargo *et al* (2018, 2016) used a subset of a multi-parent population, with a wider genetic base and higher mapping resolutions. Section 1.7.3 goes into further detail on the advantages and disadvantages of the various population types.

1.7 Quantitative Genetic analysis in wheat

Most traits of interest in plant genetics show a continuous range of variation that are controlled by the cumulative action of multiple genes, environmental factors and epistatic interactions (Lynch and Walsh, 2004).

A quantitative trait locus (QTL) is a statistically identified region of the genome that is theoretically associated with genetic variation of a given trait. The dissection of a quantitative trait requires the identification of QTLs that contribute to the expression of a quantitative phenotype by means of molecular markers associated with the phenotypic variation (Lynch and Walsh, 2004).

The success of any experiment aiming to accurately map QTLs depends on multiple factors: the size and type of mapping population, the complexity of the targeted trait, the number of molecular markers available and the quality of the linkage map (Milner *et al*., 2016). As the genetic variation of a trait can involve many minor effect QTLs, higher trait heritability is crucial for reliable results (Bradbury *et al*., 2011). To limit environmental variation on the target trait, experiments generally need to be conducted with replicates over multiple years with a large sample of individuals to ensure an appropriate level of recombination is present.

1.7.1 The experimental design challenge

Complex traits such as yield can only be accurately measured in larger field plots. Conducting field trials with multiple lines, repeats and with plots of a sufficient size can quickly become a daunting challenge for phenotyping. For example, the field experiments conducted for this thesis covered approximately 2.4ha including buffer zones between plots, which equates to around 12km to walk along every individual plot.

1.7.2 High-throughput phenotyping

To be able to dissect traits such as yield, that are the final product of a full season's growth and environmental interactions, data must be collected over the full lifecycle of the plant. Such a varied period poses its own challenges to data collection, with shorter days for phenotyping in winter, and wetter periods throughout the year meaning many instruments could not be used all the time due to sensitive electronic components. Others, such as radio spectrometers, have specific lighting conditions and times of day at which they can be used, rendering them unsuitable on a large scale. The ideal phenotyping method must be quick (lasting just seconds) and yet precise; a phenotype

acquisition time of just 1 minute per plot would result in a prohibitive 27 continuous hours of phenotyping in the context of the large yield trials described in this thesis.

Several methods have been proposed to provide a combination of mobility and automation needed to cover large scale experiments at multiple timepoints, including proximal sensing carts (White and Conley, 2013), 'Phenomobile'- a manned buggie that can collect multiple phenotypes simultaneously (Deery *et al*., 2014), 'Field Scanalyzer'- a fixed automated gantry (LemnaTec), and more flexible and variably configured tractor-mounted booms and UAVs carrying bespoke payloads of sensing instruments. All of these methods have various advantages and disadvantages, from expense and reliability to payload capacity (Table 1.1)

Platform Type	Disadvantages	Advantages
Fixed systems	Generally expensive; can only monitor a very limited number of plots	Unmanned continuous operation; after-hours operation (e.g., night-time); good repeatability
Permanent platforms based on cranes, scaffolds or cable-guided cameras	Limited area of crop, so very small plots; expensive	Give precise, high resolution images from a fixed angle
Towers/cherry-pickers	Generally varying view angle; problems with distance (for thermal), bi-directional reflectance distribution function (BRDF), plot delineation, *etc.*; difficult to move, so limited areas covered	Good for the simultaneous view of the area; can be moved to view different areas
Mobile in-field systems	Generally take a long time to cover a field, so subject to varying environmental conditions	Very flexible deployment; good capacity for GPS/GIS tagging; very good spatial resolution
Hand-held sensors	Very slow to cover a field; only one sensor at a time; different operators can give different measurements	Good for monitoring
Hand-pushed buggies	Limited payload (weight); hard operation for large experiments	Relatively low cost; flexibility with payload and view angle geometry; very adaptable
Tractor-boom	Long boom may not be stable	Easy operation; constant view angle; wide swath (if enough sensors are mounted as on a spraying bar); mounting readily available (needs modification)
Manned buggies	Requires a dedicated vehicle (expensive)	Flexibility with the design of the vehicle (e.g., tall crops, row spacing); Constant view angle; very adaptable
Autonomous robots	Expensive; no commercial solutions available; safety mechanisms required	Unmanned continuous operation; after-hours operation (e.g., night-time)
Airborne	Limitations on the weight of the payload depending on the platform; a lack of turnkey systems; spatial resolution depends on speed and altitude	Can cover the whole experiment in a very short time, getting a snapshot of all of the plots without changes in the environmental conditions
Blimps/balloons	Limited to low wind speed; not very easily moved precisely; limited payload	Relatively cheap compared with other aerial platforms
UAVs	Limited payload (weight and size); limited altitude (regulations) and total flight time (hence, total covered area); less wind-affected than blimps; regulatory issues depending on the country	Relatively low cost compared with manned aerial platforms; GPS navigation for accurate positioning
Manned aircraft	Cost of operation can be expensive and may prohibit repeated flights, thereby reducing temporal resolution; problems of availability	Flexibility with the payload (size and weight); Can cover large areas rapidly

Table 1.1 Phenotyping platforms with some relative advantages and disadvantages (Deery *et al.*, 2014)

1.7.3 Genetic mapping populations

Most studies have traditionally used bi-parental crosses. These are simple to create, needing only two lines with contrasting phenotypes at the target trait, and have proven to be highly successful. Early plant genetics experiments used backcrossing (BC) populations, typically an F_2 generation, these could be created in a relatively short time span. However, BC studies were usually based on single plants, limiting the ability to repeat trials for most crops.

The next stage of these populations is Recombinant Inbred Lines (RILs), derived from an F_2 generation which then goes through selfing for several cycles. This has the advantage of stabilising the genes across generations, allowing for replicated trials, while also increasing the potential level of genetic recombination, giving a higher mapping resolution than previous designs.

Once candidate loci for the desired traits have been identified, Near Isogenic Line (NIL) populations can be created by backcrossing to a recurrent parent several times, eliminating background genetic variation. This makes NILs a strong resource for selectively analysing single loci or genes. However, this also means that NILs are single use.

The main constraint for all of the above methods is that there are potentially large confidence intervals for many of the QTLs, potentially spanning hundreds of candidate genes (Holland, 2007), and there is a relatively low genetic base, not representing wider allelic diversity available in the germplasm (Jannink, 2007).

Genome-wide association studies (GWAS) exploit linkage disequilibrium (LD) as a function of historical recombination for QTL mapping. Until as recently as the last decade, GWAS was impractical at scale due to genotyping limitations, but decreasing costs and increasing data processing had promoted the use of GWAS across many species and studies. GWAS gives a high detection power, however is prone to return false-positives due to unknown kinship and population structure among the population analysed (Lewis, 2002; Zhao *et al*., 2007). In addition, rare variant QTLs with low frequency may remain undetected despite having relative large effects (Mackay and Powell, 2007).

Multi-parent populations have emerged as the next generation of mapping resources, combining diverse genetic founder contributions with high levels of recombination (Colin *et al*., 2008; Mackay and Powell, 2007), overcoming some of the limitations of previous populations and analysis methods. The most common form of multi-parent populations are Nested Association Mapping and Multiparent Advanced Generation InterCross (MAGIC). NAM populations are designed to increase the precision and power of QTL mapping by combining the advantages of association mapping and bi-parental crosses, and unlike GWAS are effective at identifying rare alleles (McMullen *et al*., 2009). NAM populations are derived by crossing a single inbred parent with a successive collection of diverse inbred lines, the first of which was a maize population as described by Yu *et al* (2008). These capture thousands of recombination events, but the levels of recombination and LD can vary considerably between families, potentially limiting the precision of QTL mapping (McMullen *et al*., 2009).

The advantages and disadvantages of MAGIC populations, along with their construction and current status in research, can be found below in section 1.8.

1.8 The MAGIC population

The concept of repeated intercrossing within a population was first described by Darvasi and Soller (1995), who used repeated intercrossing of a bi-parental population to increase the probability of recombination across the genome. This work was further developed by Mott *et al* (2000), creating the first multiparent advanced generation intercross (MAGIC) population to study mouse genetics.

MAGIC was first advocated in crops by Mackay and Powell (2007), based on the principles of established by Mott *et al* (2000). Several MAGIC populations are now available for a range of crop species, including rice (Bandillo *et al*., 2013), arabidopsis (Kover *et al*., 2009), wheat (Huang *et al*., 2012; Mackay *et al*., 2014), maize (Dell'Acqua *et al*., 2015), faba bean (Sallam and Martsch, 2015) and chickpea (Gaur *et al*., 2014).

The elite wheat MAGIC population of eight European varieties (Alchemy, Brompton, Claire, Hereward, Rialto, Robigus, Soissons and Xi19) was developed by the National Institute of Agricultural Botany (NIAB), as described by Mackay *et al* (2014). These parents were chosen to reflect complementary strengths in Grain Yield, Disease Resistance and Quality, as well as reflecting their importance as parents in current breeding programs (Table 1.2).

Table 1.2 - Properties of the eight wheat parents used to create the Multi-parent Advanced Generation InterCross (MAGIC) wheat population.

Variety	Breeder	Pedigree	Listing year	Seed Yield	NABIM Quality Group	Trait Attributes
Alchemy	Limagrain	Claire x (Consort x Woodstock)	2006	9.163	4	yield, disease resistance, breeding use, soft, *Rht-D1b* [a]
Brompton	Elsoms Seeds Ltd	CWW-92-1 x Caxton	2005	9.151	4	hard feed, 1BL/1RS[b], OWBM[c] - resistant, *Rht-D1b*
Claire	Limagrain	Wasp x Flame	1999	8.654	3	soft biscuit/distilling, slow apical development, *Rht-D1b*
Hereward	RAGT	Norman 's' x Disponent	1991	7.683	1	high-quality benchmark I bread- making, *Rht-D1b*
Rialto	PBI Cambridge Ltd	Haven 's' x Fresco 's'	1994	8.377	2	moderate bread-making, 1BL/1RS, *Rht-D1b*
Robigus	CPB Twyford Ltd	complex	2003	9.053	3	exotic introgression, disease resistance, breeding use, OWBM-resistant, *Rht-B1b* [d]
Soissons	Maison Florimond Desprez	Jena x HN35	1995	7.553	2	bread-making quality, early flowering, *Rht-B1b*
Xi19	Limagrain	(Cadendza x Rialto) x Cadenza	2002	8.957	1	bread-making quality, facultative type, breeding use, Rht-D1b, *Vrn-A1b* [e]

[a] Contains the dwarf allele of the D genome copy of the *Reduced height 1* gene
[b] Contains the 1BL/1RS chromosomes translocation from rye
[c] Orange wheat blossom midge
[d] Contains the dwarf allele of the B genome copy of the *Reduced height 1* gene
[e] Contains the spring type allele of the *Vrn-A1* gene
Table modified from Mackay *et al* (2014) and Benbow (2016)

The population was created following a replicated funnel crossing design, ({[AxB]x [CxD]}x {[ExF]x [GxH]}), (Figure 1.8) giving a population showing uniform kinship relationships, with minimal structure remaining. The reduction of population structure found in MAGIC populations compared to GWAS reduces the chance of false positives (Zhang *et al*., 2010). The multiple founders available in these populations contribute a greater amount of allelic variety to the population. Combined with the multiple cycles of intercrossing, that creates an increased opportunity to accumulate greater numbers of recombination events, allows for a much greater precision in QTL locations than possibly in traditional bi-parental crosses and later AM populations. The controlled allelic input and high levels of recombination improves the sampling of genetic diversity

available and facilitates the analysis of interacting and complex traits. However, MAGIC populations require high density genotyping to ensure that there is full coverage of every linkage block in the genome which allows us to take full advantage of the high recombination levels.

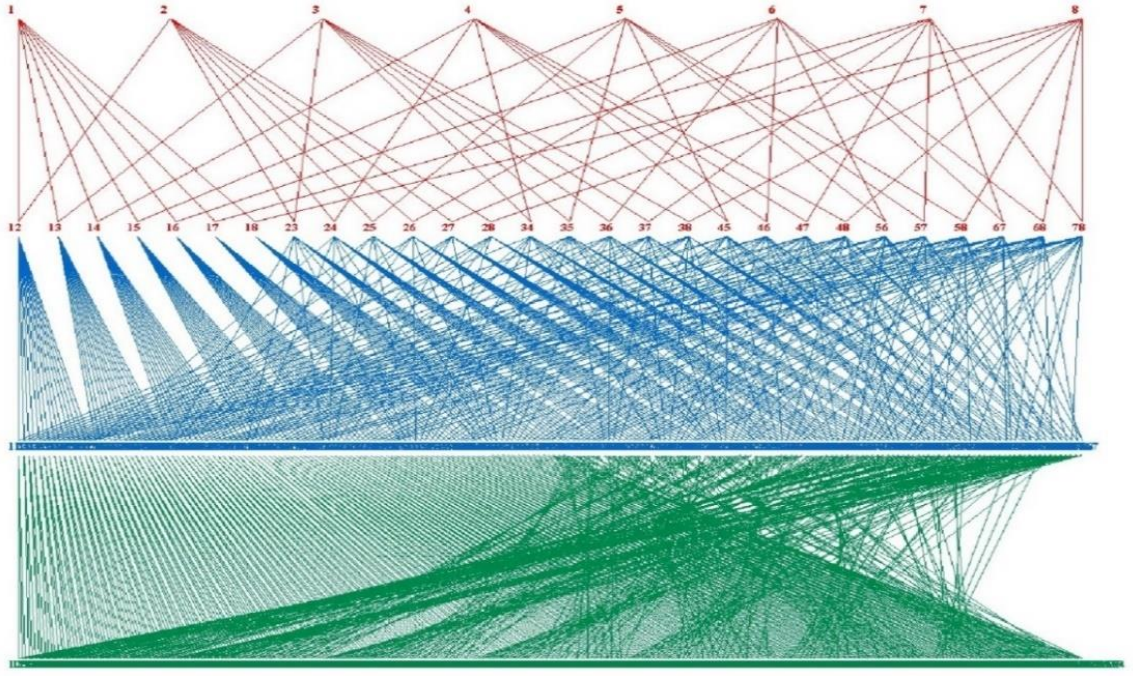

Figure 1-8 Replicated funnel crossing design from the eight founder parental lines (Table 1.1; red) to final 1091 lines (green). (source Niab.com)

Due to the multiple parentage of a MAGIC population, creating a genetic map is more difficult than in a bi-parental cross. Whilst there are multiple software packages available for mapping molecular markers in bi-parental populations (R/qtl (Broman *et al*., 2003), QTL Cartographer (Wang *et al*., 2011), Flapjack (Milne *et al*., 2010), ect.), to date only two are available for MAGIC populations (HAPPY (Mott *et al*., 2000) and mpMap (Huang and George, 2011)). A genetic linkage map for the NIAB MAGIC population was created by Gardner *et al* (2016), who use the Illumina Infinium iSelect 90k array to genotype the population. From here, they removed all markers with more

than 50% missing data, and manually recalled all markers with more than 4% missing data to ensure that only high-quality data would be used in mapping. Of the remaining markers, 20,639 SNP markers were scorable and polymorphic, of which 18,601 were mapped in the MAGIC population (Gardner *et al*., 2016; Mackay *et al*., 2014). This represents around 80% of the diversity shown in the WAGTAIL UK winter genome–wide wheat association panel genotyped with the same 90K SNP array (Gardner *et al*., 2016).

1.9 Project Outline

1.9.1 Aims

The aims of this PhD thesis are to conduct an in-depth study of the genetic underpinnings of a suit of traits spanning both source and sink potential in wheat. To accomplish this, the NIAB MAGIC population was analysed from emergence through to final yield. This population captures more than 80% of the allelic diversity found in the UK winter wheat elite breeding material, making it likely that the markers identified in this analysis are segregating in the UK population as a whole.

1.9.2 Hypotheses

1. There will be a significant heritable difference in varying aspects of biomass accumulation between MAGIC genotypes which will cause heritable differences in the final yield.
2. There will be a significant heritable difference in the components of sink capacity between MAGIC genotypes which will cause heritable differences in the final yield.
3. There will be significant genetic interactions between QTL for sink related traits.
4. There will be significant genetic interactions between QTL for source related traits.
5. There will be significant genetic interactions between QTL for combinations of all measured traits.

2. Materials and Methods

2.1 Plant Materials

All field experimentation in this thesis uses the elite wheat Multiparent Advanced Generation Intercross (MAGIC) Recombinant Inbred Line (RIL) population described in Chapter 1, section 1.7.3. The population was developed by the National Institute of Agricultural Botany (NIAB), Cambridge, UK and first described by Mackay *et al* (2014). The full population resource consists of 1,091 RILs; for logistic reasons, field trials were limited to 1,584 plots and therefore only a subset of the full population was used. The 643 RILs for which genotypic data was publicly available were prioritised, with remaining trial space being filled with a random selection of the ungenotyped lines. For convenience, this resource will henceforth be referred to as the 'MAGIC population', its progeny lines as 'MAGIC RILs' and its eight founders as 'MAGIC parents'.

2.2 Field Trial Design

At the heart of this thesis were two large-scale yield trials, conducted from 2014-16, designed to deliver the first ever evaluation of multiple traits throughout the whole crop cycle of a large eight-parent wheat RIL population, with all examined traits obtained non-destructively from plots large enough to provide a valid measure of combine yield. These field trials were conducted at University of Reading's Crop Research Unit, Sonning, UK (0°54' W, 51°29' N) where the soil type is a free-draining sandy loam overlying a gravel terrace in the field known as 'Gravelpit' and a free-draining deep sandy loam in a second field, known as 'Lamyard'.

For the 2014-15 season, the experiment comprised 783 MAGIC RILs, the 8 parents, and KWS Kielder (KWS UK Ltd.) and Skyfall as controls, all in duplicate for a total of 1584

plots in a parcel of the field known as 'Gravelpit'). The experiment was designed as a randomised complete block design using the Design of Experiments Website (DEW) software (http://www.expdesigns.co.uk) hosted by NIAB[1], comprised 2 main blocks (reps) and 16 sub-blocks (8 for each main block). For the 2015-16 season, a partially randomised incomplete block design was used to accommodate increased replication of control varieties as a means of quantifying spatial variation and consisted again of 2 blocks and 16 sub-blocks. The 2015-16 trial was located on the field known as 'Lamyard', consisted of 806 MAGIC lines, the 8 parents, and 16 replicates each of KWS Kielder and Skyfall (RAGT Seeds UK) as controls. The eight parents and 730 MEL lines were duplicated; due to lack of seed stock, only a single repetition was possible for 76 MEL lines used. All lines were randomly assigned within each rep, with one Kielder and one Skyfall in each sub-block. Field plans for both 2014-15 and 2015-16 trials, are included in the Appendix.

Both 2014-15 and 2015-16 field trials followed silage maize crops in rotation after which no farmyard manure was spread. The field was power harrowed after ploughing to a depth of 30cm. Seeds were drilled in 5.5 x 1.9m plots at 300 seeds/m^2, with a 2m discard between the ends of each plot as a buffer zone to reduce chances of contamination between lines. All plots were treated with a standard disease and nutrient regime. Weather was recorded in both seasons using an on-site weather station.

[1] www.expdesigns.co.uk is no longer available; equivalent designs to those reported here are readily generated using Genstat or packages available in R.

2.3 Phenotyping

2.3.1 Phenocart

For 2014-15 we constructed a proximal sensing cart similar to that described by White and Conley (2013). The initial designs were altered for our field dimensions and instrument requirements, with construction undertaken by Richard Casebow (Technical Manager, Crops Research Unit). Initially, this comprised a single arm where we could mount a high-resolution camera (Canon EOS 6D), triggered by remote, and a Red: Far Red sensor (Skye Instruments Ltd SKR 1800). Compared to previous testing with a monopod, the sensor cart allowed a much greater degree of repeatability and speed, with each image showing the same area within a few centimetres. This was later expanded for the 2015-16 field season to include an RTK GPS (Piksi), a Panasonic Toughbook CF-19, a deep-cycle battery with a pure sinewave inverter, and extra arms to allow further instruments to be added as needed. Pictures of the Phenocart can be seen below in Figure 2.1.

Figure 2-1 Panel A: Phenocart 2014-15 with Canon EOS 6D; Panel B: Phenocart 2015-16 with Canon EOS 6D, RTK GPS (Piksi), Panasonic Toughbook CF-19, deep-cycle battery and pure sinewave inverter.

2.3.2 Green Area Index

Images of the plots were captured throughout the growing seasons for the extraction of Green Area Index, henceforth referred to as GAI. We used the Canon EOS 6D camera at a fixed height, giving an image covering approximately 1.5m². As suggested in Physiological Breeding II (Pask *et al*., 2012), no zoom function was used, and care was taken to always approach the plots with the imaging arm pointing in a southerly direction with respect to the Phenocart body, in order to avoid shadows from the equipment appearing in the images where possible. Images were taken in RAW format with a resolution of 5472 x 3648 pixels for maximum data capture. For ease of analysis, the initial RAW images were converted to the JPEG format using Digital Photo Professional (Canon), a commercially available image editing software. These JPEG images were processed using 'PhenoHarvest', custom software that extracts the GAI from the images, based on measuring the percentage of green pixels in an image in contrast to the background of the image. This works on similar principles to Pask *et al* (2012), and BreedPix (Casadesús and Villegas, 2014). A representative subset of images before and after processing can be seen below in Figure 2.2. The software also allows for manual adjustment of the threshold for the 'greenness' of an image, which can be used to account for different lighting conditions and to remove any excess 'green' that may be in the background. The 'PhenoHarvest' software was written by Joel Potts and Samith Adhikari, undergraduate Computing Science students as part of their Undergraduate Research Opportunity Placements (UROPs), but the system specification, field testing, validation and use was conducted by myself as part of this thesis.

To verify this method and give an alternative assessment of canopy cover or "greenness", the Red: Far-Red (660:730nm) reflectance ratio of the plots was measured using the SKR 1800 (Skye Instruments Ltd, Llandrindod Wells, UK). These measurements were taken at four timepoints across the 2014-15 season, each taken within a day of the PhenoHarvest-derived GAI measurements. The R:FR was inverted (1/R:FR) to transform the data into a positive scale for better comparison with GAI. As shown below in Table 2.1, there is strong, significant ($p<0.05$), correlation between R:FR and the extracted GAI measurements at the closest overlapping timepoints (measured as days after sowing), and this correlation increases over time as the canopy closes.

	RFR 155	GAI 156	RFR 203	GAI 203	GAI 223	RFR 224	GAI 235	RFR 235
RFR 155	1							
GAI 156	0.42	1						
RFR 203	0.31	0.1	1					
GAI 203	0.22	0.03	0.74	1				
GAI 223	0.24	-0.05	0.81	0.69	1			
RFR 224	0.25	0	0.84	0.67	0.93	1		
GAI 235	0.21	-0.03	0.75	0.64	0.9	0.94	1	
RFR 235	0.19	-0.02	0.76	0.61	0.86	0.94	0.95	1

Table 2.1 Pearson's Correlation matrix of Red: Far Red (RFR) and Green Area Index (GAI). The time series measures of canopy cover are presented in chronological order with a three-digit suffix indicating the number of days after sowing when each measurement was t

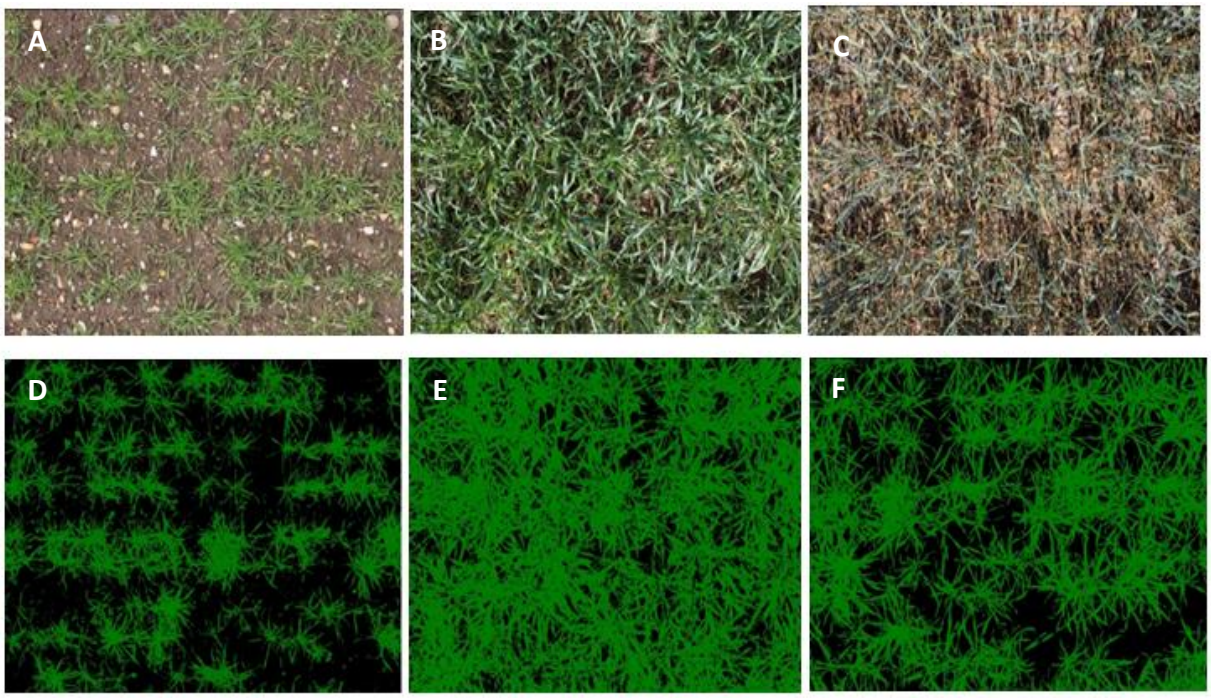

Figure 2-2 Subset of time series images before and after PhenoHarvest analysis. Panel A, B, C, D, E, F. A, B, C are RGB images taken on 2/4/15, 28/5/15 and 29/6/15 and respectively, D,E,F are the equivalent images after processing in PhenoHarvest to extract the percentage of green pixels, which is used as a proxy for GAI. Images represent approximately 1.5m x 1m area.

2.3.3 Height

Crop height was calculated for both years based on a mean value of three measurements using the rising plate method, in which a lightweight foam disk approximately 100cm in diameter is lowered onto the top of the crop until it settles, and then the height measured from that point (Sharrow, 1984). The measurements were taken pre-anthesis, at anthesis, at the end of grain filling, and at harvest maturity.

2.3.4 Growth Habit

In both seasons, growth habit was measured around G25-29 (Zadoks stages) following the scoring scheme shown in Figure 2.3.

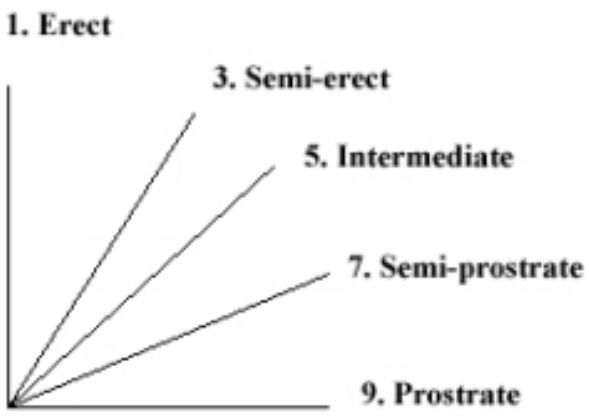

Figure 2-3 Angles for growth habit measurement. Reproduced from the CPVO Wheat Distinctness Uniformity and Stability Variety Testing guidelines (CPVO, 2009).

2.3.5 Anthesis

Anthesis was measured based on days after May 1st. This was measured as Zadoks stage 65 when over 50% of the ears in any given plot had over 75% of the anthers emerged. During the anthesis period, all plots at or near anthesis were assessed three times a week at a minimum. Where there was more than one person assessing, samples were cross-checked to ensure consistency of scoring where possible.

2.3.6 Multispectral profiling

During the 2014-15 field season, URSULA Agriculture Limited was contracted to conduct drone-based multispectral imaging of the field. This provided averaged per-plot Vegetation Index values, such as Normalised Difference Vegetation Index. Three flights were conducted across the growing season, on the May 1st, June 4th and June22nd. These dates were timed to coincide approximately with the onset of flag leaf emergence, the

peak GAI/booting, and anthesis. It was not possible to repeat this in the 2015-16 field season as the company had ceased operating.

2.3.7 Sink Traits

In both growing seasons, the individual plot sizes were manually measured before harvest, to allow for accurate calculations of the final yield. The moisture content was measured using a Harvest Master grain gauge (HM-1000), and final plot yields adjusted to a moisture content of 15%. TGW was calculated from approximately 200 seeds using an Elmor C3 seed counter (Elmor Ltd., Switzerland). Grain morphological traits were determined using digital image analysis, using the GrainScan software developed by Whan *et al* (2014), processing the same grains that were used for TGW. The Grains were scattered on a commercial flatbed scanner (HP Scanjet G2710) and scanned at a resolution of 300dpi, with no colour adjustment or cropping applied. As suggested by Whan *et al* (2014), a matt black box was upturned over the scanning surface to minimise reflection and shadows, maximising the contrast at the border of each seed.

2.3.8 Nitrogen Content

The nitrogen content of each sample was measured using Near-Infrared Reflectance Spectroscopy (NIRS). Grain samples were loaded into a FOSS NIRSystems 5000, which uses the 700-2500nm wavelength range. In order to create the calibration equation needed for NIRS, an initial 100 flour samples were dried for 72 hours, then analysed using a Leco Nitrogen analyser (model CHN628). A further 100 samples were added to encompass the extreme ends of the data range, and to fill any larger gaps in the 34

calibration curve for maximum accuracy. The final calibration equation had a correlation of 0.991 between the NIRS and Leco results.

2.3.9 Grain number m^{-2}

The number of grains m^{-2} acts as a summary of all events up to and a little beyond anthesis (Pask *et al*., 2012). The number of grains m^{-2} can be calculated using the equation:

$$Grains\ m^{-2}\ (GNO) = Yield\ (g\ m^{-2}) / TGW\ (g) \times 1000$$

2.4 Spatial Variation Modelling

In the first season (2014-15), it was noticed from the drone-based remote sensing data that there was significant spatial variability in the field experiment. Having looked at historical satellite imagery available via Google Earth during selection of the trial site, there was no prior evidence of such widespread variability. In Figure 2.4 of the URSULA aerial imagery below, the left-hand image showing Red-Green-Blue (RGB) imagery of the field with a large block appearing significantly greener than the surrounding areas. This is further highlighted in the right-hand image showing NDVI values across the field, with a significantly higher NDVI occurring in the areas appearing greener in the RGB imagery. Further URSULA imagery from alternative time series can be found in the appendix.

A level of variability was anticipated due to the large size of the experiment, with a large field area more likely to show significant variability in soil composition and hydrological features. However, the unusually low rainfall between March and June 2015 exacerbated the impact on crop growth of any variability in soil or drainage characteristics. We speculate that highly localised patches of high and low NDVI reflect

hitherto unmapped variation in the depth and distance from surface of the underlying gravel bed, causing the observed differences in water-retention ability and susceptibility to prolonged drought conditions.

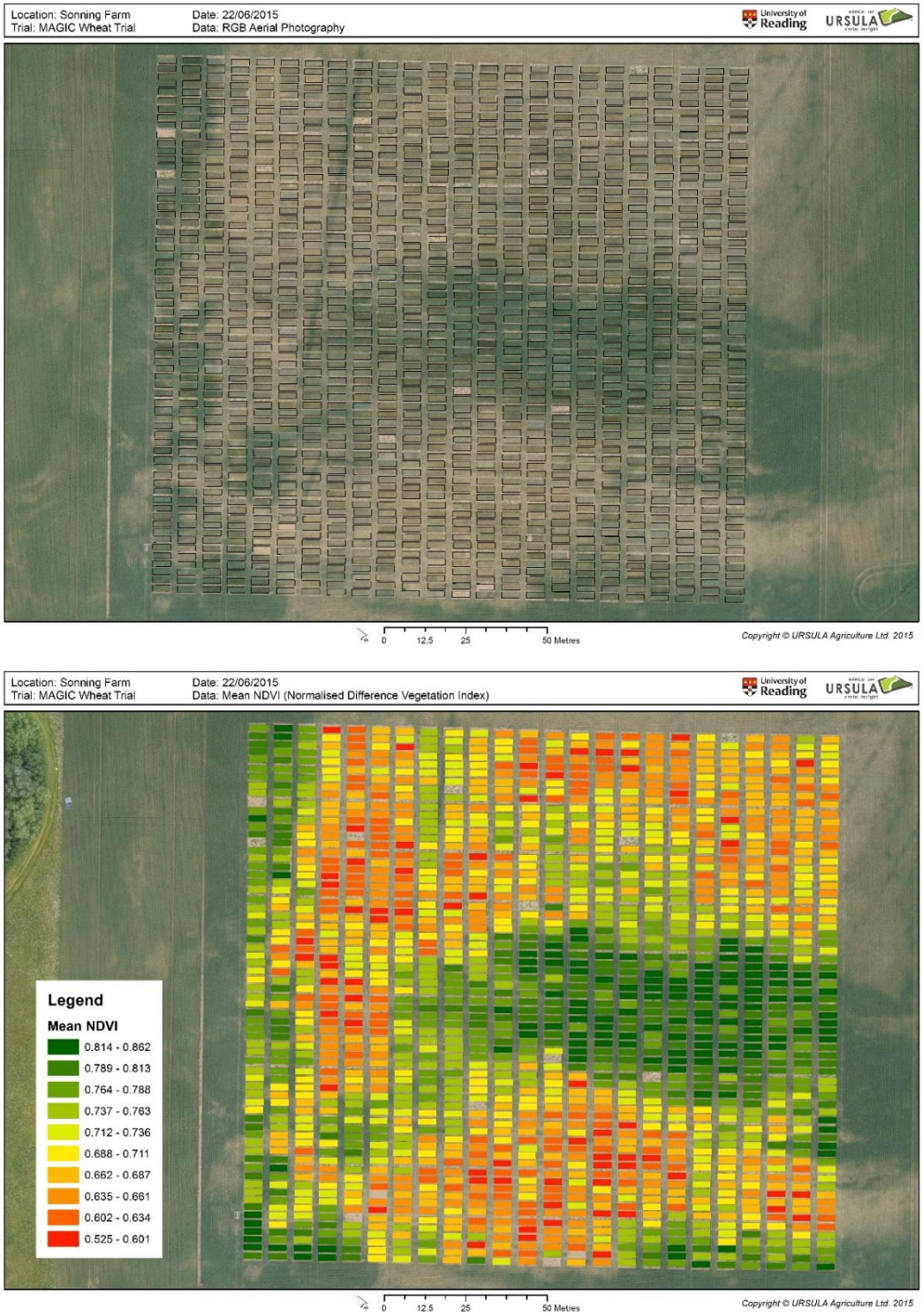

Figure 2-4 Panel A: Composite RGB image of RGB aerial imagery on 22/6/2015. Panel B: Composite false-colour NDVI image of aerial imagery on 22/6/2015.

Whatever the cause, such profoundly spatially structured patterns of variability were likely to significantly obscure the relative ranking of genotypes, given that the largest 'high NDVI' patch inconveniently straddled one end of at least six of the eight blocks, unless a bespoke approach to modelling the spatial variation was taken. In conjunction with Sam Dumble of the University of Reading Statistical Advisory Service, two models to compensate for the spatial variability were initially proposed, both of which are based in the INLA package for R (http://www.math.ntnu.no/inla/R/stable). Custom shapefiles were created for each phenotype using the QGIS software (http://qgis.osgeo.org), consisting of a 66 x 24 plot field matrix, where missing data has been removed. This step is necessary as both models would class missing data as a 0, affecting the surrounding data during modelling. Once the data and shapefile were loaded into R, the INLA package utilises a bayesian inference, continuous auto-regressive model based on the dual replication in the field and the unmodelled data surrounding each data point, with the resulting data then exported from R as BLUPs (*best linear unbiased prediction).* Spatial Model 1 makes the assumption that the genotype replicates should be identical if all underlying biotic and abiotic factors are the same. Spatial Model 2 does not assume this, with every plot being treated as an individual. Looking below at Figure 2.5 shows side-by-side heatmaps of the raw and modelled data. Both models appear to be successful in erasing visibly discernible spatial patterns. Looking at how the modelling affects the distribution of the data, as shown in Figure 2.5, Spatial Model 1 maintains a similar range and dispersion of genotypic means around the population mean, whilst Spatial Model 2 appears to pull all the values closer to the mean (~0.4), rather than effectively adjusting values to take into account the high local bias, while preserving the genotypic range.

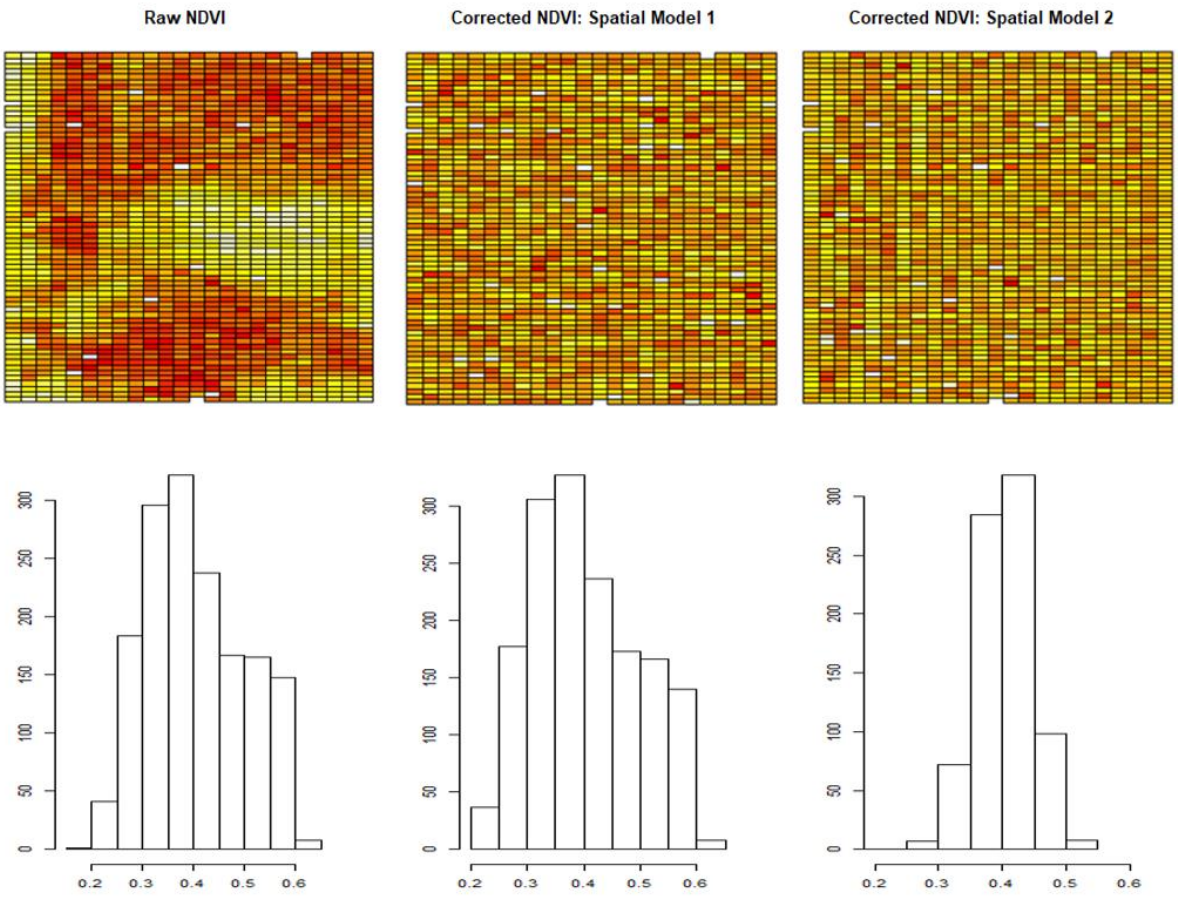

Figure 2-5 Panels A, B and C: heatmaps of NDVI data, Raw NDVI, Corrected NDVI - Spatial Model 1 and Corrected NDVI - Spatial Model 2 respectively. Panels D, E and F: NDVI data distribution, Raw NDVI, Corrected NDVI - Spatial Model 1 and Corrected NDVI - Spatial Model 2 respectively.

To discern how the different models affected QTL analysis, anthesis data for the raw and processed data was run in R/qtl. Anthesis was chosen as a model trait here because it is highly heritable, and of somewhat known genetic architecture. With one of the eight MAGIC parents (Soissons) carrying the photoperiod insensitivity allele *Ppd-D1a,* we would have expected to find a major effect QTL at the *Ppd-D1* locus on the short arm of chromosome 2D. If the spatially modelled data is effective in bringing the raw plot values closer to the true genetic mean, it is expected that the genetic signal to noise ratio will increase, and consequentially the apparent strength of the *Ppd* QTL will increase.

The resulting QTL scans for anthesis can be seen below in Figure 2.6. As expected in the raw data, *Ppd* can be clearly seen on chromosome 2D, with a LOD score in excess of 8. Application of Spatial Model 1 leads to a clear increase in the significance of the *Ppd-D1* signal, with a LOD score around 18. Spatial Model 2 appears to have completely removed the ability to detect the expected *Ppd-D1* on chromosome 2D. It is therefore likely that this second model is overcorrecting for the spatial variability and in effect spuriously reducing the genetic variation of the population. On the grounds that Spatial Model 1 was: 1. effective in removing discernible spatial patterns, whilst 2. preserving a pattern of dispersion of genotype means around the population mean and 3. increasing the signal-to-noise ratio for a well understood trait, we adopted Spatial Model 1 and implemented it to calculate BLUPs for all traits being analysed.

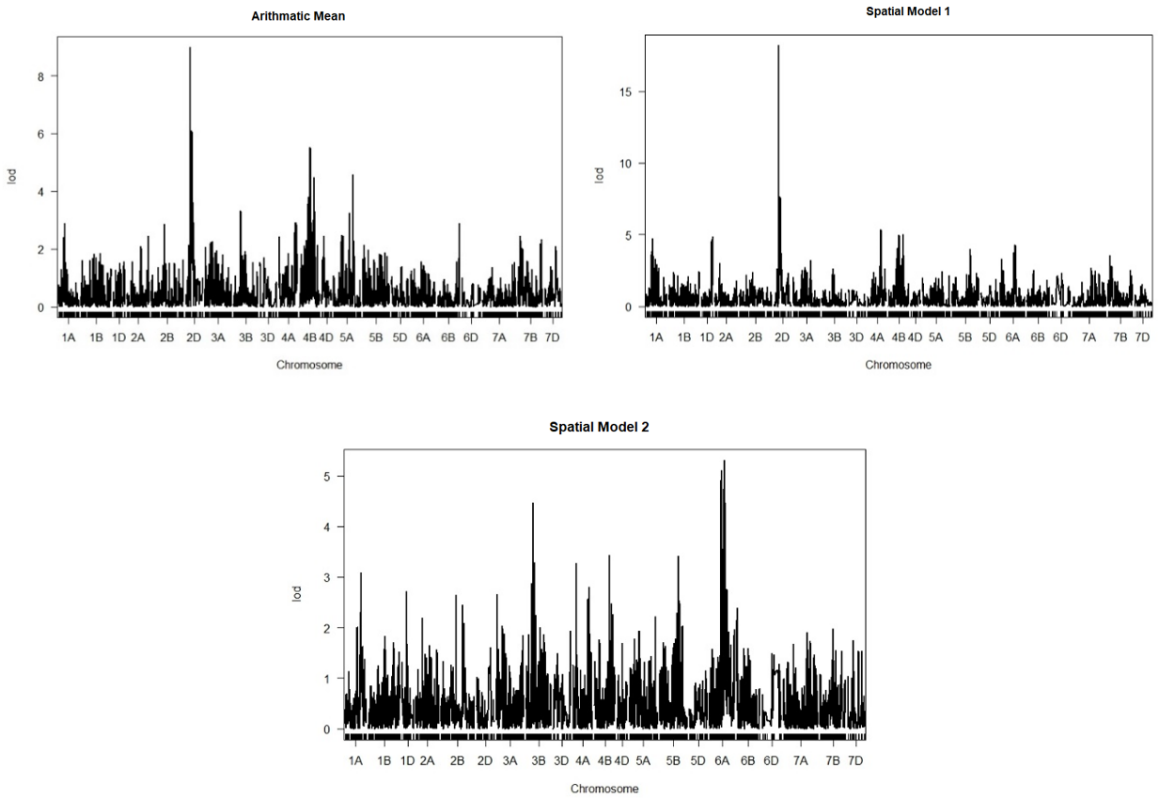

Figure 2-6 Comparison of date of anthesis (Zadoks 65) QTLs for raw and modelled data. Strength of the QTL is measured on the y-axis as LOD (Logarithm of Odds), x-axis represents the location of the QTL on each chromosome.

2.5 Genotyping

The lines were genotyped using the 90k array (Illumina Infinium iSelect, www.illumina.com - described by Wang *et al* (2014)), by Mackay *et al* (2014). 20,639 SNP markers were scorable and polymorphic, of which 18,601 were mapped in the MAGIC population (Gardner *et al*., 2016; Mackay *et al*., 2014). A comprehensive genetic linkage map for the population was reported by Gardner *et al* (2016)- the first such map for an eight-parent MAGIC population in wheat.

This map contains 4578 unique marker sites, averaging four markers per site. To simplify the genetic analysis and reduce the computational power required, the full 20,639-strong marker set was filtered and reduced by removing all but one marker from marker groups showing perfect correlation. The resulting map contained 3535 markers (Figure 2.8). In the Gardner *et al* (2016) map, around 37%, 50% and 13% of markers were mapped to the A, B and D genomes respectively. In the UoR skimmed marker set, this became around 44%, 47% and 9%. We can see that the sub-genomes with higher marker density have lost relatively more markers as a result of the filtering; however, the percentage of markers on each genome after processing are now closer to the percentages of unique marker sites reported by Gardner *et al* (2015): 41%, 47% and 12%. Where there are apparently large gaps spanning <10cM, largely on the D-genome, this is due to the well-documented lack of sequence diversity/polymorphism on the cultivated hexaploid D-genome rather than an effect of the skimming procedure.

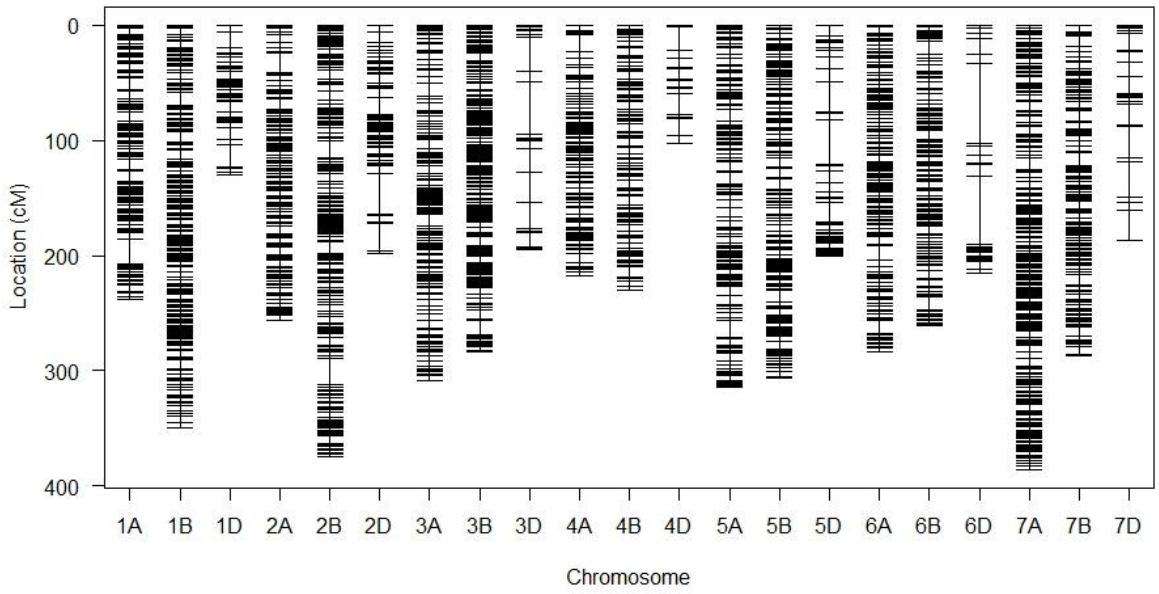

Figure 2-7 Genetic map distribution of the 'UoR skimmed marker set'. The 21 wheat chromosomes are laid out horizontally with A, B and D genome homoeologous chromosome grouped together.

2.6 Genetic Analysis

All genetic analysis was conducted in R, using the mpMap package (Huang *et al* 2011); a package specifically designed for the analysis of multi-parent populations. The genetic map was uploaded along with marker data, phenotypic data and a pedigree matrix (provided by Lukas Wittern (NIAB/University of Cambridge/Bayer CropScience) and Keith Gardner (NIAB)), which allows IBD (Identity By Descent) to be calculated for use in Composite Interval Mapping (CIM), (Zeng 1994). CIM allows for systematic inclusion of covariates in the analysis, taking into account the effects of a selected number of associated markers in the genome as surrogates for QTL.

2.6.1 Significance thresholds in QTL mapping.

Multiple methods have been proposed to set an appropriate level of significance for mapping QTL. Botstein and Lander (1989) suggested a cumulative distribution of the

LOD score, whereas Churchill and Doerge (1994) estimated the threshold for declaring QTL based on permutation testing.

For the purpose of this thesis, QTL were identified applying a threshold of 10^{-3}. While slightly lower than used in experiments such as Camargo *et al* (2016) (threshold = 10^{-4}), a lower threshold was deemed appropriate for the detection of more smaller, more subtle QTL effects for complex integrative traits.

2.6.2 QTL naming convention

All QTL were named following the Graingenes annotation (www.graingenes.org/). Briefly, the first letter has to be a "Q" to indicate it is a QTL, then follows a trait code, a period, the laboratory designator, a hyphen ("-") and the chromosome name. If there is more than one QTL for the same trait on the same chromosome, you designate each of them with numbers after the chromosome name. To differentiate between our experiments, we also added a year code, for a final format of: Q.< 3-letter trait abbreviation> - <Year in YYYY format> . <3 letter site abbreviation> - <chromosome> . <integer to make multiple QTL on same chromosome unique>.

2.6.3 Multiple peaks

In total, 245 QTLs were found over the all sink and source traits. In several cases, two or more QTL peaks for the same trait measured in different years were identified within a small map distance of each other. These multiple peaks are either real, distinct QTL that are situated in close proximity, or they could represent the same underlying QTL but where peak position for a given trait is assigned to adjacent intervals in different years because of the inherent noisiness of field phenotype data and the hidden influence of linked, environment-specific effects. Increasing the interval discovery window around

each QTL within the R/mpmap software suppressed a number of spurious 'independent' QTL; the evidence supporting this is that the final interval discovery window of 100cM used brought the sum of phenotypic variability explained close to the level predicted by the fitted model. This method worked well on individual years, however a manual approach involving application of several additional criteria was used when comparing between different analyses in order to discern if QTLs detected in different years should actually be interpreted as pleiotropic rather than linked. When combined with covariate analysis, this allows QTLs in close proximity to be detected while removing multiple peaks for the same QTL. This method worked well on individual years, however a manual approach was used when comparing between different analyses in order to discern if QTLs were the same between years.

2.7 Statistical Analysis

All descriptive statistics (mean, variance, standard error, distribution) and statistical tests (t-test, ANOVA, Pearson's product moment correlation) were carried out in R 3.3.3 (R Core Team, 2017). Broad sense heritability of phenotype data was defined as:

$$H^2 = \frac{\sigma^2 G}{\sigma^2 P}$$

Where H^2 is the broad sense heritability, $\sigma^2 G$ is the genotypic variance and $\sigma^2 P$ is the total phenotypic variance.

3. Genetic analysis of 'sink' traits in the elite wheat MAGIC population

3.1 Introduction

3.1.1 'Sink' trait definition

The genetic yield potential of wheat has been defined as the yield of a cultivar when grown in the environment to which it is adapted, with nutrients and water non-limiting and with pests, diseases, weeds, lodging, and other stresses effectively controlled (Evans and Fisher, 1999). When broken down into its component parts, yield per unit area is the product of the number of grains per ear, the grain dry mass, and the ear density, the latter in turn being a function of both plant population density and tillering. As the harvested organ, the grain is referred to as the 'sink' and the degree of remobilization of photoassimilates from the leaf canopy (i.e. the 'source') to the grain is referred to as 'sink strength'. Chapter 4 presents an analysis of 'source' traits and Chapter 5 will deal with achieving balance between source and sink. In this Chapter, genetic variation for yield components associated with the sink are treated as potential traits to ensure that sink strength is not limiting yield.

3.1.2 Tillering

After a number of weeks following germination and establishment of a primary root system and unfurling of leaves on the main shoot, a major parameter in determining the wheat plant's yield potential is the number of side shoots or tillers that it produces. In a typical season, the tillering stages, denoted in the Zadoks decimal growth stage system as GS20-30, will run from around the beginning December to the end of March

(AHDB, Wheat Growth Guide 2018). Thus, the ability to establish multiple tillers with fertile spikelets is fixed relatively early in development and is improved by early vigour via increased biomass and water use efficiency (López-Castañeda and Richards, 1994). Although a potentially interesting trait, we did not have a sufficiently accurate, high throughput system to measure tiller number and genetic dissection of tillering lies outside the scope of this thesis.

3.1.3 Grain number per ear

Once the final number of fertile tillers has been established, by the onset of stem elongation (GS31), all further potential for yield gain rests on the number and size of grains that can develop on a set number of ears per unit area. The ear itself has a complex nested branching structure consisting of a main branch (the rachis) carrying parallel rows of spikelets, each of which may bear between 2 and 5 grains. Plant dwarfing genes, the *Rht* group*,* have been attributed with the increase in the numbers of grain per ear (Ma *et al*., 2015). As well as reducing the plant height, *Rht* had a pleiotropic effect that increased the number of seeds per spikelet, rather than the number of spikelets per ear, when compared to non-dwarf plants (Youssefian *et al*., 1992). Again, although the optimisation of ear architecture is an active area of research, high throughput phenotyping of ear architecture was not possible in these large field trials and thus the further focus of this Chapter will be on grain size-related traits.

3.1.3 Grain size and shape

While the notion of a developing grain as a steadily expanding balloon has intuitive appeal, in reality grain filling is the result of a complex chain of overlapping processes which impact grain dimensions differently at different times. Grain length is the first

grain dimension to reach a maximum (Xie *et al*., 2015) and is relatively stable across more sensitive to environmental fluctuations and relies partly on the remobilisation of photosynthate during senescence. Experiments by Gebbing & Schnyder (1999) showed that remobilisation during senescence can account for 10-20% of final grain mass, or a higher proportion in stressed conditions (Foulkes *et al*., 2002).

3.1.4 Genetic variability in sink traits

It is well established that in wheat, grain numbers can have high levels of variability depending on the environment. Generally, this instability has not stopped grain number being a viable target in breeding programmes and has significantly contributed to yield increases in modern cultivars (Griffiths *et al*., 2015). In contrast, grain weight has repeatedly been shown to be more stable and has a higher heritability than grain number and yield itself (Giura and Saulescu, 1996; Kuchel *et al*., 2007). Despite grain number being the more prominent yield component; grain shape, size and density are connected directly to the economic value of wheat in the UK, as they impact the milling quality and flour yield (Gegas *et al*., 2010), with larger grains increasing flour yield.

Previous QTL and association analyses have identified QTL for grain size, shape and weight on almost every chromosome (Bogard *et al*., 2011; Bonneau *et al*., 2013; Farré *et al*., 2016; Gegas *et al*., 2010; Griffiths *et al*., 2015; Kuchel *et al*., 2007; Kumar *et al*., 2016; Simmonds *et al*., 2014; Williams and Sorrells, 2014; Xie *et al*., 2015), with stable QTL being identified on 2A (Wu *et al*., 2015); 2D (Breseghello and Sorrells, 2007); 4A (Echeverry-Solarte *et al*., 2015); 5A (Brinton *et al*., 2017; Wu *et al*., 2015); and 6A (Simmonds *et al*., 2014; Zhang *et al*., 2013).

3.1.5 Aim of this study

All the results referred to above were obtained based on analyses using biparental RIL or doubled haploid (DH) populations. Therefore, only a limited range of allelic variation was explored in each population and opportunities to detect interactions between loci was limited. My aim, in this chapter, was to conduct a thorough genetic analysis of sink-related traits in a large elite wheat eight-parent population, offering more allelic diversity and more power to detect both small effects and interactions between loci than any previous study. To date, the only instance of use of the elite wheat 8-parent MAGIC population for the genetic dissection of 'sink' traits has been a PhD thesis by Dr H. Benbow, where two experimental populations (Avalon x Cadenza and MAGIC) were utilised for the analysis of grain related traits. The combination of these populations allowed for QTL previously identified in AxC to be refined to a smaller marker interval, as well as identifying potentially novel QTL. The study used QTL mapping on AxC and GWAS on the MAGIC population, identifying regions of interest on 3D, 4B, 4D, 5A, 5B and 6A.

The aims of the work presented in this chapter are as follows:

- Estimate the heritability of traits relating to grain size and weight.
- Find out which grain weight and grain size parameters were best correlated to yield.
- Differentiate between environmentally responsive and environmentally independent QTL governing grain size and weight.
- Assess the significance of co-location of QTL governing different sink traits and yield.

3.2 Results

3.2.1 Phenotypic variation and Correlation analysis

The traits analysed in this chapter are the Grain Yield (GY), measured in tonnes per hectare; Thousand Grain Weight (TGW), the dry weight of 1000 threshed grains; Grain Length (GL) and Grain Width (GW), both measured in mm; Grain Area (GA), measured in mm^2; Length-Width Ratio (LWR); Nitrogen (N), measured as a percentage of dry weight, and Factor Form Density (FFD), a measurement of deviation from the cylindrical form.

The mean, variance, S.E., range and broad sense heritability were calculated for eight traits, spatially corrected and averaged over two years (harvest years 2015 & 2016) and are displayed in Table 3.1.

		Mean		Variance		S.E		Min		Max		Range		H^2
Trait		Parents	Progeny	Parents	Progeny	Parents	Progeny	Parents	Progeny	Parents	Progeny	Parents	Progeny	
Grain Yield	Yld	8.29	8.26	0.09	0.21	0.10	0.02	7.92	6.52	8.84	9.74	0.92	3.22	0.26
Thousand Grain Weight	TGW	38.82	38.55	2.19	9.68	0.52	0.11	36.71	28.73	41.13	48.47	4.43	19.74	0.51
Grain Width	GW	3.38	3.33	0.004	0.007	0.022	0.003	3.30	3.046	3.50	3.574	0.20	0.53	0.54
Grain Length	GL	6.91	6.82	0.03	0.05	0.10	0.01	6.65	6.16	7.20	7.69	0.55	1.53	0.74
Grain Area	GA	18.32	17.82	0.41	0.51	0.23	0.02	17.64	15.63	19.41	20.52	1.77	4.89	0.73
Nitrogen Concentration	Ntr	2.75	2.75	0.004	0.011	0.024	0.004	2.606	2.371	2.82	3.13	0.21	0.76	0.16
Length-Width Ratio	LWR	2.04	2.05	0.003	0.007	0.021	0.003	1.977	1.796	2.13	2.38	0.15	0.58	0.56
Factor Form Density	FFD	1.67E-03	1.70E-03	2.27E-09	7.59E-09	1.68E-05	3.02E-06	1.60E-03	1.37E-03	1.73E-03	2.02E-03	1.23E-04	6.46E-04	0.39

Table 3.1 - Sink traits - descriptive statistics for Parents and Progeny. S.E. – Standard Error, H2 – broad sense heritability

Using the Shapiro-Wilk test for normality, five of the eight quantitative traits could be considered normally distributed, with grain nitrogen, yield and L/W ratio deviating significantly from normality as can be seen from the density plots in Figure 3.1. However, when using large sample sizes such as these, even a small deviation from the normal will test as significant (Öztuna *et al*., 2006). From a visual inspection, yield and nitrogen appear to be normally distributed, and L/W Ratio has a skewed distribution. In this population, the phenotypic range of the progeny greatly exceeded the range of the

parental lines indicating transgressive segregation; this is clear from the density plots shown in Figure 3.1. The most heritable traits were GL, GW, GA, LWR and TGW with heritabilities between 0.51 and 0.74, which leads us to expect strong genetic signals for these traits. The least heritable traits were grain nitrogen and grain yield, with scores of 0.16 and 0.26 respectively. These low heritabilities reflect the complexity of these highly integrative traits.

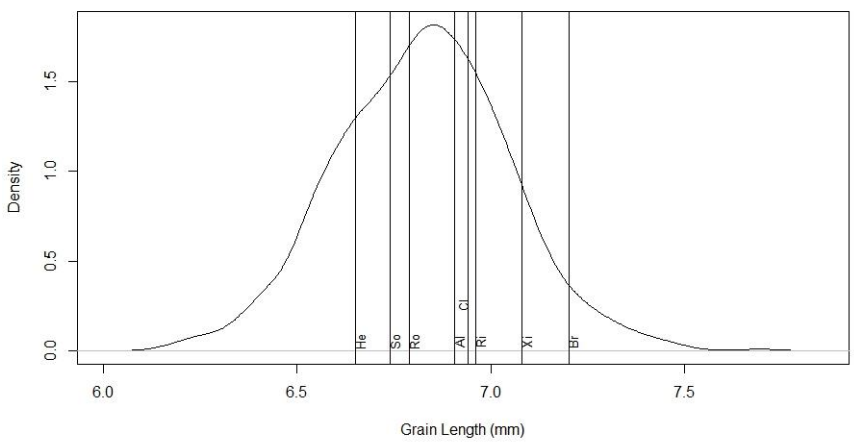
Density
Grain Length (mm)
He
So
Ro
Al
Cl
Ri
Xi
Br

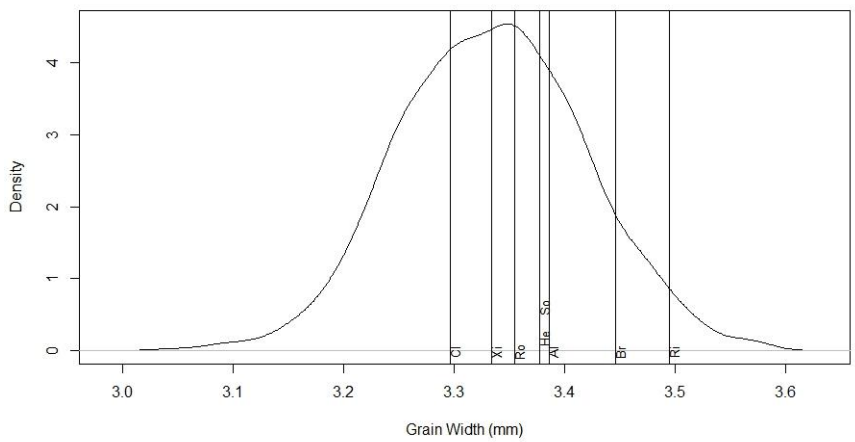
Density
Grain Width (mm)
Cl
Xi
Ro
He
So
Al
Br
Ri

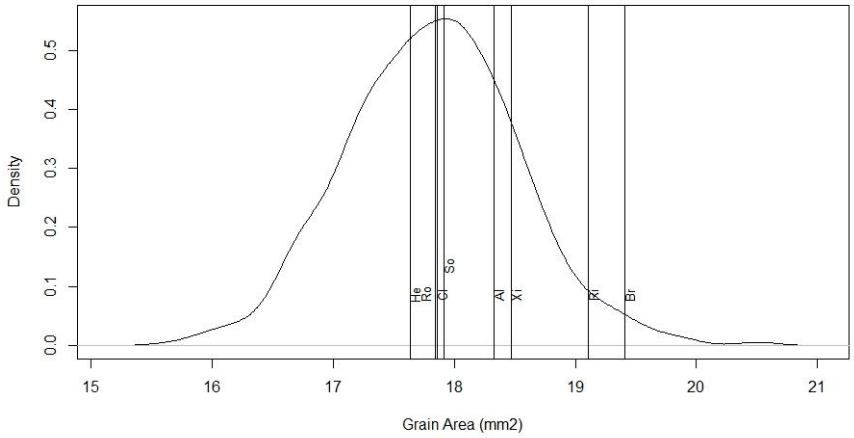
Density
Grain Area (mm2)
He
Ro
Cl
So
Al
Xi
Ri
Br

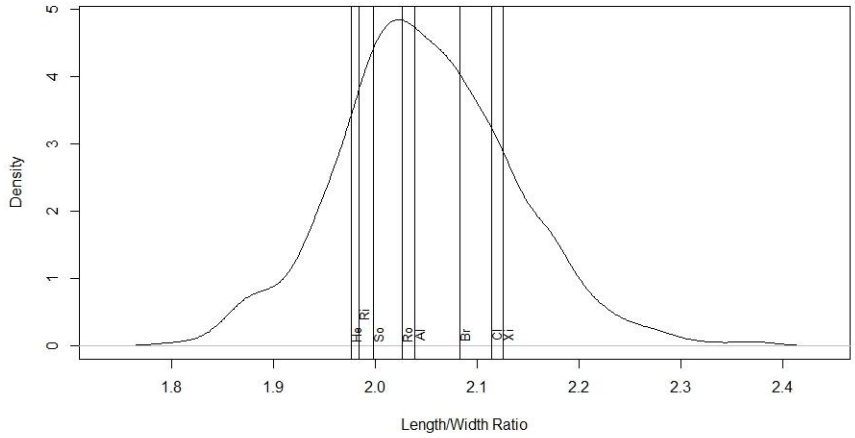
Density
Length/Width Ratio
He
Ri
So
Ro
Al
Br
Cl
Xi

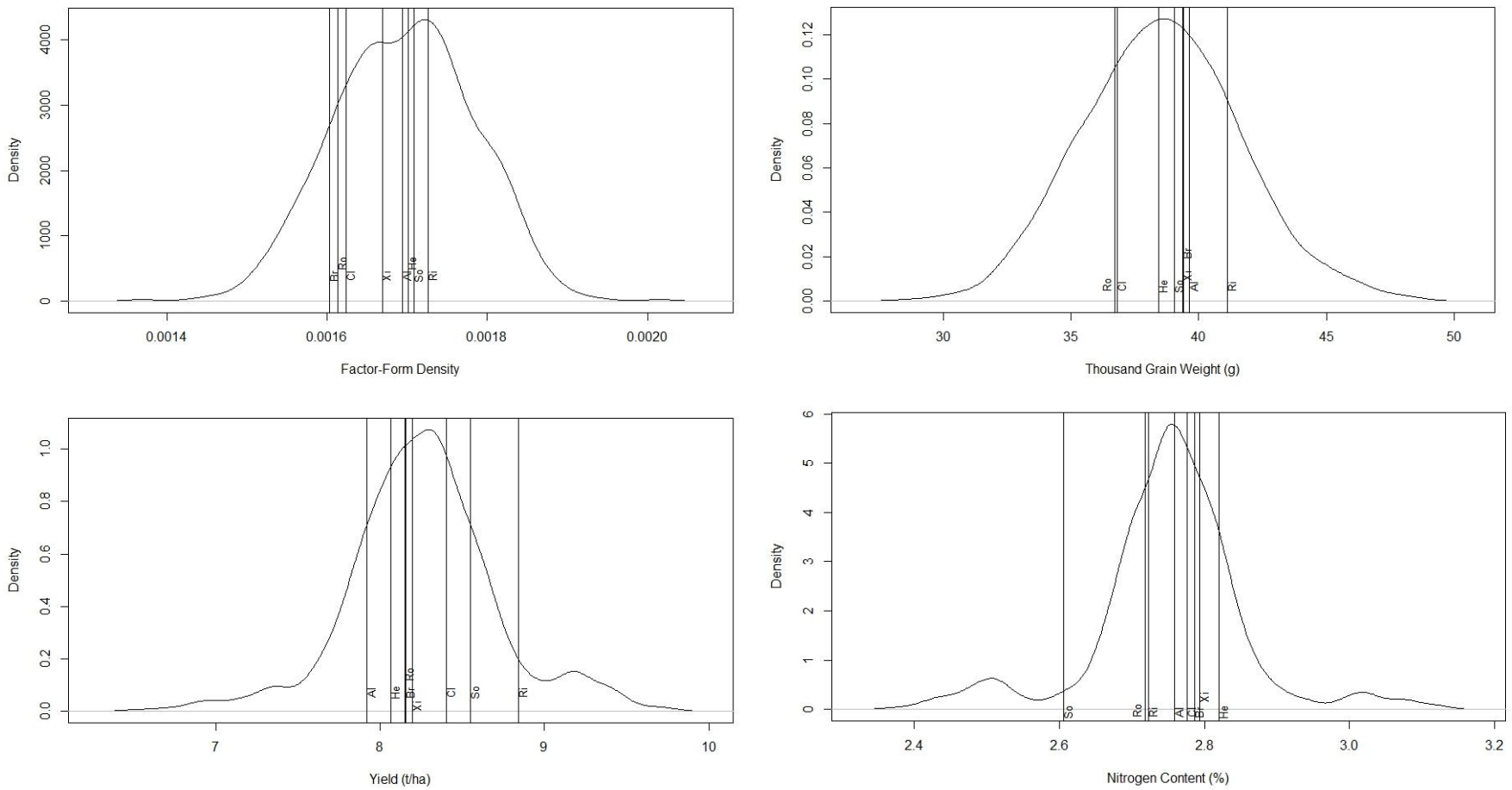

Figure 3-1 Density plots of trait data for MAGIC population. Parental values are displayed as vertical bars on the plots with two-letter codes denoting the parent cultivar as follows: Al – 'Alchemy'; Br – 'Brompton'; Cl – 'Claire'; He – 'Hereward'; Ri – 'Rialto'; Ro – 'Robigus'; So – 'Soissons'; Xi – 'Xi19'.

Of the morphological grain traits (TGW, GA, GL, GW and FFD), all were strongly correlated with themselves between years (PCC= 0.52 to 0.78, $p < 0.05$). This reflects previous research suggesting that grain morphology and weight is relatively stable across environments compared to yield (PCC= 0.11 between years).

TGW was strongly correlated with GW in both years (PCC= 0.78 and 0.87 respectively), but only moderately with GL (PCC= 0.23 and 0.38). Yield is moderately but consistently correlated with GL (PCC= 0.27 and 0.19), which is greater than yield correlations with both GW (PCC= -0.09 and 0.21) and TGW (PCC= -0.04 and 0.30). In 2015-16, both GW and TGW have more effect on the yield than GL, however in 2014-15, it appears that the opposite is true, and the yield:GL correlation is generally more consistent across environments. This is likely due to the grain length being the first morphometric measurement reaching its maximum before anthesis. Grain width is more environmentally dependant, relying on source capacity and resource remobilisation to reach its maximum, which is hindered in stressed conditions as senescence is accelerated, giving a shorter grain filling period. This in turn affects TGW, which is much more highly correlated with GW than GL. (Figure 3.2).

The impact of weather will be looked at in detail in Chapter 4.

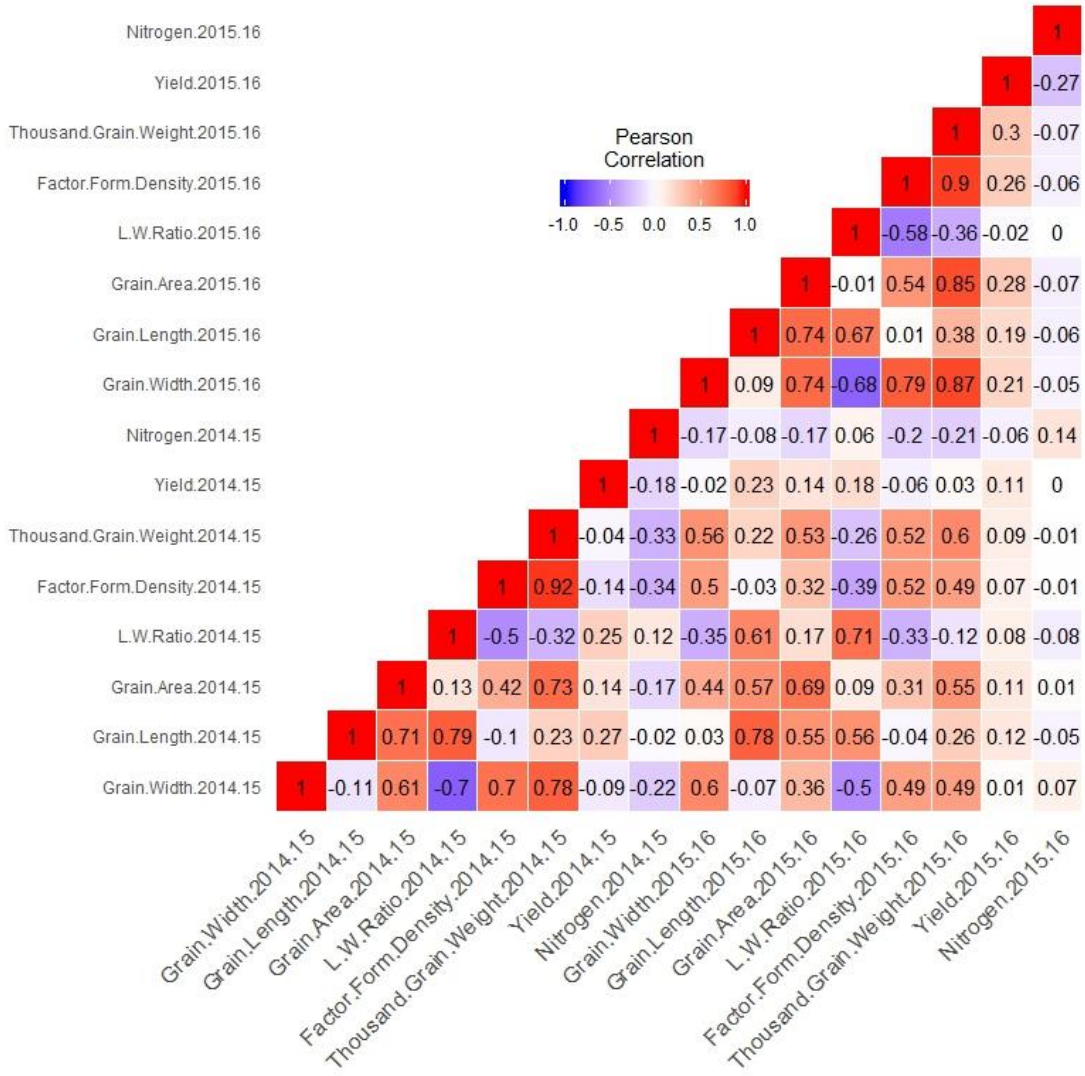

Figure 3-2 Pearson's correlation coefficients for five sink traits and yield in each of two seasons, 2014-15 and 2015-16. Increasingly negative correlations highlighted in deepening shades of blue; size of positive correlations is indicated by the depth of shade of red highlighting.

3.2.2 Mapping Quantitative Trait Loci for 'sink' traits

In total, 155 significant, non-redundant QTL were discovered for the eight studied 'sink' traits (see Chapter 2 for details of significance criteria and methodology for determining redundancy between QTL). These are shown in Table 3.2.

3.2.2.1 Thousand Grain Weight

A total of 28 significant (-log10p ≥ 3) QTL for Thousand Grain Weight (TGW) were found on chromosomes 1B, 2A, 2D, 3B, 4A, 4B, 4D, 5A, 5B, 5D and 6A (Table 3.2).

These QTL explain approximately one third of the total variation in TGW, both in 2015 and 2016 or in the across-seasons analysis. Approximately half of the variation explained by the QTL are accounted for by the two strongest QTL: *Q.TGW-2016.UoR-6A* (*p*= 9.96E-14, %var= 6.97 - 9.95); *Q.TGW-2016.UoR-4D* (*p*= 1.23E-11, %var= 4.65 - 7.6), expressed in both years and detected in identical locations in all analyses. *Q.TGW-2015.UoR-4B* (52.17 - 52.67cM), *Q.TGW-2016.UoR-4B* (54.7 - 55.2 cM) and the meta-QTL: *Q.TGW-ME.UoR-4B* (50.16 - 51.16 cM) were all highly significant (P value e-10 to e-17) and explained 3 to 3.7% variation and are likely be a single QTL, based on the magnitude and direction of the parental effect. The remaining 19 QTL were either year-specific or detected only in the across-season analysis. Smaller effects together explained the year-specific component of variation, the strongest of these being *Q.TGW-2015.UoR-7A* (254.13 - 254.63cM) which explained 3.01% of the variation and P value of 3.06E-07.

Percentage of phenotypic variation explained

QTL Name	Chromosome	Left Marker	Right Marker	QTL Position	Left Marker Position	Right Marker Position	pvalue	-log10p	Grain Length 2015	Grain Length 2016	Grain Length ME	Grain Width 2015	Grain Width 2016	Grain Width ME	Grain Area 2015	Grain Area 2016	Grain Area ME	Form Factor Density 2015	Form Factor Density 2016	Form Factor Density ME	Thousand Grain Weight 2015	Thousand Grain Weight 2016	Thousand Grain Weight ME	Grain Yield 2015	Grain Yield 2016	Grain Yield ME	Grain Nitrogen 2015	Grain Nitrogen 2016	Grain Nitrogen ME
Q.GA-ME.UoR-1B.1	1B	RAC875_rep_c109416_191	Tdurum_contig42633_1282	69.6	59.06	69.60	1.37E-05	4.86									4.1												
Q.GL-2015.UoR-1B.1	1B	RAC875_rep_c109416_191	Tdurum_contig42633_1282	69.6	59.06	69.60	2.32E-06	5.63	3.09																				
Q.GL-ME.UoR-1B.1	1B	RAC875_rep_c109416_191	Tdurum_contig42633_1282	69.6	59.06	69.60	9.44E-11	10.03			5.16																		
Q.GL-2016.UoR-1B.1	1B	RAC875_rep_c109416_191	Tdurum_contig42633_1282	69.6	59.06	69.60	5.34E-11	10.27		5.7																			
Q.GA-2016.UoR-1B.1	1B	wsnp_BE443531B_Ta_1_1	Ku_c11813_215	81.49	78.69	81.49	3.09E-10	9.51								5.63													
Q.TGW-2015.UoR-1B	1B	BS00073034_51	BS00022648_51	87.03	86.53	87.03	5.68E-05	4.25													3.59								
Q.GA-2016.UoR-1B.2	1B	BobWhite_c9881_1312	BS00074911_51	256.45	255.95	256.45	7.16E-06	5.15								3.31													
Q.GL-2015.UoR-1B.2	1B	BS00068327_51	BobWhite_c2844_569	268.54	267.04	268.54	6.88E-05	4.16	5.07																				
Q.GL-2016.UoR-1B.2	1B	RFL_Contig1823_1044	Tdurum_contig50988_500	276.38	276.38	276.88	2.53E-08	7.60		7.03																			
Q.GL-ME.UoR-1B.2	1B	RFL_Contig1823_1044	Tdurum_contig50988_500	276.38	276.38	276.88	2.06E-08	7.69			6.53																		
Q.GA-ME.UoR-1B.2	1B	RFL_Contig1823_1044	Tdurum_contig50988_500	276.88	276.38	276.88	2.91E-04	3.54									3.59												
Q.GW-2015.UoR-1D	1D	CAP8_c2401_433	D_GB5Y7FA02I369B_378	27.31	25.79	27.31	7.56E-04	3.12				0.82																	
Q.GL-ME.UoR-1D	1D	D_contig13475_402	wsnp_Ex_c12012_19240904	39.65	39.65	47.46	1.11E-04	3.95			1.31																		
Q.GW-ME.UoR-1D	1D	Kukri_rep_c112609_711	BobWhite_rep_c65565_359	61.08	59.07	61.08	1.43E-04	3.84						2															
Q.GW-2016.UoR-1D	1D	Kukri_rep_c112609_711	BobWhite_rep_c65565_359	61.08	59.07	61.08	1.00E-06	6.00					2.33																
Q.GL-2015.UoR-2A	2A	wsnp_JD_rep_c48914_33168544	RAC875_c17787_274	88.03	88.03	90.07	9.98E-07	6.00	3.79																				
Q.Yld-2016.UoR-2A	2A	Kukri_rep_c90581_382	Excalibur_c4847_631	102.38	102.38	103.90	7.75E-05	4.11																	1.83				
Q.GA-ME.UoR-2A	2A	Kukri_c45015_145	Tdurum_contig27887_55	109.94	109.94	111.95	3.30E-07	6.48									2.63												
Q.FFD-2016.UoR-2A	2A	BS00089457_51	RAC875_rep_c119471_174	115.52	112.46	115.52	9.14E-06	5.04											3.61										
Q.TGW-2016.UoR-2A	2A	BS00089457_51	RAC875_rep_c119471_174	115.52	112.46	115.52	3.37E-07	6.47														3.53							
Q.GA-2016.UoR-2A	2A	BS00045521_51	BS00083727_51	124.61	124.61	125.62	5.87E-08	7.23								0.96													
Q.GA-2015.UoR-2A	2A	BS00083727_51	RAC875_c15213_1942	125.62	125.62	127.63	3.71E-08	7.43							3.55														
Q.GL-2016.UoR-2A	2A	BS00040337_51	BS00062757_51	134.69	134.19	134.69	5.14E-06	5.29		1.57																			
Q.GL-ME.UoR-2A	2A	BS00040337_51	BS00062757_51	134.69	134.19	134.69	2.79E-08	7.55			2.28																		
Q.TGW-ME.UoR-2A	2A	BS00062757_51	BobWhite_c28819_733	135.19	134.69	135.19	3.72E-07	6.43															1.71						
Q.Yld-ME.UoR-2A	2A	Kukri_c24064_2095	BS00041816_51	140.76	140.76	141.26	1.81E-06	5.74																		3.74			
Q.FFD-ME.UoR-2A	2A	Kukri_c24064_2095	BS00041816_51	141.26	140.76	141.26	2.34E-05	4.63												2.42									
Q.TGW-2015.UoR-2A	2A	Ku_c5710_310	BS00022896_51	142.77	141.26	142.77	3.53E-05	4.45													1.04								
Q.Yld-ME.UoR-2B	2B	BS00067962_51	BS00110490_51	116.01	100.99	116.01	6.89E-04	3.16																		1.97			
Q.GA-2016.UoR-2B	2B	BS00075410_51	Jagger_c9472_305	174.88	174.38	174.88	1.20E-04	3.92								1.11													
Q.GA-ME.UoR-2B	2B	BS00072689_51	BS00039488_51	199.82	198.81	199.82	2.29E-04	3.64									1.47												
Q.Yld-2016.UoR-2B	2B	BobWhite_c22728_78	BS00022805_51	271.92	271.92	279.38	1.13E-04	3.95																	2.14				
Q.TGW-ME.UoR-2D	2D	BS00029208_51	BS00009575_51	42.21	42.21	50.33	3.17E-05	4.50															0.76						
Q.GW-2016.UoR-2D	2D	Kukri_rep_c72254_186	Kukri_c14902_1112	111.88	106.21	111.88	7.61E-05	4.12					1.38																
Q.Ntr-2015.UoR-2D	2D	BobWhite_c40561_305	BobWhite_c18906_680	170.44	164.88	170.44	9.60E-04	3.02																			3.09		
Q.GL-2016.UoR-2D	2D	BobWhite_c40561_305	BobWhite_c18906_680	170.44	164.88	170.44	1.36E-05	4.87		1.54																			
Q.GW-2015.UoR-2D	2D	BS00100539_51	BobWhite_c5756_516	196.35	171.95	196.35	4.14E-06	5.38				1.8																	
Q.GW-ME.UoR-2D	2D	BobWhite_c5756_516	BS00086534_51	198.36	196.35	198.36	1.70E-04	3.77						0.55															
Q.Ntr-2015.UoR-3A	3A	Excalibur_c12875_864	Kukri_c2123_1254	16.13	15.13	16.13	8.86E-04	3.05																			1.1		
Q.GW-2016.UoR-3A	3A	RAC875_c67998_96	BS00047668_51	188.69	186.68	188.69	4.84E-05	4.32					1.47																
Q.GA-2016.UoR-3B	3B	tplb0059m03_1516	JD_c23336_253	15.35	15.35	16.87	3.00E-04	3.52								0.64													
Q.GW-2015.UoR-3B	3B	wsnp_Ku_c17659_26797674	RAC875_c2529_1483	68.67	68.17	68.67	5.52E-05	4.26				3.48																	
Q.TGW-ME.UoR-3B	3B	BS00022072_51	Excalibur_c15944_70	89.15	87.13	89.15	1.27E-05	4.90															4.08						
Q.GL-2016.UoR-3B	3B	BS00032830_51	IACX971	94.18	94.18	95.19	1.69E-04	3.77		3.29																			
Q.TGW-2016.UoR-3B.1	3B	CAP8_rep_c4453_136	RAC875_c37608_216	105.61	105.61	106.11	1.05E-05	4.98														4.7							
Q.FFD-2016.UoR-3B.1	3B	BobWhite_s64174_119	wsnp_BE497469B_Ta_2_1	107.11	106.61	107.11	2.22E-06	5.65											3.9										
Q.TGW-2015.UoR-3B	3B	Tdurum_contig49477_187	BobWhite_c32864_250	166.02	165.01	166.02	5.24E-04	3.28													2.76								
Q.TGW-2016.UoR-3B.2	3B	BS00047274_51	Excalibur_c48047_90	175.11	171.05	175.11	5.40E-06	5.27														4.05							
Q.FFD-2016.UoR-3B.2	3B	Excalibur_c48047_90	BS00097383_51	180.42	175.11	180.42	5.23E-05	4.28											3.46										
Q.Ntr-2015.UoR-4A	4A	BS00010925_51	BS00011273_51	92.13	92.13	92.63	3.05E-04	3.52																			2.72		
Q.TGW-ME.UoR-4A	4A	wsnp_Ex_c3988_7221220	RAC875_c6939_1042	140.85	137.28	140.85	9.37E-05	4.03															1.4						
Q.Yld-2015.UoR-4A	4A	wsnp_Ex_c3988_7221220	RAC875_c6939_1042	140.85	137.28	140.85	3.45E-05	4.46																1.55					
Q.GA-2016.UoR-4A.1	4A	BS00064369_51	BS00091752_51	164.01	158.75	164.01	1.66E-05	4.78								1.66													
Q.GA-2016.UoR-4A.2	4A	Excalibur_c74390_108	BS00064419_51	211.2	210.70	211.20	4.65E-06	5.33								1.54													
Q.Yld-2016.UoR-4A	4A	Excalibur_c10699_404	BobWhite_c38832_153	214.75	214.75	217.29	1.31E-05	4.88																	2.86				
Q.FFD-ME.UoR-4B	4B	BS00084070_51	Ra_c26080_461	49.66	49.66	50.16	4.53E-06	5.34												1.87									
Q.FFD-2015.UoR-4B	4B	BS00084070_51	Ra_c26080_461	49.66	49.66	50.16	3.90E-10	9.41										2.4											
Q.Yld-2016.UoR-4B	4B	Ra_c26080_461	BS00033614_51	50.16	50.16	51.16	2.56E-04	3.59																	1.62				
Q.GA-2015.UoR-4B	4B	Ra_c26080_461	BS00033614_51	51.16	50.16	51.16	2.81E-07	6.55							1.73														
Q.GA-2016.UoR-4B.1	4B	Ra_c26080_461	BS00033614_51	51.16	50.16	51.16	2.54E-08	7.60								2.93													
Q.GW-2015.UoR-4B	4B	Ra_c26080_461	BS00033614_51	51.16	50.16	51.16	1.00E-10	10.00				3.22																	
Q.GW-2016.UoR-4B	4B	Ra_c26080_461	BS00033614_51	51.16	50.16	51.16	2.47E-11	10.61					3.03																
Q.GW-ME.UoR-4B	4B	Ra_c26080_461	BS00033614_51	51.16	50.16	51.16	1.44E-14	13.84						4.04															
Q.TGW-ME.UoR-4B	4B	Ra_c26080_461	BS00033614_51	51.16	50.16	51.16	0.00E+00	17.5*															3.53						
Q.TGW-2015.UoR-4B	4B	Tdurum_contig42229_113	BobWhite_c44691_648	52.17	52.17	52.67	6.66E-16	15.18													3.72								
Q.GA-ME.UoR-4B	4B	BS00011851_51	BS00084904_51	54.7	54.70	55.20	1.81E-08	7.74									2.77												
Q.TGW-2016.UoR-4B	4B	BS00011851_51	BS00084904_51	54.7	54.70	55.20	7.03E-11	10.15														3.03							
Q.FFD-2016.UoR-4B	4B	BS00084904_51	BS00022988_51	55.7	55.20	55.70	1.14E-06	5.94											2.05										
Q.Yld-2015.UoR-4B	4B	BS00067786_51	IACX5989	75.09	75.09	78.18	1.98E-05	4.70																3.32					
Q.GA-2016.UoR-4B.2	4B	BS00104364_51	BS00009342_51	170.66	170.66	173.22	2.89E-04	3.54								0.13													
Q.GA-2016.UoR-4D	4D	Kukri_rep_c68594_530	Excalibur_c19078_210	24.93	24.93	32.24	3.53E-06	5.45								3.25													
Q.GA-ME.UoR-4D	4D	Kukri_rep_c68594_530	Excalibur_c19078_210	24.93	24.93	32.24	5.44E-08	7.26									2.78												
Q.FFD-2016.UoR-4D	4D	Excalibur_c19078_210	RAC875_rep_c105718_304	32.24	32.24	40.11	6.89E-06	5.16											2.94										
Q.GA-2015.UoR-4D	4D	Excalibur_c19078_210	RAC875_rep_c105718_304	32.24	32.24	40.11	9.99E-08	7.00							2.48														
Q.TGW-2016.UoR-4D	4D	Excalibur_c19078_210	RAC875_rep_c105718_304	32.24	32.24	40.11	1.23E-11	10.91														4.65							
Q.FFD-ME.UoR-4D	4D	Excalibur_c19078_210	RAC875_rep_c105718_304	32.24	32.24	40.11	6.66E-14	13.18												6.34									
Q.GW-2015.UoR-4D	4D	Excalibur_c19078_210	RAC875_rep_c105718_304	32.24	32.24	40.11	5.33E-14	13.27				5.73																	
Q.FFD-2015.UoR-4D	4D	Excalibur_c19078_210	RAC875_rep_c105718_304	32.24	32.24	40.11	2.66E-15	14.58										6.87											
Q.TGW-2015.UoR-4D	4D	Excalibur_c19078_210	RAC875_rep_c105718_304	32.24	32.24	40.11	0.00E+00	21*													7.6								
Q.TGW-ME.UoR-4D	4D	Excalibur_c19078_210	RAC875_rep_c105718_304	32.24	32.24	40.11	0.00E+00	21*															7.33						
Q.GW-ME.UoR-4D	4D	Excalibur_c19078_210	RAC875_rep_c105718_304	32.24	32.24	40.11	0.00E+00	23*						8.71															
Q.GW-2016.UoR-4D	4D	Excalibur_c19078_210	RAC875_rep_c105718_304	32.24	32.24	40.11	0.00E+00	29*					9.28																
Q.GW-2015.UoR-5A.1	5A	BS00040933_51	BobWhite_rep_c50145_387	39.25	39.25	39.75	7.52E-04	3.12				1.08																	
Q.GA-2015.UoR-5A	5A	BobWhite_rep_c49700_452	wsnp_Ex_c7668_13089715	69.43	68.43	69.43	2.28E-07	6.64							3.53														
Q.GL-2015.UoR-5A	5A	BobWhite_rep_c49700_452	wsnp_Ex_c7668_13089715	69.43	68.43	69.43	6.85E-09	8.16	6.91																				
Q.GA-ME.UoR-5A	5A	wsnp_Ku_c5071_9049540	BobWhite_c15454_63	73.03	73.03	83.05	2.62E-09	8.58									5.29												
Q.GL-ME.UoR-5A	5A	wsnp_Ku_c5071_9049540	BobWhite_c15454_63	73.03	73.03	83.05	5.55E-16	15.26			9.79																		
Q.GL-2016.UoR-5A.2	5A	wsnp_Ku_c5071_9049540	BobWhite_c15454_63	73.03	73.03	83.05	0.00E+00	15.5*		11.18																			
Q.TGW-2016.UoR-5A	5A	BobWhite_c15454_63	BS00034303_51	83.55	83.05	83.55	8.40E-05	4.08														1.25							
Q.GA-2016.UoR-5A	5A	BobWhite_c15454_63	BS00034303_51	83.55	83.05	83.55	1.04E-08	7.98								5.65													
Q.TGW-2015.UoR-5A	5A	Ex_c2171_2600	BobWhite_c47401_491	310.04	310.04	310.54	2.70E-06	5.57													2.32								
Q.GW-2016.UoR-5A	5A	BS00069245_51	BobWhite_c8266_227	310.54	310.54	311.55	2.22E-11	10.65					5.07																
Q.GW-2015.UoR-5A.2	5A	BobWhite_c8266_227	Excalibur_c46261_342	311.55	311.55	312.56	6.83E-05	4.17				2.13																	
Q.GW-ME.UoR-5A	5A	BobWhite_c8266_227	Excalibur_c46261_342	311.55	311.55	312.56	6.75E-08	7.17						4.36															
Q.GA-2016.UoR-5B.1	5B	Ra_c19198_137	Kukri_c74960_427	15.68	15.68	16.69	8.33E-09	8.08								2.26													
Q.GA-ME.UoR-5B.1	5B	Kukri_c74960_427	BS00033612_51	16.69	16.69	17.19	8.57E-07	6.07									3.44												
Q.GA-2015.UoR-5B.1	5B	Tdurum_contig48658_1022	BobWhite_c8048_663	44.97	44.97	46.48	1.26E-05	4.90							2.28														
Q.GL-2015.UoR-5B.1	5B	wsnp_Ku_c3869_7094615	Ra_c44756_929	56.1	56.10	59.14	8.63E-08	7.06	4.13																				
Q.GL-2016.UoR-5B.1	5B	wsnp_Ku_c3869_7094615	Ra_c44756_929	56.1	56.10	59.14	1.29E-08	7.89		3.06																			
Q.GL-ME.UoR-5B.1	5B	wsnp_Ku_c3869_7094615	Ra_c44756_929	56.1	56.10	59.14	7.48E-10	9.13			4.31																		
Q.TGW-ME.UoR-5B	5B	IACX9261	BS00087043_51	142.56	133.91	142.56	2.08E-06	5.68															2.58						
Q.GA-2015.UoR-5B.2	5B	BS00065128_51	BS00067744_51	173.2	173.20	178.87	1.20E-05	4.92							2.37														
Q.TGW-2015.UoR-5B	5B	BS00067744_51	Excalibur_c3165_730	178.87	178.87	182.50	5.01E-04	3.30													2.04								
Q.TGW-2016.UoR-5B	5B	BS00067744_51	Excalibur_c3165_730	178.87	178.87	182.50	2.94E-04	3.53														1.97							
Q.GA-ME.UoR-5B.2	5B	BS00067744_51	Excalibur_c3165_730	178.87	178.87	182.50	3.84E-06	5.42									3.06												
Q.GL-2015.UoR-5B.2	5B	Excalibur_c3165_730	IACX9238	182.5	182.50	183.00	2.58E-07	6.59	5.05																				
Q.GL-ME.UoR-5B.2	5B	Excalibur_c3165_730	IACX9238	182.5	182.50	183.00	1.10E-07	6.96			5																		
Q.GL-2016.UoR-5B.2	5B	IACX9238	Kukri_c2955_281	183	183.00	184.00	2.17E-06	5.66		4.32																			
Q.Ntr-2016.UoR-5B	5B	BS00022673_51	BS00005860_51	199.34	199.34	202.43	3.27E-04	3.49																				2.04	
Q.GA-2016.UoR-5B.2	5B	RFL_Contig2772_1693	BobWhite_rep_c60245_107	213.01	212.00	213.01	1.05E-08	7.98								2.62													
Q.Yld-2016.UoR-5B	5B	Excalibur_c1925_2569	BobWhite_c39214_164	229.16	227.12	229.16	2.05E-12	11.69																	6.02				
Q.GW-2015.UoR-5D	5D	wsnp_Ku_rep_c72922_72561803	BS00021901_51	14.07	14.07	15.07	1.89E-04	3.72				1.27																	
Q.TGW-2016.UoR-5D	5D	wsnp_Ku_rep_c72922_72561803	BS00021901_51	14.07	14.07	15.07	1.45E-05	4.84														1.55							
Q.FFD-2016.UoR-5D	5D	BS00021901_51	Kukri_rep_c73094_348	15.07	15.07	19.57	3.05E-04	3.52											2.41										
Q.GA-2015.UoR-5D	5D	Kukri_rep_c73094_348	Kukri_c444_833	21.57	19.57	21.57	6.26E-04	3.20							0.42														
Q.GW-2016.UoR-5D	5D	Kukri_rep_c73094_348	Kukri_c444_833	21.57	19.57	21.57	3.36E-04	3.47					0.88																
Q.GW-ME.UoR-5D	5D	Kukri_rep_c73094_348	Kukri_c444_833	21.57	19.57	21.57	1.16E-04	3.94						0.48															
Q.GA-2016.UoR-6A.1	6A	wsnp_CAP7_c399_215824	wsnp_Ku_c26784_36748247	98.45	98.45	102.35	1.34E-04	3.87								2.89													
Q.FFD-ME.UoR-6A	6A	JD_c8888_741	RAC875_rep_c81239_73	119.36	119.36	119.86	1.49E-05	4.83												3.73									
Q.Ntr-2015.UoR-6A	6A	wsnp_BG262421A_Ta_2_2	BS00054054_51	125.91	124.90	125.91	2.52E-08	7.60																			8.35		
Q.FFD-2015.UoR-6A	6A	Kukri_c77911_260	BobWhite_c20706_135	131.94	131.44	131.94	9.12E-08	7.04										4.52											
Q.GA-2015.UoR-6A	6A	Kukri_c77911_260	BobWhite_c20706_135	131.94	131.44	131.94	2.91E-14	13.54							7.16														
Q.GW-2015.UoR-6A	6A	Kukri_c77911_260	BobWhite_c20706_135	131.94	131.44	131.94	1.41E-14	13.85				7.75																	
Q.GW-ME.UoR-6A	6A	Kukri_c77911_260	BobWhite_c20706_135	131.94	131.44	131.94	0.00E+00	22.5*						10.96															
Q.FFD-2016.UoR-6A	6A	BobWhite_c20706_135	BS00022605_51	132.95	131.94	132.95	3.23E-04	3.49											2.43										
Q.TGW-2016.UoR-6A	6A	BobWhite_c20706_135	BS00022605_51	132.95	131.94	132.95	9.96E-14	13.00														6.97							
Q.TGW-2015.UoR-6A	6A	BobWhite_c20706_135	BS00022605_51	132.95	131.94	132.95	0.00E+00	20.5*													9.48								
Q.TGW-ME.UoR-6A	6A	BobWhite_c20706_135	BS00022605_51	132.95	131.94	132.95	0.00E+00	21*															9.95						
Q.GW-2016.UoR-6A	6A	RAC875_c23305_563	BS00041481_51	134.48	134.48	137.00	0.00E+00	24*					11.91																
Q.GA-2016.UoR-6A.2	6A	Tdurum_contig53138_302	BS00021689_51	139.52	139.52	140.53	1.11E-16	15.95								9.47													
Q.GA-ME.UoR-6A	6A	Tdurum_contig53138_302	BS00021689_51	139.52	139.52	140.53	0.00E+00	18*									9.26												
Q.Ntr-2016.UoR-6A	6A	BS00023893_51	BS00065082_51	180.47	176.94	180.47	6.27E-04	3.20																				3.2	
Q.GA-2016.UoR-6A.3	6A	Excalibur_c7002_314	RAC875_c40653_612	229.11	229.11	230.12	4.29E-07	6.37								3.36													
Q.Ntr-2015.UoR-6B.1	6B	BS00091262_51	BS00103275_51	152.64	152.64	153.14	5.32E-04	3.27																			1.75		
Q.Ntr-2015.UoR-6B.2	6B	RAC875_c12907_515	BS00023080_51	201.81	199.77	201.81	3.85E-05	4.41																			3.78		
Q.FFD-2015.UoR-6D	6D	BS00021881_51	BobWhite_c22280_104	130.85	130.85	190.15	1.75E-04	3.76										1.67											
Q.TGW-ME.UoR-7A.1	7A	BS00026702_51	BS00082055_51	6.6	5.60	6.60	4.09E-05	4.39															1.07						
Q.GW-ME.UoR-7A.1	7A	Excalibur_c24750_504	Excalibur_rep_c69170_602	8.61	7.10	8.61	5.03E-04	3.30						1.39															
Q.GA-2016.UoR-7A	7A	Excalibur_c60134_182	BS00110940_51	65.98	65.98	74.73	1.40E-05	4.85								0.39													
Q.GL-ME.UoR-7A.1	7A	BobWhite_s63403_99	Kukri_s118416_65	180.5	178.46	180.50	1.57E-04	3.80			1.82																		
Q.GL-2016.UoR-7A.1	7A	BobWhite_s63403_99	Kukri_s118416_65	180.5	178.46	180.50	2.06E-05	4.69		2.19																			
Q.TGW-2015.UoR-7A	7A	Kukri_rep_c105999_572	BobWhite_c47283_127	254.13	254.13	254.63	3.06E-07	6.51													3.01								
Q.FFD-2015.UoR-7A	7A	Kukri_rep_c105999_572	BobWhite_c47283_127	254.63	254.13	254.63	1.51E-04	3.82										2.17											
Q.TGW-ME.UoR-7A.2	7A	Excalibur_c63900_370	BobWhite_c1441_1123	265.69	264.18	265.69	5.65E-06	5.25															2.27						
Q.Yld-2016.UoR-7A	7A	BS00063458_51	RAC875_c67826_84	276.69	275.17	276.69	2.14E-05	4.67																	1.11				
Q.GW-2016.UoR-7A	7A	BS00009838_51	BS00021657_51	311.26	310.25	311.26	3.03E-06	5.52					2.58																
Q.GL-ME.UoR-7A.2	7A	BS00004257_51	Excalibur_c14451_1313	312.27	312.27	313.79	1.35E-05	4.87			1.87																		
Q.GL-2016.UoR-7A.2	7A	BS00004257_51	Excalibur_c14451_1313	312.27	312.27	313.79	1.32E-05	4.88		2.37																			
Q.Yld-2015.UoR-7A	7A	RAC875_c13093_86	wsnp_Ex_c7071_12171619	318.37	318.37	321.39	1.21E-07	6.92																4.33					
Q.GW-ME.UoR-7A.2	7A	Tdurum_contig54832_139	Tdurum_contig61864_1352	352.64	351.63	352.64	1.85E-04	3.73						1.11															
Q.GW-2015.UoR-7A	7A	Tdurum_contig27856_230	BobWhite_c25105_507	355.66	355.16	355.66	2.08E-04	3.68				1.61																	
Q.Yld-2015.UoR-7B.1	7B	RFL_Contig6075_1128	Tdurum_contig5352_556	0	0.00	6.39	3.30E-04	3.48																1.55					
Q.Yld-2016.UoR-7B.1	7B	RFL_Contig6075_1128	Tdurum_contig5352_556	0	0.00	6.39	7.77E-06	5.11																	1.68				
Q.Yld-2016.UoR-7B.2	7B	RAC875_c10932_1697	BS00022550_51	66.08	64.06	66.08	1.81E-04	3.74																	0.9				
Q.Ntr-ME.UoR-7D	7D	Excalibur_c33002_123	BS00022463_51	148.98	148.98	180.19	9.07E-04	3.04																					2.57
						Total Variation Explained			28	42.25	38.1	28.9	40.12	33.6	23.5	47.8	38.4	17.6	20.8	14.4	35.6	31.7	34.7	10.75	18.16	5.71	20.8	5.24	2.57

Table 3.2 – QTL table for sink-related traits. QTL names follow standard format as described in Chapter 2. Trait abbreviations are as shown in Table 3.1. Left and Right Marker Positions are the location of the markers in cM, p-value is the significance of the QTL and -log10p is the strength of the QTL

3.2.2.2 Grain Length

A total of 25 significant (-log10p ≥ 3) QTL for Grain Length (GL) were found on chromosomes 1B, 1D, 2A, 2D, 3B, 5A, 5B and 7A.

These QTL explain on average one third of the total variation in Grain Length, both in 2015 and 2016 or in the across-seasons analysis. Approximately one third of the variation explained by the QTL are accounted for by the two strongest QTL: *Q.GL-ME.UoR-5A* (*p*= 5.55E-16, %var= 6.91 – 11.18); *Q.GL-2016.UoR-1B.1* (*p*= 5.34E-11, %var= 3.09 – 5.7), expressed in both years and detected in identical locations in all analyses. A further two stable QTL were identified across all analyses on chromosome 5B, *Q.GL-2015.UoR-5B.1* located between 56.10 - 59.14cM and *Q.GL-ME.UoR-5B.2* 182.50 – 184.00cM explaining between 3.06 - 5.05% variation explained. A further four dual co-locating were identified on 1B, 2A, and 2 sets on 7A. The remaining five QTL were either year-specific or detected only in the across-season analysis. Smaller effects together explained the year-specific component of variation, the strongest of these being *Q.GL-2015.UoR-1B.2* (267.04 - 268.54cM) which explained 5.07% of the variation and P value of 6.88E-05.

3.2.3.3 Grain Width

A total of 29 Significant (-log10p ≥ 3) Grain Width (GW) were found on chromosomes 1B, 1D, 2D, 3A, 3B, 4B, 4D, 5A, 5D, 6A and 7A.

These QTL explain between 28.9 and 40.12% of the total variation in Grain Width, both in 2015 and 2016 or in the across-seasons analysis. Approximately half of the variation explained by the QTL are accounted for by the two strongest QTL: *Q.GW-2015.UoR-6A*

(*p*= 1.41E-14, %var= 7.75 – 11.91); *Q.GW-2015.UoR-4D* (*p*= 5.33E-14, %var= 5.73 – 9.28), located at the locus for *Rht-D1*.

The four largest effect QTL were on 4B (50.16 - 51.16cM), 4D (32.24 - 40.11cM), 5A (310.54 - 312.56cM) and 6A (131.44 - 137.00cM). These QTL were expressed in both years and multi-environment analysis, suggesting they are relatively stable in their effects. The QTL on 4B and 4D are likely to be *Rht-B1b* and *Rht-D1b* respectively. All stable QTL have variation in the effects between years, suggesting that there is some genotype by environment interaction remaining. Eight QTL only appeared in single year analysis, suggesting that these are environmentally specific. However, within their environment these QTL explain between 0.82% and 3.48% of phenotypic variation in the environments.

3.2.2.4 Grain Yield

Grain Yield has a relatively low heritability (H^2 =0.26), leading us to expect that there would be fewer significant QTL explaining a lower percentage of the total phenotypic variation. This reflects the complexity of yield as a trait reliant on the output of many other traits.

A total of 14 Significant (-log10p ≥ 3) QTL for Grain Yield (GY) were found on chromosomes 2A, 2B, 4A, 4B, 5B, 7A and 7B.

These QTL collectively explain between 5.71 and 18.16% of the total variation in Grain Yield, both in 2015 and 2016 or in the across-seasons analysis. In the 2014-15 analysis, three quarters of the variation is explained by the strongest two QTL: *Q.Yld-2015.UoR-4B* (*p*= 1.98E-05, %var= 3.32); *Q.Yld-2015.UoR-7A* (*p*= 1.21E-07, %var= 4.33). In the 2015-

16 analysis, one third of the variation explained was due to the single strongest QTL: *Q.Yld-2016.UoR-5B* (*p*= 2.05E-12, %var= 6.02). In the multi-environment analysis, there were only two QTL detected *Q.Yld-ME.UoR-2A* (*p*= 1.81E-06, %var= 3.74) and *Q.Yld-ME.UoR-2B* (*p*= 6.9E-04, %var= 1.97).

For this trait*, Q.Yld-2015.UoR-7B and Q.Yld-2016.UoR-7B.1* were the only overlapping QTL between years, located between 0.000- 6.392cM. Both were significant (*p*= e-4 to e-6) and explained 1.55 to 1.68% of the total variation. All remaining QTL were year specific.

12 QTL only appeared in single year analysis, suggesting that these are environmentally unstable. However, within their environment the QTL explain between 0.9% and 6.02% of phenotypic variation in the environments.

3.2.2.5 Nitrogen Content

The low heritability of this trait (H^2 =0.16) would lead us to expect that there would be fewer, less significant QTL for Nitrogen Content. A total 9 Significant (-log10p ≥ 3) QTL for Nitrogen content (N) were found on chromosomes 2D, 3A, 4A, 5B, 6A, 6B and 7D.

These QTL collectively explained between 2.57 and 20.8% of the total variation found in Nitrogen Content both in 2015 and 2016 or in the across-seasons analysis. The strongest of the individual QTL was *Q.Ntr-2015.UoR-6A* (*p*= 2.52E-08, %var= 8.35).

All nine QTL only appeared in single year analysis, suggesting that these are environmentally unstable. However, within their environment explain between 1.1% and 8.35% of phenotypic variation in the environments.

3.2.3 Co-location of QTL for driver and output traits.

Multi-trait QTL analysis enables us to identify groupings of QTL that may have effects on several agronomically important traits. By analysing the co-location of QTL, it is likely that several traits will appear genetically linked. Some may be controlled by the same gene, while others may be controlled by adjacent genes that are close enough together that it is unlikely a recombination event would happen between their locations. With 155 QTL distributed over all 21 chromosomes, it is likely that some QTL will randomly co-locate. However, at least a portion of the major GW and GL effects are likely to be additive, rather than working as trade-offs between different grain dimensions. This would lead directly to an increase in TGW, and indirectly to an increase in yield. This can be seen in co-locations between GL, GA and TGW on chromosomes 5A (73.03 – 83.55cM) and 5B (173.20 – 184.00cM), and co-locations between GW, GA and TGW on chromosomes 4B (50.2 – 55.2cM) and 6A (131.44 – 132.95cM).

These regions show that both grain length and width can drive increases in TGW individually. The co-location of GA, GW, TGW and Yield on chromosome 4B (50.2 – 55.2cM) is the only genetic observation of the indirect effect that the primary drivers of TGW (GL and GW) affecting yield as well. However, TGW does impact yield on 4A (137.28 - 140.85cM).

In principle, looking at co-location also provides the opportunity to identify QTL for yield which are relatively independent from phenology. Such QTL would be extremely significant for breeding purposes (Pinto *et al*., 2010; Reynolds *et al*., 2009). A total of 75 co-locating QTL were identified on chromosomes 1B, 2A, 2D, 3B, 4A, 4B, 4D, 5A, 5B, 5D and 6A.

									Percentage of phenotypic variation explained																							
									Grain Length			Grain Width			Grain Area			Form Factor Density			Thousand Grain Weight			Grain Yield			Grain Nitrogen		
QTL Name	Chromosome	Left Marker	Right Marker	QTL Position	Left Marker Position	Right Marker Position	pvalue	-log10p	2015	2016	ME	2015	2016	ME	2015	2016	ME	2015	2016	ME	2015	2016	ME	2015	2016	ME	2015	2016	ME
Q.GA-ME.UoR-1B.1	1B	*RAC875_rep_c109416_191*	*Tdurum_contig42633_1282*	69.6	59.06	69.60	1.37E-05	4.86									4.1													
Q.GL-2015.UoR-1B.1	1B	*RAC875_rep_c109416_191*	*Tdurum_contig42633_1282*	69.6	59.06	69.60	2.32E-06	5.63	3.09																				
Q.GL-ME.UoR-1B.1	1B	*RAC875_rep_c109416_191*	*Tdurum_contig42633_1282*	69.6	59.06	69.60	9.44E-11	10.03			5.16																		
Q.GL-2016.UoR-1B.1	1B	*RAC875_rep_c109416_191*	*Tdurum_contig42633_1282*	69.6	59.06	69.60	5.34E-11	10.27		5.7																			
Q.GL-2016.UoR-1B.2	1B	*RFL_Contig1823_1044*	*Tdurum_contig50988_500*	276.38	276.38	276.88	2.53E-08	7.60		7.03																			
Q.GL-ME.UoR-1B.2	1B	*RFL_Contig1823_1044*	*Tdurum_contig50988_500*	276.38	276.38	276.88	2.06E-08	7.69			6.53																		
Q.GA-ME.UoR-1B.2	1B	*RFL_Contig1823_1044*	*Tdurum_contig50988_500*	276.88	276.38	276.88	2.91E-04	3.54									3.59													
Q.FFD-2016.UoR-2A	2A	*BS00089457_51*	*RAC875_rep_c119471_174*	115.52	112.46	115.52	9.14E-06	5.04											3.61											
Q.TGW-2016.UoR-2A	2A	*BS00089457_51*	*RAC875_rep_c119471_174*	115.52	112.46	115.52	3.37E-07	6.47														3.53							
Q.GL-2016.UoR-2A	2A	*BS00040337_51*	*BS00062757_51*	134.69	134.19	134.69	5.14E-06	5.29		1.57																			
Q.GL-ME.UoR-2A	2A	*BS00040337_51*	*BS00062757_51*	134.69	134.19	134.69	2.79E-08	7.55			2.28																		
Q.TGW-ME.UoR-2A	2A	*BS00062757_51*	*BobWhite_c28819_733*	135.19	134.69	135.19	3.72E-07	6.43															1.71						
Q.Yld-ME.UoR-2A	2A	*Kukri_c24064_2095*	*BS00041816_51*	140.76	140.76	141.26	1.81E-06	5.74																	3.74				
Q.FFD-ME.UoR-2A	2A	*Kukri_c24064_2095*	*BS00041816_51*	141.26	140.76	141.26	2.34E-05	4.63												2.42									
Q.Ntr-2015.UoR-2D	2D	*BobWhite_c40561_305*	*BobWhite_c18906_680*	170.44	164.88	170.44	9.60E-04	3.02																				3.09	
Q.GL-2016.UoR-2D	2D	*BobWhite_c40561_305*	*BobWhite_c18906_680*	170.44	164.88	170.44	1.36E-05	4.87		1.54																			
Q.TGW-2016.UoR-3B.2	3B	*BS00047274_51*	*Excalibur_c48047_90*	175.11	171.05	175.11	5.40E-06	5.27														4.05							
Q.FFD-2016.UoR-3B.2	3B	*Excalibur_c48047_90*	*BS00097383_51*	180.42	175.11	180.42	5.23E-05	4.28											3.46										
Q.TGW-ME.UoR-4A	4A	*wsnp_Ex_c3988_7221220*	*RAC875_c6939_1042*	140.85	137.28	140.85	9.37E-05	4.03															1.4						
Q.Yld-2015.UoR-4A	4A	*wsnp_Ex_c3988_7221220*	*RAC875_c6939_1042*	140.85	137.28	140.85	3.45E-05	4.46																1.55					
Q.FFD-ME.UoR-4B	4B	*BS00084070_51*	*Ra_c26080_461*	49.66	49.66	50.16	4.53E-06	5.34												1.87									
Q.FFD-2015.UoR-4B	4B	*BS00084070_51*	*Ra_c26080_461*	49.66	49.66	50.16	3.90E-10	9.41										2.4											
Q.Yld-2016.UoR-4B	4B	*Ra_c26080_461*	*BS00033614_51*	50.16	50.16	51.16	2.56E-04	3.59																	1.62				
Q.GA-2015.UoR-4B	4B	*Ra_c26080_461*	*BS00033614_51*	51.16	50.16	51.16	2.81E-07	6.55							1.73														
Q.GA-2016.UoR-4B.1	4B	*Ra_c26080_461*	*BS00033614_51*	51.16	50.16	51.16	2.54E-08	7.60								2.93													
Q.GW-2015.UoR-4B	4B	*Ra_c26080_461*	*BS00033614_51*	51.16	50.16	51.16	1.00E-10	10.00				3.22																	
Q.GW-2016.UoR-4B	4B	*Ra_c26080_461*	*BS00033614_51*	51.16	50.16	51.16	2.47E-11	10.61					3.03																
Q.GW-ME.UoR-4B	4B	*Ra_c26080_461*	*BS00033614_51*	51.16	50.16	51.16	1.44E-14	13.84						4.04															
Q.TGW-ME.UoR-4B	4B	*Ra_c26080_461*	*BS00033614_51*	51.16	50.16	51.16	0.00E+00	17.5*															3.53						
Q.TGW-2015.UoR-4B	4B	*Tdurum_contig42229_113*	*BobWhite_c44691_648*	52.17	52.17	52.67	6.66E-16	15.18													3.72								
Q.GA-ME.UoR-4B	4B	*BS00011851_51*	*BS00084904_51*	54.7	54.70	55.20	1.81E-08	7.74									2.77												
Q.TGW-2016.UoR-4B	4B	*BS00011851_51*	*BS00084904_51*	54.7	54.70	55.20	7.03E-11	10.15														3.03							
Q.FFD-2016.UoR-4B	4B	*BS00084904_51*	*BS00022988_51*	55.7	55.20	55.70	1.14E-06	5.94											2.05										
Q.GA-2016.UoR-4D	4D	*Kukri_rep_c68594_530*	*Excalibur_c19078_210*	24.93	24.93	32.24	3.53E-06	5.45								3.25													
Q.GA-ME.UoR-4D	4D	*Kukri_rep_c68594_530*	*Excalibur_c19078_210*	24.93	24.93	32.24	5.44E-08	7.26									2.78												
Q.FFD-2016.UoR-4D	4D	*Excalibur_c19078_210*	*RAC875_rep_c105718_304*	32.24	32.24	40.11	6.89E-06	5.16											2.94										
Q.GA-2015.UoR-4D	4D	*Excalibur_c19078_210*	*RAC875_rep_c105718_304*	32.24	32.24	40.11	9.99E-08	7.00							2.48														
Q.TGW-2016.UoR-4D	4D	*Excalibur_c19078_210*	*RAC875_rep_c105718_304*	32.24	32.24	40.11	1.23E-11	10.91														4.65							
Q.FFD-ME.UoR-4D	4D	*Excalibur_c19078_210*	*RAC875_rep_c105718_304*	32.24	32.24	40.11	6.66E-14	13.18												6.34									
Q.GW-2015.UoR-4D	4D	*Excalibur_c19078_210*	*RAC875_rep_c105718_304*	32.24	32.24	40.11	5.33E-14	13.27				5.73																	
Q.FFD-2015.UoR-4D	4D	*Excalibur_c19078_210*	*RAC875_rep_c105718_304*	32.24	32.24	40.11	2.66E-15	14.58										6.87											
Q.TGW-2015.UoR-4D	4D	*Excalibur_c19078_210*	*RAC875_rep_c105718_304*	32.24	32.24	40.11	0.00E+00	21*													7.6							
Q.TGW-ME.UoR-4D	4D	*Excalibur_c19078_210*	*RAC875_rep_c105718_304*	32.24	32.24	40.11	0.00E+00	21*															7.33						
Q.GW-ME.UoR-4D	4D	*Excalibur_c19078_210*	*RAC875_rep_c105718_304*	32.24	32.24	40.11	0.00E+00	23*						8.71															
Q.GW-2016.UoR-4D	4D	*Excalibur_c19078_210*	*RAC875_rep_c105718_304*	32.24	32.24	40.11	0.00E+00	29*					9.28																
Q.GA-2015.UoR-5A	5A	*BobWhite_rep_c49700_452*	*wsnp_Ex_c7668_13089715*	69.43	68.43	69.43	2.28E-07	6.64							3.53														
Q.GL-2015.UoR-5A	5A	*BobWhite_rep_c49700_452*	*wsnp_Ex_c7668_13089715*	69.43	68.43	69.43	6.85E-09	8.16	6.91																				
Q.GA-ME.UoR-5A	5A	*wsnp_Ku_c5071_9049540*	*BobWhite_c15454_63*	73.03	73.03	83.05	2.62E-09	8.58									5.29												
Q.GL-ME.UoR-5A	5A	*wsnp_Ku_c5071_9049540*	*BobWhite_c15454_63*	73.03	73.03	83.05	5.55E-16	15.26			9.79																		
Q.GL-2016.UoR-5A.2	5A	*wsnp_Ku_c5071_9049540*	*BobWhite_c15454_63*	73.03	73.03	83.05	0.00E+00	15.5*		11.18																			
Q.TGW-2016.UoR-5A	5A	*BobWhite_c15454_63*	*BS00034303_51*	83.55	83.05	83.55	8.40E-05	4.08														1.25							
Q.GA-2016.UoR-5A	5A	*BobWhite_c15454_63*	*BS00034303_51*	83.55	83.05	83.55	1.04E-08	7.98								5.65													
Q.GA-2015.UoR-5B.2	5B	*BS00065128_51*	*BS00067744_51*	173.2	173.20	178.87	1.20E-05	4.92							2.37														
Q.TGW-2015.UoR-5B	5B	*BS00067744_51*	*Excalibur_c3165_730*	178.87	178.87	182.50	5.01E-04	3.30													2.04								
Q.TGW-2016.UoR-5B	5B	*BS00067744_51*	*Excalibur_c3165_730*	178.87	178.87	182.50	2.94E-04	3.53														1.97							
Q.GA-ME.UoR-5B.2	5B	*BS00067744_51*	*Excalibur_c3165_730*	178.87	178.87	182.50	3.84E-06	5.42									3.06												
Q.GL-2015.UoR-5B.2	5B	*Excalibur_c3165_730*	*IACX9238*	182.5	182.50	183.00	2.58E-07	6.59	5.05																				
Q.GL-ME.UoR-5B.2	5B	*Excalibur_c3165_730*	*IACX9238*	182.5	182.50	183.00	1.10E-07	6.96			5																		
Q.GL-2016.UoR-5B.2	5B	*IACX9238*	*Kukri_c2955_281*	183	183.00	184.00	2.17E-06	5.66		4.32																			
Q.GW-2015.UoR-5D	5D	*wsnp_Ku_rep_c72922_72561803*	*BS00021901_51*	14.07	14.07	15.07	1.89E-04	3.72				1.27																	
Q.TGW-2016.UoR-5D	5D	*wsnp_Ku_rep_c72922_72561803*	*BS00021901_51*	14.07	14.07	15.07	1.45E-05	4.84														1.55							
Q.FFD-2016.UoR-5D	5D	*BS00021901_51*	*Kukri_rep_c73094_348*	15.07	15.07	19.57	3.05E-04	3.52											2.41										
Q.GA-2015.UoR-5D	5D	*Kukri_rep_c73094_348*	*Kukri_c444_833*	21.57	19.57	21.57	6.26E-04	3.20							0.42														
Q.GW-2016.UoR-5D	5D	*Kukri_rep_c73094_348*	*Kukri_c444_833*	21.57	19.57	21.57	3.36E-04	3.47					0.88																
Q.GW-ME.UoR-5D	5D	*Kukri_rep_c73094_348*	*Kukri_c444_833*	21.57	19.57	21.57	1.16E-04	3.94						0.48															
Q.FFD-2015.UoR-6A	6A	*Kukri_c77911_260*	*BobWhite_c20706_135*	131.94	131.44	131.94	9.12E-08	7.04										4.52											
Q.GA-2015.UoR-6A	6A	*Kukri_c77911_260*	*BobWhite_c20706_135*	131.94	131.44	131.94	2.91E-14	13.54							7.16														
Q.GW-2015.UoR-6A	6A	*Kukri_c77911_260*	*BobWhite_c20706_135*	131.94	131.44	131.94	1.41E-14	13.85				7.75																	
Q.GW-ME.UoR-6A	6A	*Kukri_c77911_260*	*BobWhite_c20706_135*	131.94	131.44	131.94	0.00E+00	22.5*						10.96															
Q.FFD-2016.UoR-6A	6A	*BobWhite_c20706_135*	*BS00022605_51*	132.95	131.94	132.95	3.23E-04	3.49											2.43										
Q.TGW-2016.UoR-6A	6A	*BobWhite_c20706_135*	*BS00022605_51*	132.95	131.94	132.95	9.96E-14	13.00														6.97							
Q.TGW-2015.UoR-6A	6A	*BobWhite_c20706_135*	*BS00022605_51*	132.95	131.94	132.95	0.00E+00	20.5*													9.48							
Q.TGW-ME.UoR-6A	6A	*BobWhite_c20706_135*	*BS00022605_51*	132.95	131.94	132.95	0.00E+00	21*															9.95						
Q.TGW-2015.UoR-7A	7A	*Kukri_rep_c105999_572*	*BobWhite_c47283_127*	254.13	254.13	254.63	3.06E-07	6.51													3.01								
Q.FFD-2015.UoR-7A	7A	*Kukri_rep_c105999_572*	*BobWhite_c47283_127*	254.63	254.13	254.63	1.51E-04	3.82										2.17											
						Total Variation Explained			15.05	31.34	28.76	19.77	13.19	24.74	21.24	12.79	21.59	15.96	16.9	10.63	25.85	27	23.92	1.55	1.62	3.74	3.09	0	0

*Table **Error! No text of specified style in document.**3.3 – Co-locating QTL table for sink-related traits. QTL names follow standard format as described in Chapter 2. Trait abbreviations are as shown in Table 3.1. Left and Right Marker Positions are the location of the markers in cM, p-value is the significance of the QTL and -log10p is the strength of the QTL*

3.2.3.1 Chromosome 1B

On chromosome 1B, two sets of co-locating QTL were observed (Figure 3.3). *Q.GA-ME.UoR-1B.1* and a grain length QTL consistent across all analyses are co-located between markers *RAC875_rep_c109416_191* and *Tdurum_contig42633_1282* (59.06 - 69.60cM), explaining between 3.09 and 5.7% of the total phenotypic variation. The Grain Area meta-QTL *Q.GA-ME.UoR-1B.2* also co-located with a grain length QTL detected in 2016 and the multi-environment analysis. These QTL were co-located between *RFL_Contig1823_1044* and

Tdurum_contig50988_500 (276.38 - 276.88cM), explaining between 3.59 and 7.03% of the total phenotypic variation.

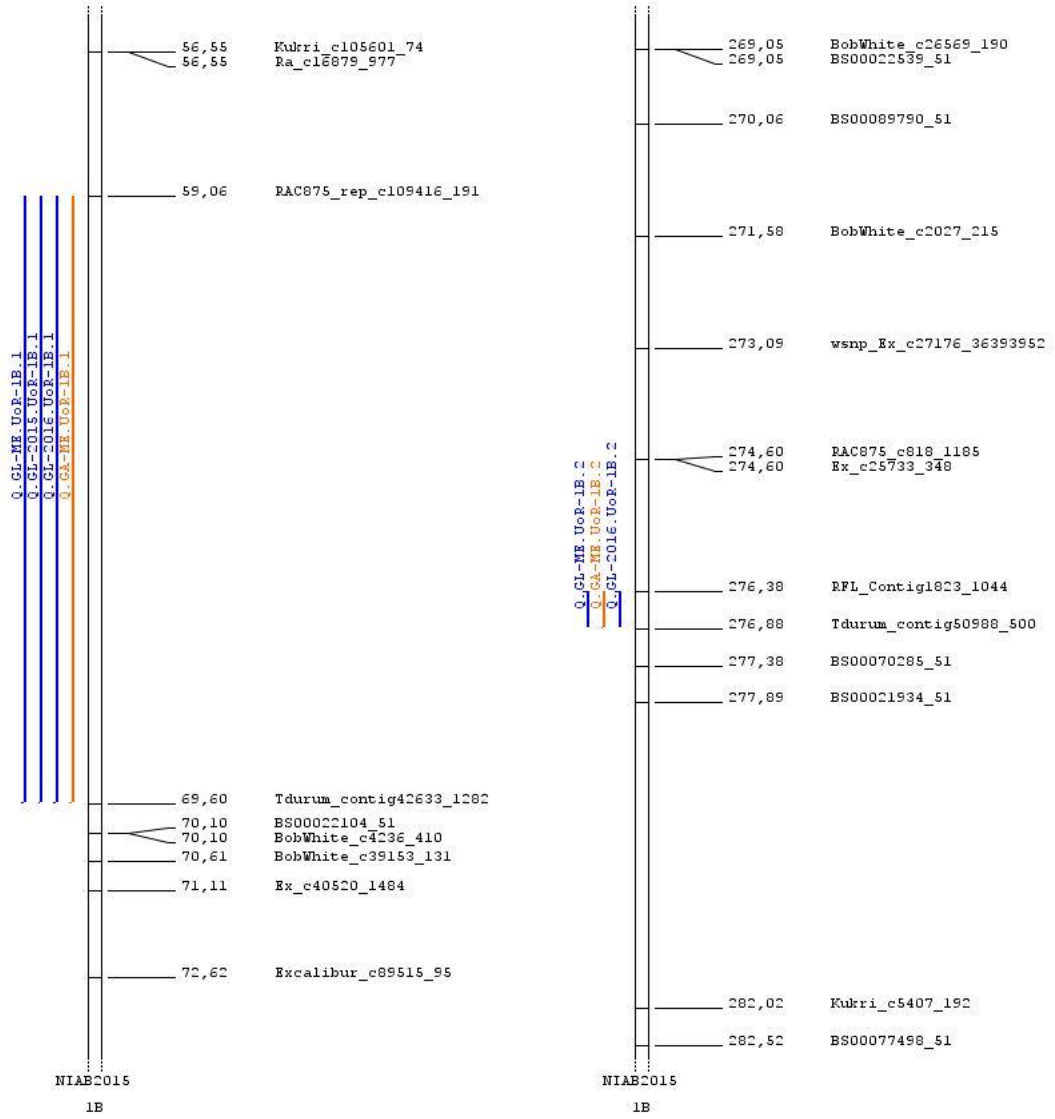

Figure 3-3 Fragments of genetic linkage map of chromosome 1B with marker positions as reported in Gardner et al (2016). QTL intervals are displayed as coloured bars labelled with QTL names as reported in Table 3.3.

3.2.3.2 Chromosome 2A

On chromosome 2A, three sets of co-locating QTL were observed (Figure 3.4). *Q.FFD-2016.UoR-2A* and *Q.TGW-2016.UoR-2A* were co-located between markers *BS00089457_51* and *RAC875_rep_c119471_174* (112.46 - 115.52cM), explaining 3.61 and 3.53% of the total phenotypic variation respectively. Q.TGW-ME.UoR-2A co-located with a grain length QTL that was identified in 2016 and multi-environment analysis, between markers *BS00040337_51* and *BobWhite_c28819_733* (134.19 – 135.19cM), explaining between 1.57 and 2.28% of the total phenotypic variation. *Q.Yld-ME.UoR-2A* and *Q.FFD-ME.UoR-2A* co-locate between markers *Kukri_c24064_2095* and *BS00041816_51* (140.76 - 141.26cM), explaining 3.74 and 2.42% of the total phenotypic variation respectively.

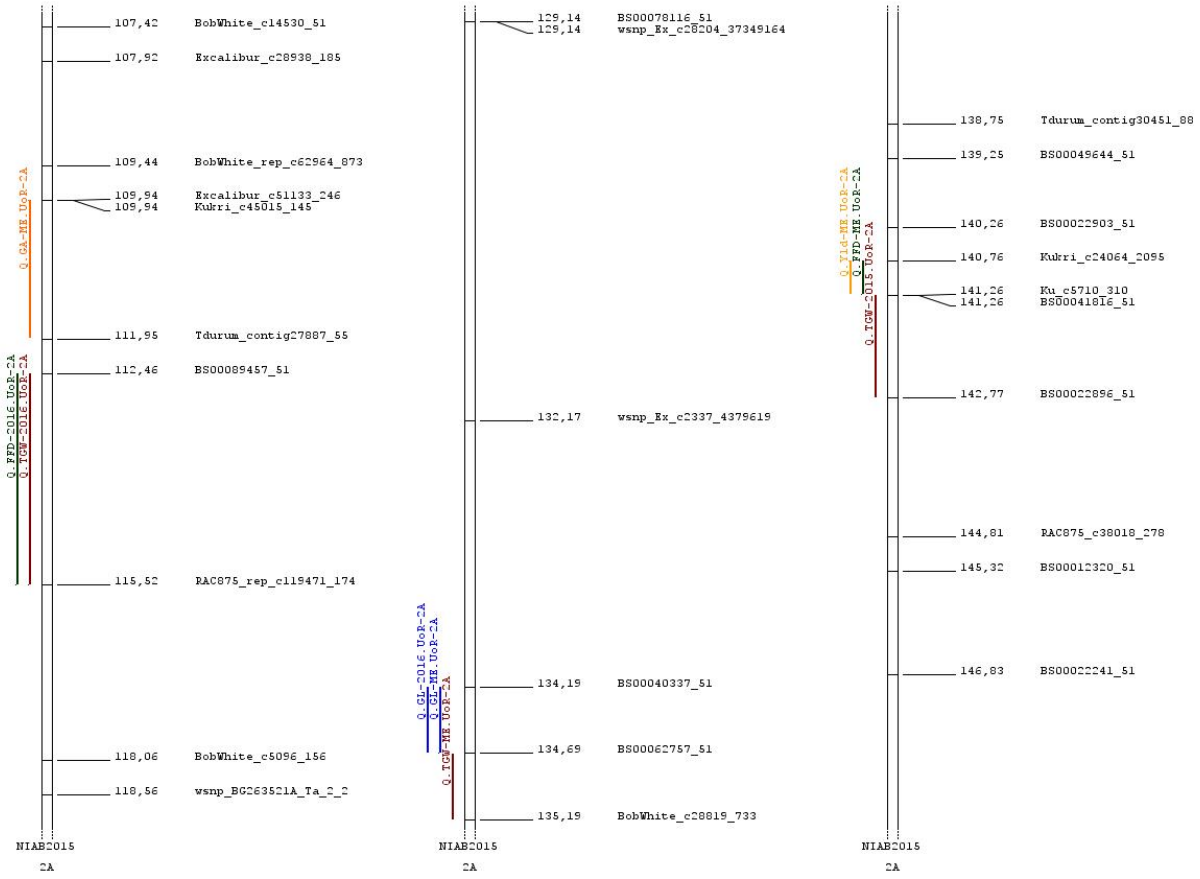

Figure 3-4 - Fragments of genetic linkage map of chromosome 2A with marker positions as reported in Gardner et al (2016) and rendered using Biomercator (Sosnowski *et al*., 2012)*. QTL intervals are displayed as coloured bars labelled with QTL names as reported in Table 3.3.*

3.2.3.3 Chromosome 2D

Co-locating QTL for Grain Nitrogen and Grain Length observed on chromosome 2D (Figure 3.5) *Q.Ntr-2015.UoR-2D* and *Q.GL-2016.UoR-2D* co-located between markers *BobWhite_c40561_305* and *BobWhite_c18906_680* (164.88 - 170.44cM), explaining 1.54 and 3.09% of the total phenotypic variation respectively. These QTL are independent of *Ppd-D1,* which is located approximately 100cM away from this location. It is not clear why Grain Nitrogen from the 2014-15 season would share an element of genetic control with Grain Length in the 2015-16 season, especially given the lack of correlation between these two traits (PCC = -0.08, Figure 3.2), but this is a 5.6cM interval and it is entirely possible, therefore, that these are independent QTL that fall in the same interval by chance.

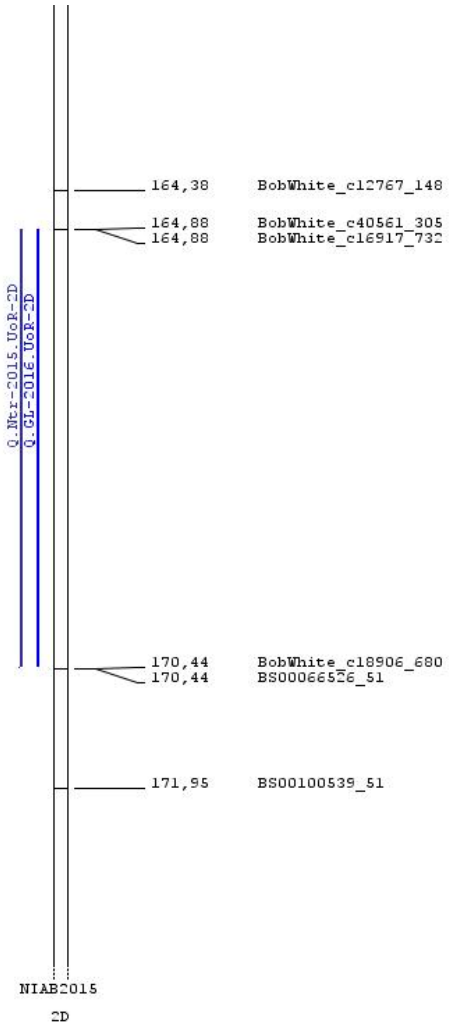

Figure 3-5 Fragments of genetic linkage map of chromosome 2D with marker positions as reported in Gardner et al (2016) and rendered using Biomercator (Sosnowski *et al*., 2012)*. QTL intervals are displayed as coloured bars labelled with QTL names as reported in Table 3.3.*

3.2.3.4 Chromosome 3B

There was only one set of co-locating QTL observed on chromosome 3B (Figure 3.6) *Q.TGW-2016.UoR-3B.2* and *Q.FFD-2016.UoR-3B.2* co-located between markers *BS00047274_51* and *BS00097383_51* (171.05 – 180.42cM), explaining 4.05 and 3.46% of the total phenotypic variation.

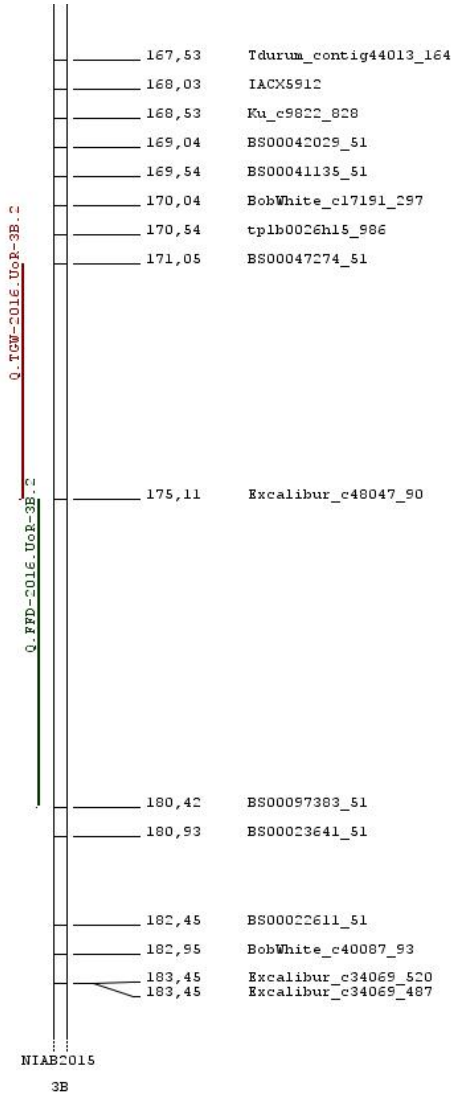

Figure 3-6- Fragments of genetic linkage map of chromosome 3B with marker positions as reported in Gardner et al (2016) and rendered using Biomercator (Sosnowski *et al*., 2012)*. QTL intervals are displayed as coloured bars labelled with QTL names as reported in Table 3.3.*

3.2.3.5 Chromosome 4A

Co-locating QTL for TGW and Yield were observed on chromosome 3B (Figure 3.7) *Q.TGW-ME.UoR-4A* and *Q.Yld-2015.UoR-4A* co-located between markers *wsnp_Ex_c3988_7221220* and *RAC875_c6939_1042* (137.28 - 140.85cM), explaining 1.4 and 1.55% of the total phenotypic variation.

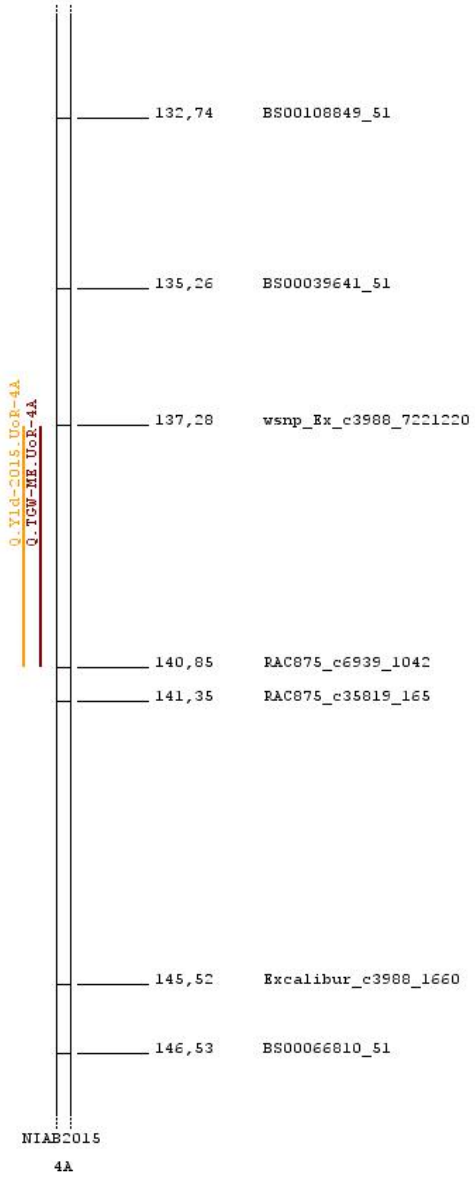

Figure 3-7 - Fragments of genetic linkage map of chromosome 4A with marker positions as reported in Gardner et al (2016) and rendered using Biomercator (Sosnowski *et al.*, 2012)*. QTL intervals are displayed as coloured bars labelled with QTL names as reported in Table 3.3.*

3.2.3.5 Chromosome 4B

On chromosome 4B, there was one large group of co-locating QTL (Figure 3.8). Initially, this contains 13 QTL, but can be refined down to five QTL where the same QTL appears in all analyses.

Q.Yld-2016.UoR-4B is co-locating with QTL for FFD, GA, GW and TGW; the four of which are stable across both years and detected in the meta-analysis. This QTL cluster is located between markers *BS00084070_51* and *BS00022988_51* (49.66 – 55.70cM) and explains between 1.62 and 4.04% of the total phenotypic variation. TGW and GW consistently had the highest -log10p scores and explained the most variation. These QTL are co-locating with *Rht-B1b.*

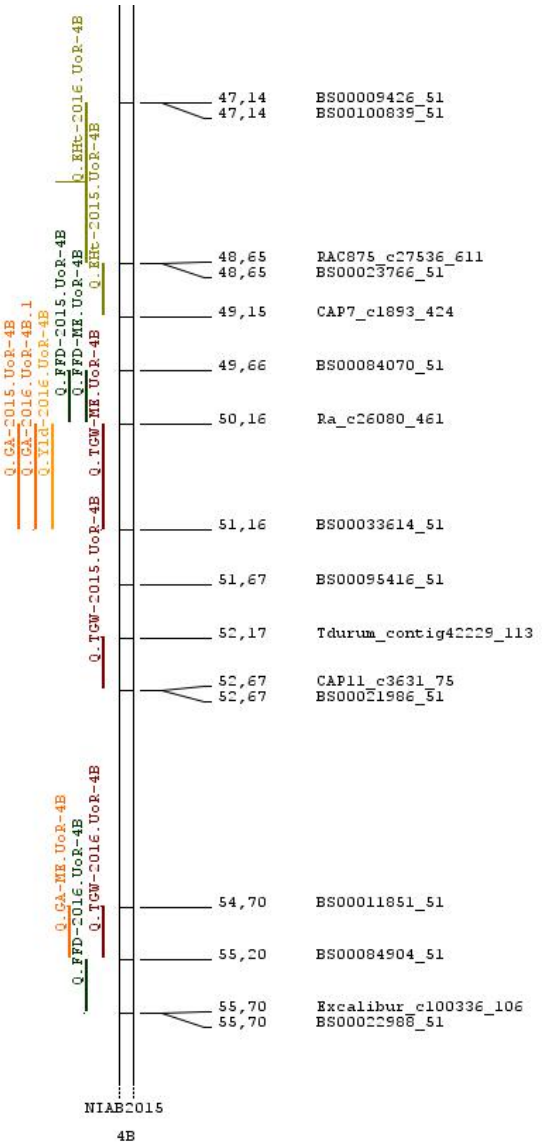

Figure 3-8 - Fragments of genetic linkage map of chromosome 4B with marker positions as reported in Gardner et al (2016) and rendered using Biomercator (Sosnowski *et al*., 2012). *QTL intervals are displayed as coloured bars labelled with QTL names as reported in Table 3.3.*

3.2.3.5 Chromosome 4D

On chromosome 4D, there was one large group of co-locating QTL (Figure 3.9). Initially, this contains 12 QTL, but can be refined down to four QTL where the same QTL appears in all trait analyses- for example *Q.TGW-2015.UoR-4D, Q.TGW-2016.UoR-4D* and *Q.TGW-ME.UoR-4D* are all located between *Excalibur_c19078_210* and *RAC875_rep_c105718_304.* QTL for GW, GA, TGW and FFD appeared in all analyses between markers *Kukri_rep_c68594_530* and *RAC875_rep_c105718_304* (24.93 - 40.11cM) and explains between 2.48 and 9.28% of the total phenotypic variation. As with chromosome 4B, TGW and GW consistently had the highest -log10p values and explained the most variation. These QTL are co-locating with *Rht-D1b.*

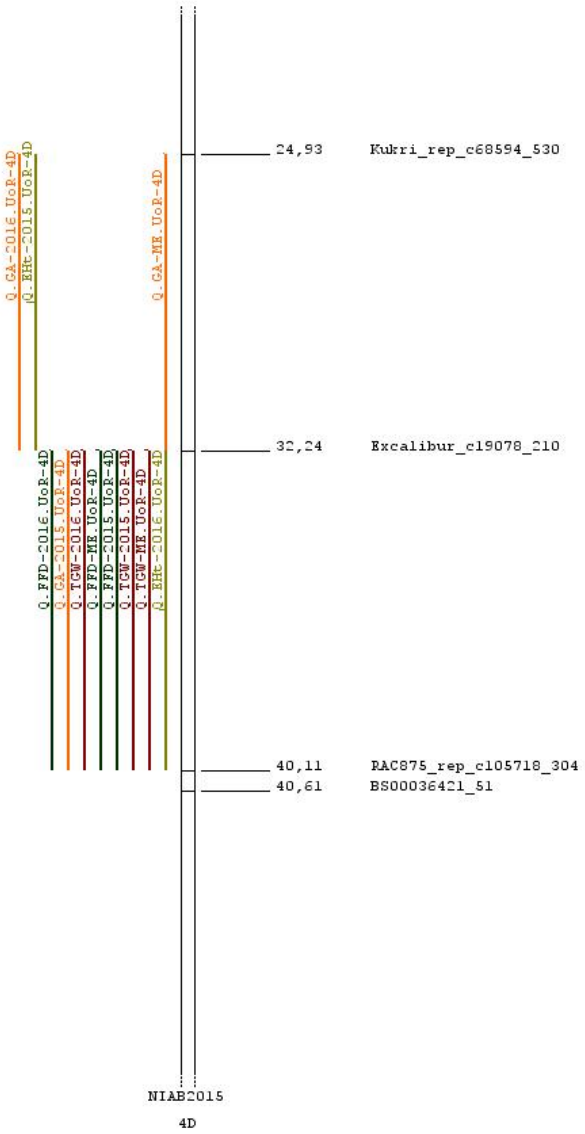

Figure 3-9 - Fragments of genetic linkage map of chromosome 4D with marker positions as reported in Gardner et al (2016) and rendered using Biomercator (Sosnowski *et al*., 2012)*. QTL intervals are displayed as coloured bars labelled with QTL names as reported in Table 3.3.*

3.2.3.6 Chromosome 5A

On chromosome 5A, there was one moderate group of co-locating QTL (Figure 3.10). Initially, this contains seven QTL, but can be refined down to three where the same QTL appears in all trait analyses, with the magnitude and direction of effects from the parents being comparable. *Q.TGW-2016.UoR-5A* co-locates with QTL for GL and GA, between markers

BobWhite_rep_c49700_452 and *BS00034303_51* (68.43 – 83.55cM), explaining between 1.25 and 11.2% of the total phenotypic variance. GL is the strongest QTL in this cluster, explaining between 6.91 and 11.2% of the total variation.

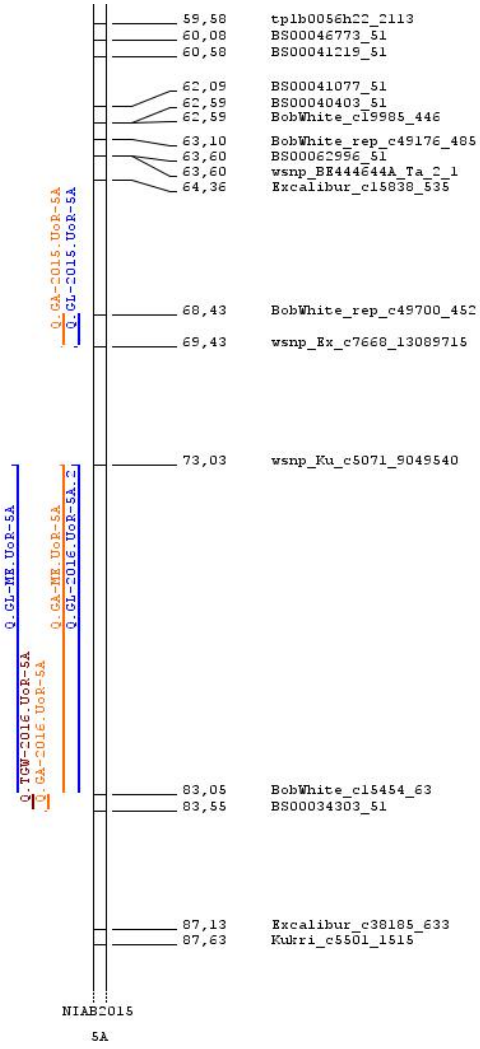

Figure 3-10 - Fragments of genetic linkage map of chromosome 5A with marker positions as reported in Gardner et al (2016) and rendered using Biomercator (Sosnowski *et al.*, 2012)*. QTL intervals are displayed as coloured bars labelled with QTL names as reported in Table 3.3.*

3.2.3.7 Chromosome 5B

On chromosome 5B, there was one moderate sized group of co-locating QTL (Figure 3.11). Here, a QTL for GL detected in all analyses co-locates with QTL for GA (2015 and ME) and TGW

(2015 and 2016), between markers *BS00065128_51* and *Kukri_c2955_281* (173.20 – 183.00cM), explaining between 0.48 and 2.41% of total phenotypic variation.

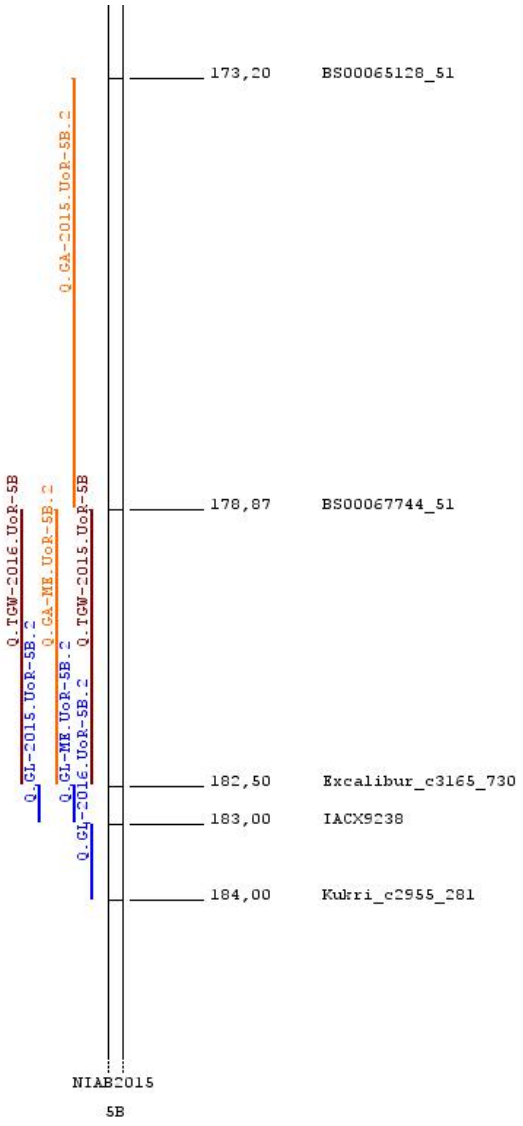

Figure 3-11- Fragments of genetic linkage map of chromosome 5B with marker positions as reported in Gardner et al (2016) and rendered using Biomercator (Sosnowski *et al*., 2012)*. QTL intervals are displayed as coloured bars labelled with QTL names as reported in Table 3.3.*

3.2.3.8 Chromosome 5D

On chromosome 5D, there was one moderate sized group of co-locating QTL (Figure 3.12). Here, a consistent QTL for GW co-located with *Q.TGW-2016.UoR-5D, Q.FFD-2016.UoR-5D* and *Q.GA-2015.UoR-5D* between markers *wsnp_Ku_rep_c72922_72561803* and *Kukri_c444_833* (14.07 – 21.57cM), explaining between 0.42 and 2.41% of the total phenotypic variation.

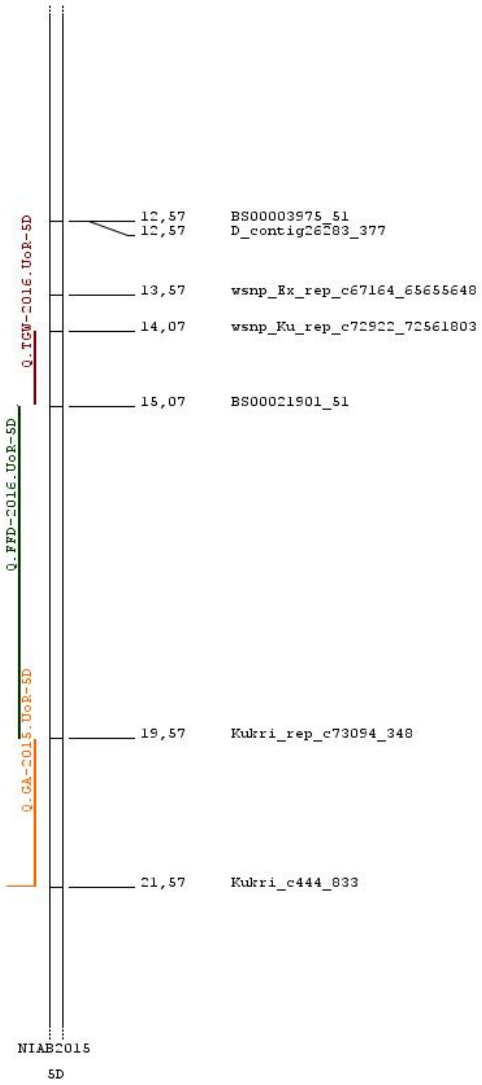

Figure 3-12 - Fragments of genetic linkage map of chromosome 5D with marker positions as reported in Gardner et al (2016) and rendered using Biomercator (Sosnowski *et al*., 2012). *QTL intervals are displayed as coloured bars labelled with QTL names as reported in Table 3.3.*

3.2.3.9 Chromosome 6A

On chromosome 6A, there was one moderate sized group of co-locating QTL (Figure 3.13). Here, a consistent QTL for TGW co-located with FFD (2015 and 2016), GW (2015 and ME) and Q.GA-2015.UoR-6A, between markers *Kukri_c77911_260* and *BS00022605_51* (131.94 – 132.95cM), explaining between 2.43 and 11.00% of the total phenotypic variation.

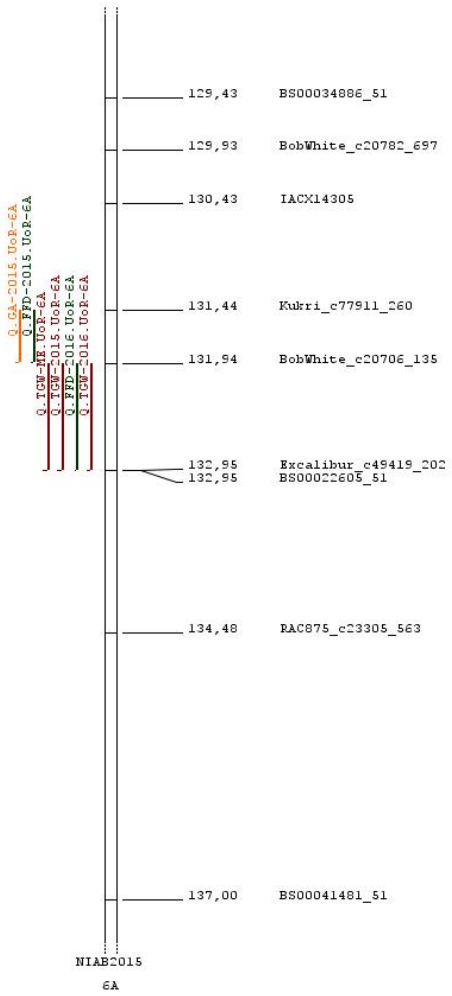

Figure 3-13 - Fragments of genetic linkage map of chromosome 6A with marker positions as reported in Gardner et al (2016) and rendered using Biomercator (Sosnowski *et al*., 2012)*. QTL intervals are displayed as coloured bars labelled with QTL names as reported in Table 3.3.*

3.2.3.10 Chromosome 7A

On chromosome 7A, there is a single set of co-locating QTL (Figure 3.14). *Q.TGW-2015.UoR-7A* and *Q.FFD-2015.UoR-7A* are co-locating between markers *Kukri_rep_c105999_572* and *BobWhite_c47283_127* (254.13 - 254.63cM), explaining 3.01 and 2.17% of total phenotypic variation respectively.

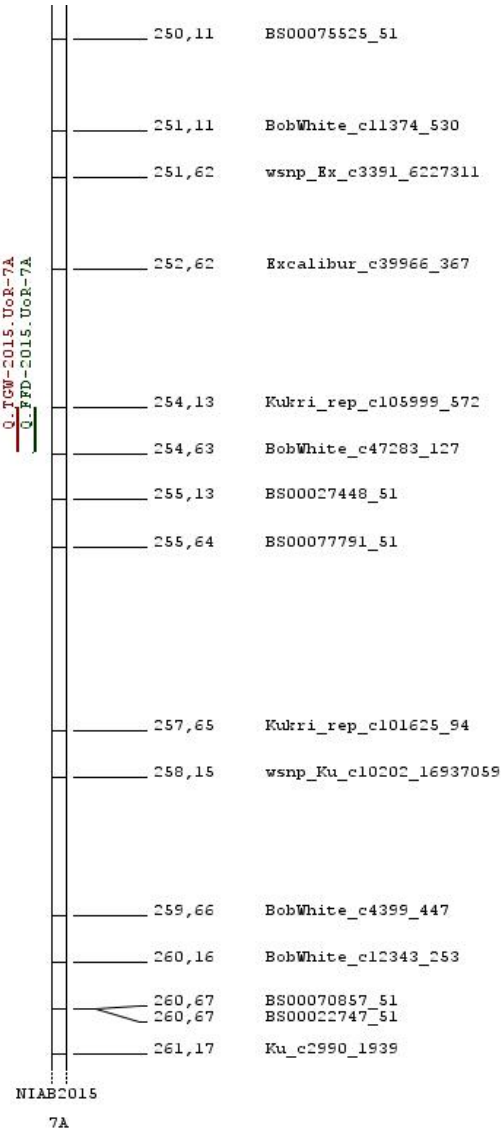

Figure 3-14 - Fragments of genetic linkage map of chromosome 7A with marker positions as reported in Gardner et al (2016) and rendered using Biomercator (Sosnowski *et al.*, 2012)*. QTL intervals are displayed as coloured bars labelled with QTL names as reported in Table 3.3.*

3.3 Discussion

3.3.1 Phenotypic variation in yield traits in the MAGIC population

The experiments described in this chapter were designed to investigate sink-related traits by breaking down yield into as many individual components as can be reasonably measured. The eight seed traits analysed in this chapter: Grain Yield, Thousand Grain Weight, Grain Width, Grain Length, Grain Area, Nitrogen Content, Length-Width Ratio and Factor-Form Density were measured over 2 years, in 2015 and 2016. Multiple years are critical when measuring quantitative field traits, as most countries have environmental variability year on year, which will affect crop production and yields. For example, 2012 was an environmentally unfavourable year in the UK compared to other years (Figure 3.15), averaging around 6.6t/ha, where successive years have averaged between 7.3 -8.9t/ha (FAOSTAT, 2018)

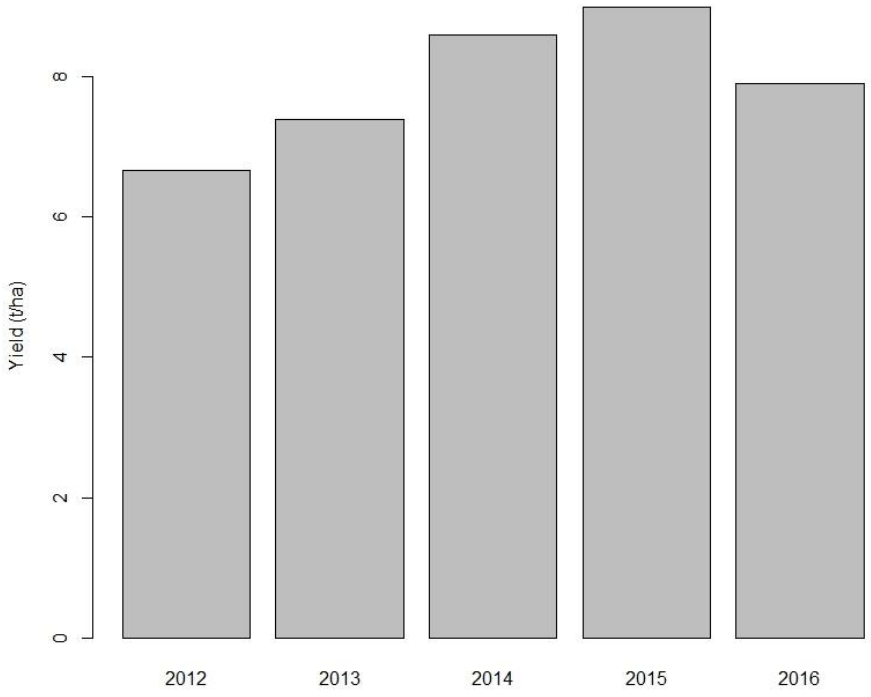

Figure 3-15 - Average UK wheat yields from 2012-2016. Data retrieved from FAOSTAT.

This environmental variability can be seen between the 2014-15 and 2015-16 seasons in our field conditions. Average yield increased from 7.14t/ha to 9.34t/ha, an increase of around 30%, and the average nitrogen concentration declined from 3.03 to 2.47%, a decrease of almost 20%. These traits are typically affected in opposite directions due to well established negative correlations between yield and nitrogen concentration. In the context of environmental influence, the stressed season in 2014-15 led to an earlier senescence, therefore less time for grain filling, decreasing yield. However, the later senescence in 2015-16 increased the grain filling period, diluting the nitrogen content with starch to a lower overall concentration.

The environmental conditions had little effect on grain area, width and length overall. Average grain length decreased by 0.21mm (3%) in 2015-16. However, this is likely to be due to an increased amount of grains coming from the apex and base of the ear, which are typically smaller than grains in the middle of the ear. These smaller grains are usually aborted in any form of sub-optimal conditions (Friend, 1965). The average grain width only increased by 0.13mm (4%) in 2015-16. Despite a much longer grain filling period, there were significantly more grain to fill. Average thousand grain weight increased from 35.60 to 40.98g (15% increase); while this is a significant amount, overall it is much more stable than yield.

3.3.2 Heritability of phenotypes

Heritability of phenotypes is key to plant breeding, as the extent to which the trait value reflects genetically programmed ‘merit’ rather than environmentally-influenced ‘response’ determines the rate of gain in selection. Highly heritable traits are also consistently expressed over a range of growing conditions, providing reliability for growers. Over the 2 years of field trials, between 5.71 and 18.16% of the total phenotypic variation in yield between the 800

tested progeny lines of the MAGIC population was accounted for in this analysis. It is likely that some of the remaining variation is caused by genetic factors not detected in the analysis, however a larger proportion of the remaining phenotypic variance will be due to indirect cumulative effects of other traits and environmental interactions. It has been repeatedly shown that final yield is unstable and is largely influenced by environmental factors (Snape *et al*., 2007; Tyagi *et al*., 2015; Wu *et al*., 2012). This vulnerability to environmental variables is undesirable in UK elite varieties, as weather conditions are rarely consistent between areas or years. Grain yield is unlikely to be suitable for marker-assisted breeding, as any QTL are unlikely to be stable across environments or have large phenotypic effects. This is backed up by our analysis where we found only one QTL stable (7B) across seasons, and this only explained around 1.6% of the phenotypic variation. Final yield is the product of complex interactions between multiple genetically determined traits (such as the number of grains per ear, potential grain dry mass and the ear density, to name but a few) and environmental factors (such as temperature and rainfall patterns, nutrient availability and biotic stress). The low heritability of the grain yield found in the MAGIC population reflects the polygenic nature of the trait and the complexity of grain yield inheritance. In direct contrast, thousand grain weight and grain dimensions have significantly higher heritability (H^2= 0.39 to 0.74) in the MAGIC population. This indicates that grain morphological traits may be more suitable targets for identifying QTL and marker assisted breeding, as they are more environmentally stable. Moreover, grain morphological measurements can be semi-automated using instruments like MARVIN (GTA Sensorik GmbH, Neubrandenburg, Germany) used by Simmonds *et al* (2014) - although there are some cheaper image analysis methods now available, such as GrainScan (Whan *et al*., 2014), giving a variety of options to drive systematic genetic dissection of this category of sink trait.

3.3.3 Correlation

Of the traits analysed in this chapter, all but yield and nitrogen concentration were strongly correlated across years (PCC= 0.49 - 0.78 for grain traits, PCC= 0.11 and 0.14 for yield and nitrogen concentration respectively). This followed the expected pattern, as it has been well established that grain morphology and weight are more stable across environments than yield itself.

Most grain morphological traits were inconsistently correlated with yield. Only grain length appeared to be the more stably correlated with yield, with a moderate correlation coefficient of 0.27 and 0.19 in 2014-14 and 2015-16 respectively. The remaining grain morphology traits (GW, GA and FFD) varied each year, with significantly lower correlation in 2014-15 compared to 2015-16. It would appear that the relationships between sink-related traits are partially environmentally dependant. Grain width and factor-form density have higher correlations with yield in 2015-16 compared to 2014-15, showing that they can have significant impact on yield under favourable conditions, and little effect under stressed conditions. Grain length is likely to be the most stable across years in relation to yield because it is the first grain morphological trait to reach it maximum (Xie *et al*., 2015), whereas grain width is dependent on the grain filling period.

The inconsistent correlations between thousand grain weight and yield might reflect the conclusions of Fischer (2008), stating that increasing grain yield potential has been achieved by increasing the numbers of grain per unit land, rather than the size of individual seed. However, the moderate correlation between TGW and yield in 2015-16 (PCC= 0.30) and strong heritability (H^2= 0.6), suggests that a significant measure of yield potential is embodied

in thousand grain weight, subject to that potential being realised by favourable conditions immediately preceding and during grain filling.

Grain length and width have relatively low correlations in both years (PCC= -0.11 and 0.09 respectively), however both are positively correlated to various degrees with thousand grain weight. The low correlations between grain length and width suggests that these traits are controlled independently with minimal interaction, although there is some research suggesting that it is possible that increasing grain length would allow for further enhancements of grain width as well (Brinton *et al*., 2017). As both grain length and width have either low correlation (PCC= -0.09) or moderate positive correlation (PCC= 0.19 - 0.27) with yield, grain morphology could potentially be improved for economic traits such as milling quality without adversely affecting the yield.

In the context of thousand grain weight, grain width (PCC= 0.78 and 0.87) is a more important contributor than grain length (PCC = 0.23 and 0.38). However, grain area, which is heavily influenced by both grain width and length, has a strong correlation (PCC= 0.73 and 0.85) with thousand grain weight, indicating that increasing grain length may have a positive effect on the thousand grain weight via grain area. Of the traits measured, only Nitrogen content had a consistent negative correlation with yield, a well-documented trade off.

Grain number m^{-2} will be discussed in Chapters 4 and 5 as the culmination of a season's growth and pre-grain filling source capacity and the link between source and sink traits, representing the final sink capacity and the ability of source to provide assimilates to fill it.

3.3.4 Quantitative Trait Loci Analysis for Grain Yield Traits in the MAGIC population

3.3.4.1 Co-locating QTL

Across eleven chromosomes, QTL for two or more traits were detected, either co-locating between the two same markers, spanning adjacent marker intervals or having a shared flanking marker. Once QTL had been grouped into non-redundant intervals, consolidating adjacent QTL as described above, there were a total of 85 unique QTL locations, of which 16 QTL locations involved two or more different traits. As many of the traits analysed here are correlated with each other, it is expected that some QTL, especially the stronger effect ones, will either be pleiotropic, directly affecting several phenotypes simultaneously, or that variability in one trait will indirectly affect another trait. QTL that are co-locating for the yield and grain morphological traits suggest that some of the variability in yield can be explained by variation in the size and shape of the grain, rather than the number of grains alone. The chromosomes of interest to this analysis are 1B, 2A, 2D, 3B, 4A, 4B, 4D, 5A, 5B, 5D 6A and 7A - the twelve chromosomes where we have identified with co-locating QTL. Previous studies have identified QTL for yield, thousand grain weight, grain quality and grain morphology on all of these chromosomes, using both bi-parental and association panels (Bennett *et al*., 2012; Bonneau *et al*., 2013; Breseghello and Sorrells, 2007; Brinton *et al*., 2017; Cabral *et al*., 2018; Echeverry-Solarte *et al*., 2015; Giura and Saulescu, 1996; Griffiths *et al*., 2015; Li *et al*., 2015; Simmonds *et al*., 2014; Tyagi *et al*., 2015; Williams and Sorrells, 2014). It is possible that many of the QTL detected in the MAGIC population are homologues of QTL found in other wheat populations; however, it is difficult to directly compare studies due to differences in marker sets and maps. Nonetheless, where appropriate, the most relevant previously discovered grain size and weight QTL are considered as candidates to explain the effects observed.

3.3.4.2 Major Effect QTL

Within the analysed co-locating QTL, 29 had a -log10p value of greater than 10, accounting for 11 trait/chromosome combinations over multiple analyses. The higher -log10p values and effect sizes suggest that these are major effect QTL. Within this group were major co-locating QTL on chromosomes 4B, 4D, 5A and 6A.

3.3.4.3 Chromosome 4B

Major effect QTL were located on chromosome 4B between markers *BS00084070_51* and *BS00022988_51.* The strongest QTL detected were for grain width and thousand grain weight. In this case, it is likely that variation in expansion of grain width is acting as a driver of thousand grain weight, which in turn has an effect on yield. This chromosome contains the only observation of the indirect effect of a primary component (grain width) on the final yield, and then *Q.Yld-2016.UoR-4B* has been detected in 2016 alone, the only year where grain width and thousand grain weight had a significant correlation with yield. These QTL are co-locating with the B-genome copy of the Reduced height (*Rht-B1*) gene. From looking at parental effects, it is apparent that *Rht-B1b*, inherited from Robigus and Soissons, has a small negative effect on grain width. A probable pleiotropic effect of *Rht-B1b* on Grain Width and Thousand Grain Weight has been reported previously by Simmonds *et al* (2014); and earlier, at a cruder level, analysis of monosomic lines with substituted whole chromosomes of large-grained line G603-86 in the 'Favorit' background showed the 4B monosomic to have narrower, longer grains than average (Giura and Saulescu, 1996).

3.3.4.4 Chromosome 4D

The most noticeable QTL was for grain width between markers *Excalibur_c19078_210* and *RAC875_rep_c105718_304*. This co-locates with QTL for grain area, FFD, and thousand grain

weight. These are likely to be located near the D-genome copy of the Reduced height (*Rht-D1b*) gene, inherited from six of the eight parents in the MAGIC population. The 'perfect' marker for *Rht-D1b* (*wMAS000002_Rht-D1*) was not included on the genetic map used in the MAGIC population, however there is strong evidence that these markers are closely linked with *Rht-D1b* (Benbow, 2016), and the negative effect of *Rht-D1b* on grain weight was demonstrated over a range of tillage and production systems by Casebow *et al* (2016).

This leads to the conclusion that variability in grain width and weight is caused by the dwarfing effect of *Rht,* supported by previous work by Flintham *et al* (Flintham *et al*., 1997); Gale and Youssefian (1985); and Fischer and Stockman (1986), showing that *Rht* has no effect on the number of spikelets per ear, but does increase the number of fertile florets per spikelet, which would tend to bring down the mean grain weight since the higher the grain positions within a given spikelet, the lower the grain weight (Acreche and Slafer, 2006).

3.3.4.5 Chromosome 5A

A QTL for grain length was identified co-locating with grain area thousand grain weight, between markers *BobWhite_rep_c49700_452* (69.4cM) and *BS00034303_51* (83.6cM). This is likely to be the same QTL identified and fine mapped by Brinton *et al* (2017), which led to a significant increase in thousand grain weight driven by longer grains associated with increased pericarp cell length. A direct comparison cannot be made between studies, as there is only one common marker between the genetic maps on chromosome 5A.

QTL for grain width and thousand grain weight were co-locating between markers *BS00069245_51* (68.4cM) and *Excalibur_c46261_342* (83.6cM). This region has been identified as being associated with numerous beneficial traits (Bariana *et al*., 2006), including the B1 awning locus (Mackay *et al*., 2014) and SnTox1 sensitivity (Cockram *et al*., 2015). Both

the B1 and SnTox1 loci co-locate with the identified QTL once the markers were transposed from the Wang *et al* (2014) map used in the original studies to the newer Gardner *et al* (2016) map. The Q locus may also co-locate to this area, which has been shown to have multiple roles in plant growth and reproductive development. However, no markers between the MAGIC population overlap with previous mapping studies of the Q locus, making it difficult to compare studies.

3.3.4.6 Chromosome 6A

The fourth major QTL set is on chromosome 6A, between markers *Kukri_c77911_260* and *BS00022605_51*. Simmonds *et al* (2014) has already identified and validated a QTL for thousand grain weight on 6A using near isogenic lines (NILs). The *TaGW2* gene was found in this QTL region, which is the homologue of *OsGW2* found in rice, *Oryza sativa. OsGW2* encodes for a ubiquitin ligase, which has been shown to negatively regulate grain width and grain weight. Loss of function in *OsGW2* in rice leads to increased cell numbers in the spikelet hull, resulting in wider grains and indirectly affecting the rate of grain filling (Song *et al*., 2007). This affect has shown to be lower in wheat, with some evidence suggesting that *TaGW2* may have the opposite effect (Bednarek *et al*., 2012; Yang *et al*., 2012). Based on the location of a common adjacent marker, the QTL is less than 10cM from the Simmonds marker, suggesting that the QTL detected here is the same that was previously validated. The common parent, Rialto, between the populations used in these experiments also supports the QTL found on 6A of the MAGIC population being the same one as found in the Spark x Rialto DH population, as Rialto had positive effect alleles in both studies.

3.3.5 Conclusions

The results in this chapter present a set of SNP markers that have significant associations with grain yield, weight and dimensions in the MAGIC population. Compared to previous studies, the use of the MAGIC population bypasses some of the problems in traditional association panels or bi-parental crosses - such as limited allelic diversity, few recombination points, and population structure effects. Our results show that grain width is responsible for a greater proportion of grain weight, than grain length. There is still scope to increase grain length as a way of affecting grain area, which has a much greater correlation with grain weight than grain length does, which will affect the economic value of the grain consistently, whereas thousand grain weight is only significantly correlated with yield in the 2016 conditions. When looking directly at correlations with yield, grain length is the more stable trait across environments. From this multi-year analysis, a combined total of 155 QTL were identified in all analyses, refined to 85 unique QTL when multi-trait pleiotropic QTL and multi-year QTL for a single trait are consolidated. Of these, 16 loci were associated with two or more traits (as opposed to just multiple environments for the same trait). Only seven of the multi-trait QTL were the pleiotropic multi-trait effects wholly consistent from year to year.

There are several loci that have been identified in this chapter that are potential candidates for further investigation. There are several notable yield QTL that appear to be independent of other measured traits. *Q.Yld-2015.UoR-7B.1* and *Q.Yld-2016.UoR-7B.1* are located on chromosome 7B and on average explain 1.6% of the phenotypic variation in yield. *Q.Yld-2016.UoR-5B* explains 6.02%, warranting further investigation due to the relatively large effect for such a complex trait, despite only occurring in a single environment. Likewise, the

strongest QTL for nitrogen concentration, *Q.Ntr-2015.UoR-6A,* explained 8.35% and only occurred in a single year.

Some of these have been reported in previous studies but have yet to be fully validated, whereas others, such as those found on 1B, 1D, 5B and 5D, have not been reported in any of the several studies of grain size and shape parameters conducted on winter wheat in UK environments, and thus appear to be novel QTL. The capacity to detect variation that was not previously seen is expected due to the additional allelic diversity captured by the eight parents, the high levels of recombination in the MAGIC population and extensive marker coverage not found in many previous studies.

4. Genetic analysis of 'source' traits in the elite wheat MAGIC population

4.1 Introduction

4.1.1 'Source' trait definition

As mentioned in Chapter 3, the genetic yield potential of wheat has been defined as the yield of a cultivar when grown in the environment to which it is adapted, with nutrients and water non-limiting and with pests, diseases, weeds, lodging, and other stresses effectively controlled (Evans and Fisher, 1999). As the harvested organ, the grain is referred to as the 'sink'. The capability of the plant to fill the sink to its full potential capacity reliant on the 'source'. In plant physiology, the total capacity of a plant to accumulate biomass is referred to as the 'source'. The source capacity is principally limited by the rate at which a plant can fix carbon through photosynthesis. Plant photosynthesis, and therefore biomass, is dependent on multiple factors; the canopy architecture and its ability to intercept and capture light, the duration of light capture, and the photosynthetic capacity/efficiency of the canopy (Parry *et al*., 2011). In this chapter, genetic variation in the rate, duration and absolute quantity of biomass accumulation are treated as potential traits to ensure that source capacity is not limiting yield.

4.1.2 Canopy Architecture

For wheat grown in modern high-input agricultural systems, canopy architecture has already been targeted extensively in breeding programs, and has largely been optimised for light capture, with few obvious opportunities for further improvement (Horton, 2000).

4.1.3 Duration of light capture

There may still be opportunities to extend the duration of light capture by increasing early development of leaf area so that the formation of a full canopy coincides with periods when radiation intensities are highest in any given season. For example, rapid canopy formation may be useful in colder climates where developmental processes, such as leaf emergence, are temperature limited (Hay and Porter, 2006). Alternatively, the duration of light capture could be improved by introducing 'stay green' phenotypes, increasing the total photosynthesis accumulation by delaying senescence (Dohleman *et al*., 2009; Dohleman and Long, 2009).

4.1.4 Photosynthetic capacity

Potentially, the largest improvements to the source capacity could be achieved through increasing the photosynthetic rate per unit leaf area (Long *et al*., 2006; Parry *et al*., 2011; Raines, 2006). Previous experiments conducted by Fischer *et al*. (2009), using eight historic bread wheat cultivars, suggest that there have been some improvements in photosynthesis per unit leaf area in line with improvements in harvest index, although there appears to be little difference in the total biomass produced.

Currently, most research on increasing photosynthesis per unit leaf area is focused on optimising the properties of Rubisco as it is currently a slow and inefficient catalyst, although several groups are also working on transgenic lines that would allow C4 enzyme pathways and CO2 concentrating mechanisms to be deployed in wheat (Hu *et al*., 2012; Miyao, 2003; Qi *et al*., 2017). There are several strategies that could increase photosynthesis, which may be developed individually or in combination. The first approach, and most obvious, would be to simply increase the amount of Rubisco present - this would be particularly useful in high-

irradiance environments. However, Rubisco already accounts for approximately 25% of leaf nitrogen and 50% of the soluble protein within the leaf (Reynolds *et al*., 2009), making any further increase difficult on a resource level. Another option would be to identify or engineer 'better' Rubisco, by increasing the catalytic rate and the relative specificity for CO2-reducing competitive, and wasteful, oxygenase reactions. Driever *et al*. (2014), has shown that there is still vast potential to be exploited in the natural variation found in different genotypes. While there is potential in this area, there has not yet been any substantial increase in catalytic rate or enzyme specificity (Parry *et al*., 2007). As well as increasing the photosynthetic rate, it is also important to maintain that higher level once achieved. Lobell and Field (2007) show that heat stress has a significant negative impact on photosynthesis, translating to a decrease in yield. Modern cultivars are adapted to current environmental conditions, however increased heat-tolerance will be needed in the face of climate change. There is already evidence that the thermotolerance of photosynthesis can be improved, as shown by Kumar *et al*. (2009) in Arabidopsis.

An often-overlooked contributor to photosynthetic capacity is that of spike photosynthesis. The spikes are displayed above the crop canopy for a significant amount of time, with less competition for radiation interception between plants than you find at the canopy level. It has been shown that spike photosynthesis can significantly contribute to grain filling (Tambussi *et al*., 2007). This is likely to be of particular importance in stressed environments. Despite this potential, little research has been conducted on this trait, and there has been no known attempts to improve it in breeding programmes (Parry *et al*., 2011). Recent work by Molero *et al.* (2014) has identified high variation in spike photosynthesis, and Sanchez-Bragado *et al.* (2014) showed that the spike has a photosynthetic capacity comparable to that

of the flag leaf. Within spike photosynthesis, there is also the role of awns, where present. Research by Li *et al*. (2006) concluded that awns play a significant role in carbohydrate production and are considered the main photosynthetic tissues in the ear (Tambussi *et al*., 2007). Despite the recent progress in this area, estimates of the contribution to grain filling vary considerably, ranging from 10% to 76% (Aranjuelo *et al*., 2011; Gebbing and Schnyder, 1999; Tambussi *et al*., 2007). This could be part of the genetic diversity reported by Molero *et al*. (2014), however it may also by caused by the limitations in the individual methodologies used, as it is a particularly difficult phenotype to measure.

4.1.5 Aims of this study

All of the results referred to above were obtained based on analyses using biparental RIL or doubled haploid (DH) populations. Therefore, only a limited range of allelic variation was explored in each population and opportunities to detect interactions between loci was limited. My aim, in this chapter, was to conduct a thorough genetic analysis of source-related traits in a large elite wheat eight-parent population offering more allelic diversity and more power to detect both small effects and interactions between loci than any previous study. To date, the only instance of use of the elite wheat 8-parent MAGIC population for the genetic dissection of 'source' traits has been conducted by Camargo *et al* (2018, 2016), based on a limited number of lines and a single growth season in a controlled environment.

The aims of the work presented in this chapter are as follows:

- Estimate the heritability of traits relating to biomass accumulation
- Calculate correlations between grain yield and crop biomass parameters
- Detect environmentally stable QTL regulating biomass accumulation
- Assess the significance of co-locating QTL governing different source traits

4.2 Results

4.2.1 Phenotypic variation and Correlation analysis

4.2.1.1 'Source' Traits

The primary traits analysed in this chapter are Crop Height - measured at multiple time points in cm, Green Area Index (GAI) - the percentage of green cover per unit area and Date of Anthesis - measured in days after the 1st May. As with the sink traits dealt with in Chapter 3, the 'source' traits dealt with in this Chapter are examined for their correlation with and impact on Grain Yield (GY) - measured in tonnes per hectare.

As the time series GAI data are capable of charting the growth and decline of the vegetative canopy, biologically relevant secondary traits were extracted from a spline curve model that interpolates data between points and extract potential growth indicators for biomass accumulation: Canopy Duration - measured as the number of days spent above 50% of maximum value; Maximum Green Value and Accumulated Green Cover - the area under the plotted curve and the Senescence Rate, measured as a percentage loss of green area per day from time of Maximum GAI to maturity.

4.2.1.2 Trait variability

The mean, variance, S.E., range and broad sense heritability were calculated for four primary and five derived traits, averaged over two years (harvest 2015 & 2016) and are displayed in Table 4.1.

Table 4.1 Sink phenotypes - descriptive statistics for Parents and Progeny. S.E. – Standard Error, H^2 – broad sense heritability. Three letter trait abbreviations will be used throughout the remainder of the Chapter and in the QTL names.

Trait	Trait Abbreviation	Mean		Variance		S.E		Min		Max		Range		H^2
		Parents	Progeny	Parents	Progeny	Parents	Progeny	Parents	Progeny	Parents	Progeny	Parents	Progeny	
Early Height	Eht	40.00	40.90	12.26	17.74	1.24	0.15	36.40	30.80	47.90	57.50	11.60	26.70	0.63
Final Height	Fht	64.70	66.80	15.87	37.32	1.41	0.21	58.10	48.10	72.00	88.40	13.90	40.3	0.70
Canopy Duration	Cdu	96.94	99.86	202.39	216.39	5.03	0.51	80.00	65.00	128.50	165.00	48.50	100	0.27
Maximum Green Value	Mgv	0.810	0.810	0.002	0.004	0.016	0.002	0.730	0.560	0.880	1.000	0.140	0.440	0.19
Accumulated Green Cover	Agc	81.32	84.00	12.99	155.82	1.27	0.44	75.34	42.84	87.70	132.47	12.35	89.63	0.12
Date of Anthesis	Da	39.61	39.65	17.38	11.90	1.47	0.12	29.93	26.47	43.46	48.35	13.54	21.89	0.71
Grain Yield	Yld	8.46	8.21	0.13	0.60	0.13	0.03	7.98	4.11	8.95	10.86	0.97	6.75	0.29
Senescence Rate	Snr	3.55	3.50	0.12	0.18	0.12	0.01	3.08	2.02	3.97	4.77	0.89	2.75	0.54

Using the Shapiro-Wilk test for normality, only two traits were statistically normally distributed; Accumulated Green Area and Maximum Green Value, both in 2014-15. However, when using large sample sizes such as these, even a small deviation from the normal will test as significant (Öztuna *et al*., 2006). Visually (Figure 4.1), most traits appear to follow a near-normal distribution, with notable exceptions: Anthesis Date in 2014-15 showed a bimodal distribution with a minority of the population flowering several days earlier than the mean, while in 2015-16 there was a more complex multi-modal distribution of Anthesis Dates, Maximum Green Value in 2015-16 has a truncated distribution due to the large number of lines reaching the maximum possible GAI of 1. For all traits, the phenotypic range of the progeny greatly exceeded the range of the parental lines indicating transgressive segregation; this can be clearly seen in Table 4.1 above and Figure 4.1 below. Predictably, Height and Anthesis Date were the most heritable traits, with heritabilities between 0.63 and 0.71, followed by Senescence Rate and Grain number m^{-2} at 0.54 and 0.38 respectively. These strong heritabilities lead us to expect strong genetic signals for these traits. The least heritable traits were Accumulated Green Area, Maximum Green Value and Time of Maximum Green Value, with heritabilities between 0.12 and 0.22, reflecting the inherent complexity of traits that represent integrative properties of the canopy growth curve over a prolonged period of time.

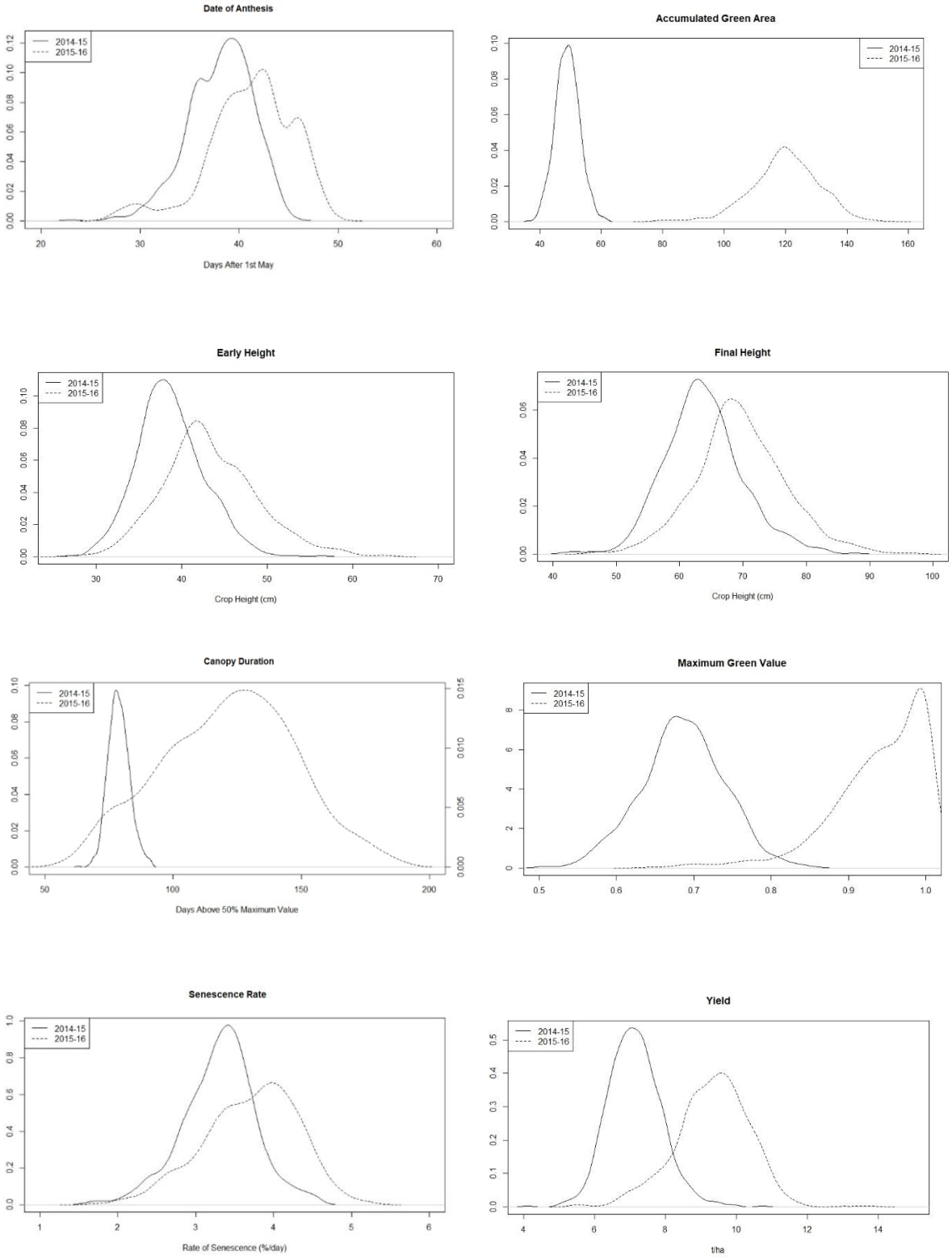

Figure 4-1 - Density plots showing the distribution of the spatially corrected trait data for the MAGIC RIL population in the 2014-15 vs 2015-16 field trials.

4.2.1.3 Between year correlations

Of the source traits measured, height and anthesis are the only traits that are highly correlated (PCC>0.5) across years (Figure 4.2). It was expected that these traits should be highly correlated between years due to their overall strong heritability and the large individual effects of the *Rht* and *Ppd* loci. Grain number m^{-2} was moderately correlated between years (PCC= 0.34). The lack of strong correlation (PCC= -0.05 – 0.16) between years for other traits suggests that more subtle, quantitative effects on canopy development are highly responsive to year-to-year variation in environmental parameters such as temperature and rainfall patterns (see Section 4.2.2).

4.2.1.4 Trait-trait correlations

Early Height is consistently negatively correlated with the date of anthesis in each year (PCC = -0.46 and -0.52); this probably reflects the fact that the minority of lines inheriting photoperiod-insensitivity from 'Soissons' begin stem extension some weeks earlier than the remainder of the population (the 'Soissons' *Ppd-D1a* allele confers an advancement in GS55 of 42d in a study of isogenic pairs – (Bentley *et al*., 2013)) and therefore there is a strong causal link between a determinant of Anthesis Date (the *Ppd-D1a* allele) and height of the canopy pre-booting (as only photoperiod-insensitive lines have begun stem extension at the date of measurement of Early Height (11-13th May). Anthesis and senescence maintain negative correlations in both years (PCC = -0.1 and -0.36 respectively), possibly reflecting the fact that late flowering lines fill grain and mature in the longest, hottest days of the year which hastens the rate of senescence relative to earlier flowering lines. All other trait-trait correlations were inconsistent from year to year. For example, the correlation between final height and yield obtained in 2014-15 (PCC = 0.02) was negligible compared to that seen in

2015-16 (PCC = 0.46). This is likely due to environmental stress reducing yields across the board in 2014-15 but without affecting height variation so strongly. The maximum green value and accumulated green area are inconsistently correlated (PCC= 0.88 and 0.17 in 2014-15 and 2015-16 respectively), as were maximum green value and the canopy duration (PCC= 0.01 and -0.45 in 2014-15 and 2015-16 respectively) and accumulated green area and canopy duration (PCC= 0.37 and 0.73 in 2014-15 and 2015-16 respectively). Grain number m^{-2} was inconsistently correlated with all traits with the exception of yield (PCC= 0.62 and 0.57 in 2014-15 and 2015-16 respectively). This strong correlation was expected as it is well established that increases in the grain number has traditionally been responsible for increases in yield.

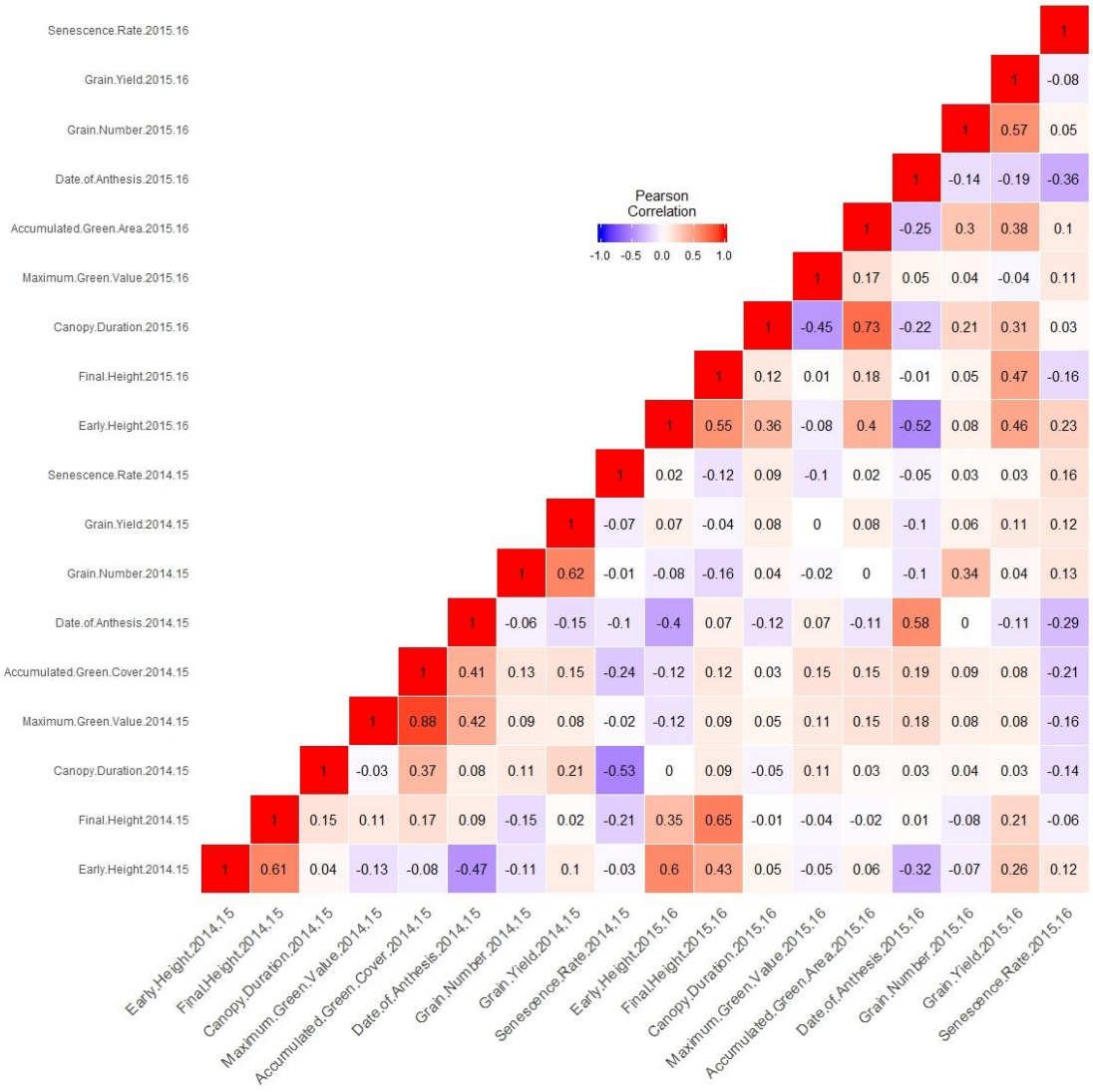

Figure 4-2 - Correlation matrix of Source phenotype data

4.2.2 Weather differences between seasons

Since most traits were poorly correlated between 2014/15 and 2015/16, weather data was examined with a view for identifying potential sources of differences in abiotic stress between the two seasons, which might be triggering differential genotype-dependant responses. As previously described, weather data was retrieved from the weather station at Sonning Farm, Sonning UK. Data can be seen below in Figure 4.3.

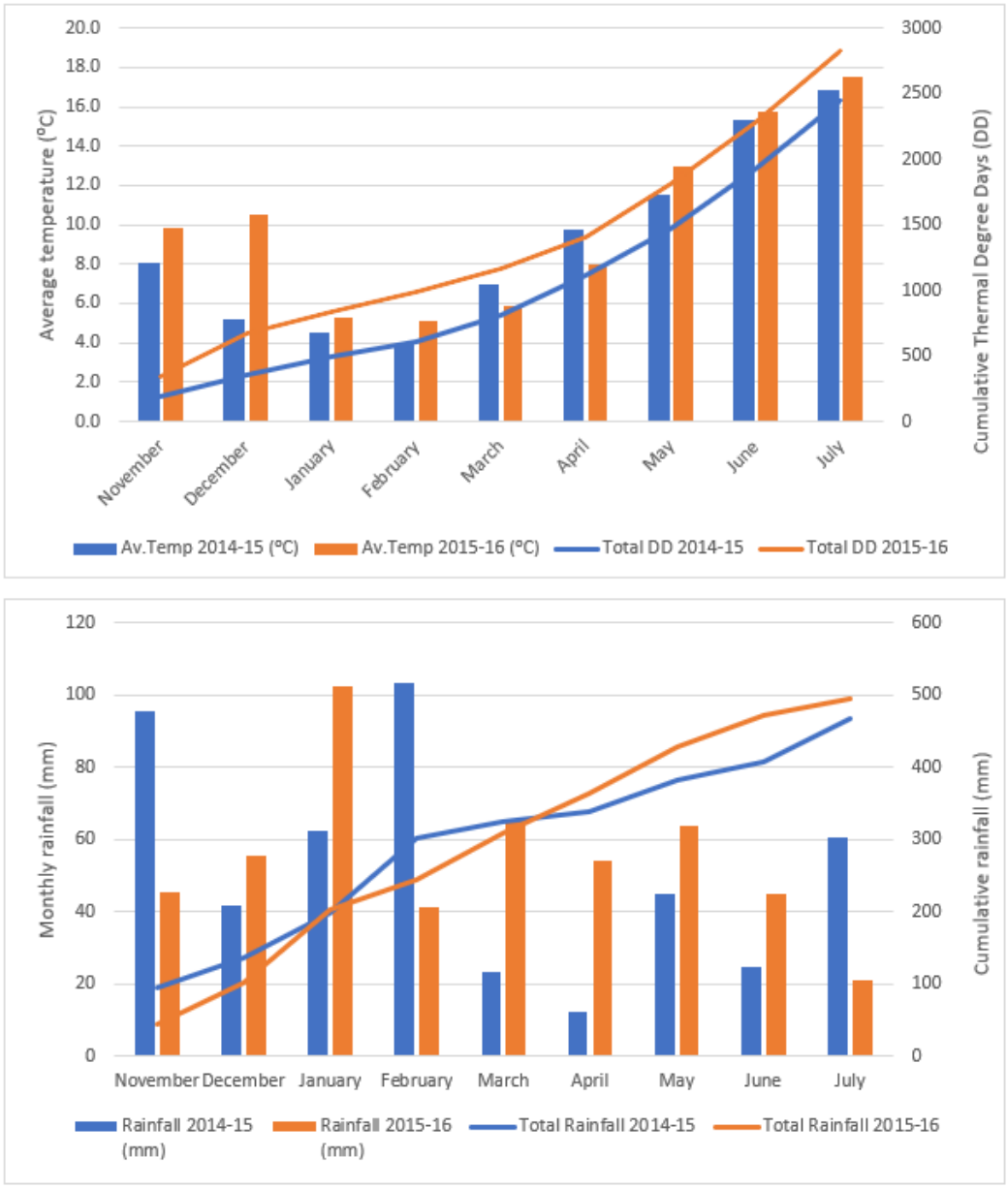

Figure 4-3 - A. Monthly average temperature (in °C, LHS y-axis) is plotted for 2014-15 (blue bars) and 2015-16 (orange bars) and as cumulative Thermal Degree Days (DD, RHS y-axis) for 2014-15 (blue line) and 2015-16 (orange line). Monthly average rainfall (in mm, LHS y-axis) is plotted for 2014-15 (blue bars) and 2015-16 (orange bars) and as cumulative rainfall (mm, RHS y-axis) for 2014-15 (blue line) and 2015-16 (orange line).

As shown in Figure 4.3, the 2014-15 season was characterised by a cool winter and relatively dry spring/early summer. In contrast, the 2015-16 season featured an unusually mild winter and a much more average rainfall with a well-distributed pattern across the spring and summer. Average temperatures between January and July are relatively comparable. However, looking at average rainfall between March and June, the main growth periods,

there was a total of 104.9mm rain in the period in 2015 compared to 227.8mm of rain in 2016 - a twofold increase. This sporadic rainfall in the 2014-15 season would have exacerbated the underlying spatial variability issue as described in Chapter 2 of this thesis. Overall, 2014-15 was lower yielding than 2015-16 by an average of 2.2t/ha, reached anthesis 3 days sooner and had a lower overall biomass (plant height, maximum green cover, accumulated green cover), all of which are highlighted in the density plots shown in Figure 4.1.

4.2.3 Mapping Quantitative Trait Loci for 'source' traits

In total, 106 significant, non-redundant QTL were discovered for the nine 'source' traits studied, plus yield (see Chapter 2 for details of significance criteria and methodology for determining redundancy between QTL). These are shown below in Table 4.2.

QTL	Chromosome	Left Marker	Right Marker	QTL Position	Left Marker Position	Right Marker Position	pvalue	-log10p	Percentage of phenotypic variation explained															
									Early Height		Final Height		Canopy Duration		Maximum Green Value		Accumulated Green Cover		Date of Anthesis		Grain Yield		Senescence Rate	
									2015	2016	2015	2016	2015	2016	2015	2016	2015	2016	2015	2016	2015	2016	2015	2016
Q.Agc-2016.UoR-1A	**1A**	***BS00010488_51***	***RAC875_c42700_264***	**0.00**	**0.00**	**1.01**	**8.39E-09**	**8.08**										**5.19**						
Q.Cdu-2016.UoR-1A	**1A**	***BS00010488_51***	***RAC875_c42700_264***	**0.00**	**0.00**	**1.01**	**4.09E-06**	**5.39**						**4.01**										
Q.Cdu-2015.UoR-1A	1A	*Tdurum_contig47183_205*	*RAC875_c11899_366*	57.08	57.08	63.47	1.84E-06	5.74					2.33											
Q.Da-2015.UoR-1A	**1A**	***BS00009866_51***	***BobWhite_c46349_402***	**75.12**	**73.62**	**75.12**	**4.82E-04**	**3.32**											**3.2**					
Q.Snr-2016.UoR-1A	**1A**	***BS00009866_51***	***BobWhite_c46349_402***	**75.12**	**73.62**	**75.12**	**1.15E-07**	**6.94**																**5.2**
Q.Agc-2016.UoR-1B	1B	*BS00037387_51*	*BobWhite_c14271_1379*	28.79	26.75	28.79	2.61E-05	4.58										3.1						
Q.Cdu-2016.UoR-1B	1B	*BobWhite_c44460_821*	*IACX8074*	299.25	291.21	299.25	3.08E-04	3.51						1.69										
Q.Da-2016.UoR-1B	1B	*Excalibur_c55186_351*	*wsnp_Ex_c11461_18489681*	349.59	345.42	349.59	2.39E-04	3.62												2.37				
Q.Da-2016.UoR-1D	1D	*Excalibur_c15692_532*	*tplb0061f07_1411*	25.28	24.28	25.28	1.26E-07	6.90												3.05				
Q.Cdu-2015.UoR-1D	1D	*D_F5XZDLF01A85DT_301*	*Excalibur_c24303_1145*	32.03	32.03	35.60	2.44E-04	3.61					2.07											
Q.Fht-2015.UoR-1D	**1D**	***Kukri_rep_c112609_711***	***BobWhite_rep_c65565_359***	**61.08**	**59.07**	**61.08**	**2.83E-09**	**8.55**			**4.95**													
Q.Fht-2016.UoR-1D	**1D**	***Kukri_rep_c112609_711***	***BobWhite_rep_c65565_359***	**61.08**	**59.07**	**61.08**	**2.41E-07**	**6.62**				**4.85**												
Q.Eht-2015.UoR-1D	1D	*BS00004282_51*	*BS00003816_51*	89.52	89.52	99.08	5.90E-07	6.23	2.26															
Q.Fht-2016.UoR-2A	2A	*Excalibur_rep_c105284_131*	*Excalibur_c25235_1178*	84.49	83.99	84.49	5.22E-04	3.28				1.41												
Q.Yld-2016.UoR-2A	**2A**	***Kukri_rep_c90581_382***	***Excalibur_c4847_631***	**102.38**	**102.38**	**103.90**	**7.75E-05**	**4.11**														**1.83**		
Q.Da-2016.UoR-2A	**2A**	***BS00021739_51***	***BobWhite_c12252_476***	**106.42**	**106.42**	**106.92**	**2.78E-04**	**3.56**												**3.02**				
Q.Agc-2016.UoR-2A	**2A**	***wsnp_Ex_c28204_37349164***	***wsnp_Ex_c2337_4379619***	**132.17**	**129.14**	**132.17**	**7.44E-12**	**11.13**										**7.03**						
Q.Cdu-2016.UoR-2A	**2A**	***BS00062757_51***	***BobWhite_c28819_733***	**135.19**	**134.69**	**135.19**	**3.45E-10**	**9.46**						**6.51**										
Q.Snr-2015.UoR-2B	2B	*Kukri_c19266_779*	*BobWhite_c12144_216*	3.53	2.53	3.53	1.12E-04	3.95															4.75	
Q.Cdu-2015.UoR-2B	2B	*RAC875_c5577_1682*	*BS00084668_51*	11.09	11.09	12.10	3.80E-06	5.42					4.23											
Q.Agc-2015.UoR-2B	2B	*Excalibur_c14396_1629*	*Excalibur_c1787_1199*	28.32	27.82	28.32	1.86E-09	8.73									5.25							
Q.Agc-2016.UoR-2B.1	2B	*Kukri_c63748_1453*	*wsnp_Ex_c19371_28311667*	35.38	34.88	35.38	6.38E-04	3.20										2.21						
Q.Mgv-2015.UoR-2B.2	2B	*Kukri_c3067_398*	*RFL_Contig1863_250*	48.39	39.92	48.39	2.58E-05	4.59							2.95									
Q.Mgv-2016.UoR-2B.1	2B	*BobWhite_c7786_376*	*BS00037345_51*	168.84	167.33	168.84	5.77E-05	4.24								2.32								
Q.Mgv-2016.UoR-2B.2	2B	*Ku_c34010_1016*	*Kukri_c6973_344*	188.99	188.49	188.99	8.49E-04	3.07								1.14								
Q.Agc-2016.UoR-2B.2				**243.11**	**241.07**	**243.11**	**3.08E-04**	**3.51**										**2.61**						
Q.Eht-2016.UoR-2B	**2B**	***Ex_c16948_754***	***BobWhite_c38001_528***	**243.11**	**241.07**	**243.11**	**1.90E-04**	**3.72**		**2.89**														
Q.Cdu-2016.UoR-2B				**243.11**	**241.07**	**243.11**	**4.56E-05**	**4.34**						**4.29**										
Q.Eht-2015.UoR-2B	2B	*Kukri_c4294_371*	*Excalibur_c1353_1364*	253.98	251.45	253.98	6.57E-04	3.18	0.93															
Q.Yld-2016.UoR-2B	2B	*BobWhite_c22728_78*	*BS00022805_51*	271.92	271.92	279.38	1.13E-04	3.95														2.14		
Q.Mgv-2016.UoR-2D	2D	*BS00010043_51*	*D_contig17313_245*	18.85	18.85	21.94	3.34E-04	3.48								4.06								
Q.Snr-2015.UoR-2D	2D	*BS00010043_51*	*D_contig17313_245*	18.85	18.85	21.94	4.91E-06	5.31															3.62	
Q.Da-2015.UoR-2D				**62.71**	**55.40**	**62.71**	**0.00E+00**	**20***											**10.78**					
Q.Da-2016.UoR-2D	**2D**	***Kukri_c27309_590***	***wsnp_CAP12_c1503_764765***	**62.71**	**55.40**	**62.71**	**1.04E-13**	**12.98**												**6.98**				
Q.Cdu-2016.UoR-2D				**62.71**	**55.40**	**62.71**	**4.36E-04**	**3.36**						**1.35**										
Q.Mgv-2015.UoR-2D				**62.71**	**55.40**	**62.71**	**5.99E-05**	**4.22**							**4.48**									
Q.Snr-2016.UoR-2D	2D	*Excalibur_c39215_100*	*D_contig28346_467*	78.27	77.77	78.27	2.06E-04	3.69																0.97
Q.Fht-2015.UoR-3A	3A	*BS00034334_51*	*BS00022516_51*	88.10	87.60	88.10	9.47E-06	5.02			3.33													
Q.Fht-2016.UoR-3A	3A	*RAC875_c30443_966*	*Ku_c103671_362*	97.97	97.47	97.97	6.39E-11	10.19				4.75												
Q.Eht-2015.UoR-3A	3A	*wsnp_Ku_c30545_40369365*	*BobWhite_c28950_147*	110.76	107.22	110.76	4.43E-04	3.35	2.39															
Q.Da-2015.UoR-3A	3A	*Excalibur_c60452_196*	*BS00078430_51*	111.27	111.27	111.77	1.51E-04	3.82											2.45					
Q.Agc-2015.UoR-3A	**3A**	***BS00056089_51***	***wsnp_Ex_c26887_36107413***	**176.22**	**174.70**	**176.22**	**3.42E-04**	**3.47**									**2.35**							
Q.TMgv-2015.UoR-3A	**3A**	***BS00056089_51***	***wsnp_Ex_c26887_36107413***	**176.22**	**174.70**	**176.22**	**7.72E-05**	**4.11**																
Q.Cdu-2015.UoR-3A	3A	*RAC875_c67998_96*	*BS00047668_51*	186.68	186.68	188.69	7.49E-04	3.13					2.02											
Q.Eht-2016.UoR-3A	3A	*Tdurum_contig56731_335*	*BS00100626_51*	194.73	194.23	194.73	3.78E-06	5.42		4.15														
Q.Mgv-2015.UoR-3B	3B	*RAC875_c60169_200*	*BS00044752_51*	44.77	44.77	47.31	4.10E-04	3.39							2.14									
Q.Agc-2015.UoR-3B	3B	*Excalibur_c5977_440*	*BS00035137_51*	165.01	164.00	165.01	5.80E-04	3.24									2.05							
Q.Yld-2015.UoR-4A	4A	*wsnp_Ex_c3988_7221220*	*RAC875_c6939_1042*	140.85	137.28	140.85	3.45E-05	4.46													1.55			
Q.Da-2016.UoR-4A	4A	*D_F5XZDLF02G9H4M_286*	*BobWhite_c43728_100*	154.19	151.14	154.19	1.70E-04	3.77												2.59				
Q.Da-2015.UoR-4A	4A	*BS00021957_51*	*Kukri_c3948_209*	158.24	157.74	158.24	8.70E-07	6.06											3.58					
Q.Fht-2016.UoR-4A	4A	*BobWhite_c25163_178*	*Excalibur_c74390_108*	210.20	210.20	210.70	3.73E-07	6.43				1.96												
Q.Yld-2016.UoR-4A	4A	*Excalibur_c10699_404*	*BobWhite_c38832_153*	214.75	214.75	217.29	1.31E-05	4.88														2.86		
Q.Snr-2015.UoR-4B	4B	*Kukri_c23338_624*	*Kukri_c26488_139*	25.91	19.24	25.91	1.17E-05	4.93															3.74	
Q.Eht-2016.UoR-4B	**4B**	***BS00100839_51***	***BS00023766_51***	**48.65**	**47.14**	**48.65**	**6.29E-06**	**5.20**		**0.43**														
Q.Eht-2015.UoR-4B	**4B**	***RAC875_c27536_611***	***CAP7_c1893_424***	**49.15**	**48.65**	**49.15**	**6.14E-12**	**11.21**	**1.89**															
Q.Fht-2015.UoR-4B				**50.16**	**50.16**	**51.16**	**2.61E-14**	**13.58**			**2.69**													
Q.Fht-2016.UoR-4B	**4B**	***Ra_c26080_461***	***BS00033614_51***	**50.16**	**50.16**	**51.16**	**1.23E-13**	**12.91**				**4.45**												
Q.Yld-2016.UoR-4B				**50.16**	**50.16**	**51.16**	**2.56E-04**	**3.59**														**1.62**		
Q.Yld-2015.UoR-4B	4B	*BS00067786_51*	*IACX5989*	75.09	75.09	78.18	1.98E-05	4.70													3.32			
Q.Snr-2016.UoR-4B	4B	*Ex_c32540_659*	*BS00096604_51*	92.89	92.39	92.89	1.70E-06	5.77																4
Q.Mgv-2015.UoR-4B	4B	*Jagger_c1432_289*	*wsnp_Ra_c2711_5148302*	105.13	105.13	105.63	4.07E-08	7.39							3.46									
Q.Agc-2015.UoR-4B	4B	*BS00022653_51*	*Kukri_c11415_1074*	111.24	111.24	112.25	5.55E-07	6.26									3.78							
Q.Da-2015.UoR-4B	4B	*BS00022830_51*	*Ku_c101046_1063*	159.51	158.50	159.51	1.58E-07	6.80											3.47					
Q.Eht-2015.UoR-4D	**4D**	***Kukri_rep_c68594_530***	***Excalibur_c19078_210***	**24.93**	**24.93**	**32.24**	**0.00E+00**	**35***	**12.32**															
Q.Eht-2016.UoR-4D				**32.24**	**32.24**	**40.11**	**2.22E-11**	**10.65**		**8.38**														
Q.Fht-2015.UoR-4D	**4D**	***Excalibur_c19078_210***	***RAC875_rep_c105718_304***	**32.24**	**32.24**	**40.11**	**0.00E+00**	**68***			**21.2**													
Q.Fht-2016.UoR-4D				**32.24**	**32.24**	**40.11**	**0.00E+00**	**25***				**8.48**												
Q.Mgv-2015.UoR-5A	5A	*BS00079189_51*	*RFL_Contig3674_847*	28.29	28.29	34.11	1.71E-06	5.77							1.51									
Q.Da-2016.UoR-5A.1	5A	*BS00041077_51*	*BobWhite_c19985_446*	62.59	62.09	62.59	5.39E-05	4.27												2.33				
Q.Snr-2016.UoR-5A	5A	*wsnp_Ex_c3838_6980774*	*BobWhite_c11512_157*	128.21	128.21	137.43	9.35E-04	3.03																2.6
Q.Eht-2016.UoR-5A	**5A**	***Tdurum_contig43844_1266***	***Excalibur_c1208_72***	**139.96**	**139.96**	**141.98**	**1.49E-06**	**5.83**		**3.47**														
Q.Da-2015.UoR-5A	**5A**	***Tdurum_contig43844_1266***	***Excalibur_c1208_72***	**141.98**	**139.96**	**141.98**	**1.25E-04**	**3.90**											**1.51**					
Q.Da-2016.UoR-5A.2	5A	*wsnp_Ex_c1279_2451582*	*BS00094342_51*	144.55	144.55	146.06	1.36E-05	4.87												2.25				
Q.Eht-2015.UoR-5A	5A	*Jagger_c6106_119*	*BS00068178_51*	169.34	169.34	169.84	3.01E-05	4.52	1.45															
Q.Agc-2016.UoR-5B	5B	*Kukri_c33299_519*	*BS00010213_51*	75.62	75.62	76.12	6.27E-04	3.20										3.33						
Q.Eht-2016.UoR-5B	5B	*BS00105054_51*	*Tdurum_contig12995_722*	156.19	155.69	156.19	3.20E-05	4.49		4.34														
Q.Da-2015.UoR-5B	5B	*BS00037103_51*	*Tdurum_contig50731_961*	218.58	218.58	220.08	4.67E-05	4.33											2.79					
Q.Yld-2016.UoR-5B	5B	*Excalibur_c1925_2569*	*BobWhite_c39214_164*	229.16	227.12	229.16	2.05E-12	11.69														6.02		
Q.Cdu-2015.UoR-5B	5B	*Excalibur_c71712_180*	*RFL_Contig3285_1009*	301.22	300.72	301.22	1.96E-04	3.71					2.62											
Q.Da-2016.UoR-5D	5D	*BS00108733_51*	*BobWhite_c7263_337*	49.43	38.25	49.43	1.33E-04	3.88												2.55				
Q.Fht-2015.UoR-6A	6A	*Kukri_c27958_334*	*wsnp_CAP7_c399_215824*	96.41	96.41	98.45	4.64E-05	4.33			4.09													
Q.Mgv-2016.UoR-6A	6A	*Kukri_c21413_107*	*BS00003881_51*	122.39	122.39	123.90	1.43E-05	4.84								3.08								
Q.Eht-2016.UoR-6A	**6A**	***Kukri_c77911_260***	***BobWhite_c20706_135***	**131.94**	**131.44**	**131.94**	**6.92E-06**	**5.16**		**2.58**														
Q.Fht-2016.UoR-6A	**6A**	***BobWhite_c20706_135***	***BS00022605_51***	**132.95**	**131.94**	**132.95**	**5.15E-08**	**7.29**				**2.92**												
Q.Eht-2016.UoR-6B	6B	*BobWhite_c11301_226*	*Excalibur_c20083_433*	142.38	137.71	142.38	1.84E-05	4.74		2.66														
Q.Da-2016.UoR-6B	6B	*BS00054287_51*	*Excalibur_c22998_621*	158.18	158.18	159.18	1.89E-04	3.72												1.53				
Q.Fht-2016.UoR-6D	6D	*Kukri_c31995_1948*	*wsnp_Ra_c13881_21836489*	120.26	120.26	120.76	3.43E-08	7.46				3.13												
Q.Da-2015.UoR-7A	7A	*BS00078460_51*	*Ex_c9615_1202*	105.98	104.98	105.98	8.38E-05	4.08											2.31					
Q.Fht-2016.UoR-7A	7A	*BobWhite_c8366_563*	*BS00044040_51*	204.19	204.19	205.19	1.70E-04	3.77				2.44												
Q.Cdu-2015.UoR-7A	7A	*CAP7_c10038_214*	*Excalibur_c47990_159*	243.07	242.57	243.07	4.70E-04	3.33					2.36											
Q.Yld-2016.UoR-7A	7A	*BS00063458_51*	*RAC875_c67826_84*	276.69	275.17	276.69	2.14E-05	4.67														1.11		
Q.Yld-2015.UoR-7A	7A	*RAC875_c13093_86*	*wsnp_Ex_c7071_12171619*	318.37	318.37	321.39	1.21E-07	6.92													4.33			
Q.Yld-2015.UoR-7B	**7B**	***RFL_Contig6075_1128***	***Tdurum_contig5352_556***	**0.00**	**0.00**	**6.39**	**3.30E-04**	**3.48**													**1.55**			
Q.Yld-2016.UoR-7B.1	**7B**	***RFL_Contig6075_1128***	***Tdurum_contig5352_556***	**0.00**	**0.00**	**6.39**	**7.77E-06**	**5.11**														**1.68**		
Q.Yld-2016.UoR-7B.2	7B	*RAC875_c10932_1697*	*BS00022550_51*	66.08	64.06	66.08	1.81E-04	3.74														0.9		
Q.Eht-2015.UoR-7B	7B	*RAC875_c34012_983*	*BS00023884_51*	237.78	237.78	238.79	7.13E-05	4.15	3.04															
						Total Variation Explained			24.28	28.90	36.26	34.39	15.63	17.85	19.59	10.60	13.43	23.47	30.09	26.67	10.75	18.16	12.11	12.77

Table 4.2 – QTL table for source-related traits, QTL names follow standard format as described in Chapter 2. Trait abbreviations are as shown in Table 4.1. Left and Right Marker Positions are the location of the markers in cM, p-value is the significance of the QTL and -log10p is the strength of the QTL.

4.2.3.1 Maximum Green Value

A total of 10 significant (-log10p ≥ 3) QTL for the Maximum Green Value were found on chromosomes 2B, 2D, 3B, 4B, 4D, 5A and 6A (Table 4.2).

Combined, these QTL explained 19.6% and 10.6% of the total variation in the Maximum Green Value in the 2015-16 and 2015-14 seasons analyses respectively. In the 2014-15 analysis, approximately half of the variation explained by the QTL are accounted for by the two strongest QTL: *Q.Mgv-2015.UoR-2B.1* (*p*= 1.72E-06, %var= 5.05); *Q.Mgv-2015.UoR-2D* (*p*= 5.99E-05, %var= 4.48). In the 2015-16 analysis, the single strongest QTL, *Q.Mgv-2016.UoR-2D* (*p*= 3.34E-04, %var= 4.06%) accounted for less than half of the total variation. The remaining 7 QTL explained between 1.14% and 3.46% of the variation in the relevant year. For this trait, all 10 significant QTL were year-specific i.e. no QTL was found in the same location in both years.

4.2.3.2 Canopy Duration

A total of 11 significant (-log10p ≥ 3) QTL for the canopy duration were found on chromosomes 1A, 1B, 1D, 2A, 2B, 2D, 3A, 5B and 7A (Table 4.2).

Combined, these QTL explain 15.63% and 17.85% of the total variation in the canopy duration in the 2015-14 and 2015-16 seasons respectively. In 2014-15, the strongest QTL explained approximately a quarter of the variation; *Q.Cdu-2015.UoR-2B* (*p*= 3.80E-06, %var= 4.23). The remaining QTL from this analysis each averaged 2.28% of the variation explained. In the 2015-16 analysis, the strongest three QTL explain the majority of the total variation explained: *Q.Cdu-2016.UoR-1A* (*p*= 4.09E-06, %var= 4.01)*; Q.Cdu-2016.UoR-2A* (*p*= 3.45E-10, %var= 6.51); *Q.Cdu-2016.UoR-2B* (*p*= 4.56E-05, %var= 4.29). The remaining 7 QTL explained between 1.35% and 2.62% of the variation in the

relevant year. For this trait again, all 11 significant QTL were year-specific, with no overlap between years.

4.2.3.3 Accumulated Green Cover

A total of 10 significant (-log10p ≥ 3) QTL for the Accumulated Green Cover were found on chromosomes 1A, 1B, 2A, 2B, 3A, 3B, 4B and 5B (Table 4.2).

Combined, these QTL explain 13.43% and 23.47% of the total variation in Accumulated Green Cover in the 2015-14 and 2015-16 seasons respectively. In 2014-15, the two strongest QTL explained over half of the total variation explained: *Q.Agc-2015.UoR-2B* (*p*= 1.86E-09, %var= 5.25); *Q.Agc-2015.UoR-4B* (*p*= 5.55E-07, %var= 3.78). In the 2015-16 analysis, the two strongest QTL explained approximately half of the total variation explained: *Q.Agc-2016.UoR-1A* (*p*= 8.39E-09, %var= 5.19); *Q.Agc-2016.UoR-2A* (*p*= 7.44E-12, %var= 7.03). *Q.Agc-2015.UoR-2B* (27.8-28.3cM) and *Q.Agc-2016.UoR-2B.1* (34.9- 35.4cM) were both significant (*p value* e-4 to e-9), explained 2.21 and 5.25% variation respectively and may actually be a single QTL. The remaining QTL explained between 2.05 and 3.33% of the variation in the relevant year and were all year-specific.

4.2.3.4 Senescence

A total of 7 significant (-log10p ≥ 3) QTL for Senescence were found on chromosomes 1A, 2B, 2D, 3A, 3B, 4B and 5A (Table 4.2).

Combined, these QTL explain 12.11% and 12.77% of the total variation in the Senescence in the 2015-14 and 2015-16 seasons analyses respectively. In 2014-15, three QTL explained similar amounts of variation: *Q.Snr-2015.UoR-2B* (*p*= 1.12E-04, %var= 4.75); *Q.Snr-2015.UoR-2D* (*p*= 4.91E-06, %var= 3.62); *Q.Snr-2015.UoR-4B* (*p*= 1.17E-05,

%var= 3.74). In the 2015-16 season, three quarters of the variation is explained by the strongest two QTL: *Q.Snr-2016.UoR-1A* (*p*= 1.15E-07, %var= 5.20); *Q.Snr-2016.UoR-4B* (*p*= 1.70E-06, %var= 4.00). The remaining QTL explained between 0.97 and 2.6% of the variability. Yet again, all seven QTL were year specific.

4.2.3.5 Grain Yield

A total of 12 significant (-log10p ≥ 3) QTL for Yield were found on chromosomes 2A, 2B, 4A, 4B, 5B, 7A and 7B (Table 4.2).

Combined, these QTL explain 10.75% and 18.16% of the total variation in Grain Yield in the 2015-14 and 2015-16 seasons respectively. In 2014-15, three quarters of the variation is explained by the strongest two QTL: *Q.Yld-2015.UoR-4B* (*p*= 1.98E-05, %var= 3.32); *Q.Yld-2015.UoR-7A* (*p*= 1.21E-07, %var= 4.33). In 2015-16, one third of the variation explained was due to the single strongest QTL: *Q.Yld-2016.UoR-5B* (*p*= 2.05E-12, %var= 6.02). *Q.Yld-2015.UoR-7B (p=3.30E-04, %var =1.55) and Q.Yld-2016.UoR-7B.1 (p=7.77E-06, %var =1.68)* were the only Yield QTL found in both years, located between 0.0- 6.39cM on chromosome 7B. Both were significant (*p*= e-4 to e-6) and explained 1.55 to 1.68% of the total variation. All remaining Yield QTL were year specific.

4.2.3.5 Grain number m^{-2}

A total of 10 significant (-log10p ≥ 3) QTL for grain number were found on chromosomes 2B, 3A, 3B, 4D, 5B, 6A and 7A (Table 4.2).

Combined, these QTL explain 11.76% and 21.49% of the total variation in Grain number m^{-2} in the 2015-16 and 2015-14 seasons respectively. In 2014-15, half of the variation explained is explained by the strongest two QTL: *Q.GNO-2015.UoR-4D* (p= 2.10E-08, %var=

6.11); *Q.GNO-2015.UoR-2B* (p= 6.35E-06, %var= 3.98). In 2015-16, half of the variation explained is explained by the strongest two QTL: *Q.GNO-2016.UoR-4D* (p= 1.19E-05, %var= 3.51); *Q.GNO-2016.UoR-7A* (p= 5.30E-06, %var= 3.02). Two pairs of QTL were consistent across both years: *Q.GNO-2015.UoR-4D* and *Q.GNO-2016.UoR-4D,* located 32.24 - 40.61cM, explaining 6.11 and 3.51% of the total variation; Q.GNO-2015.UoR-7A.2 and Q.GNO-2016.UoR-7A, located at 361.19 - 366.73cM, explaining 3.44 and 3.02% of the total variation. All remaining grain number QTL were year specific.

4.2.4 Co-location of QTL for driver and output traits

Multi-trait QTL analysis enables us to identify QTL that may have pleiotropic effects on several agronomically important traits. Pleiotropy, according to K.B.Low is defined as "the condition where a single mutation causes more than one observable phenotypic effect or change in characteristic." In examining the co-location of QTL for different traits, therefore, we are entertaining the hypothesis that the same gene variant may impact either directly or indirectly on the expression of two or more traits, although it may not be easy to differentiate between pleiotropy and tight linkage, where the traits in question may be controlled by adjacent genes that are so close together that we are unlikely to observe recombination between them. With 102 QTL distributed over 20 chromosomes (7D being the exception), it is likely that some pairs of QTL for different traits will co-locate merely by chance. However, as we have seen in section 4.2.1.4, some traits are highly and consistently correlated from year to year, and therefore there is an expectation that correlated traits will share overlapping genetic architecture. Different criteria are used here to judge whether QTL for different traits co-locate due to pleiotropy or chance linkage. First, pleiotropy is favoured over chance linkage if there are well-founded biological reasons to suppose that an increase in the value of trait *x*

would lead to the observed direction of change in trait *y*. However, if the biological or mechanistic reasoning is supported by observation of consistent relative size and direction of parental effects for the traits in question, pleiotropy is far more likely to be the correct explanation. In principle, looking at co-location also provides the opportunity to identify QTL for yield which are relatively independent from phenology i.e. rather than impacting shifting key stages of development with respect to the peak of resource availability within the testing environment, they encode additive effects that increase efficiency of resource capture, leading to increased biomass and better yield. Such QTL would be extremely significant for breeding purposes (Pinto *et al*., 2010; Reynolds *et al*., 2009). Loci where two or more QTL co-located were identified on chromosomes 1A, 2A, 2B, 2D, 3A, 4B, 4D, 5A, 6A and 7B.

4.2.4.1 Chromosome 1A

On chromosome 1A, two sets of co-locating QTL were observed for: accumulated green cover and canopy duration; date of anthesis and senescence rate (Figure 4.4). *Q.Agc-2016.UoR-1A* and *Q.Cdu-2016.UoR-1A* are co-located between markers *BS00010488_51* and *RAC875_c42700_264* (0.00 - 1.00cM), explaining 4.01 and 5.19% of the total phenotypic variation respectively. *Q.Da-2015.UoR-1A* and *Q.Snr-2016.UoR-1A* also co-locate on 1A, between markers *BS00009866_51* and *BobWhite_c46349_402* (73.61 - 75.12cM), explaining 3.5 and 5.2% of the total phenotypic variation respectively. The two QTL are likely to be pleiotropic as: A. the correlation between Agc and Cdu in 2016 was 0.73, B. the same subsets of parents had increasing and decreasing alleles for the QTL and biologically, it is plausible that an increase in Canopy Duration (Cdu) would be

accompanied by an increase in the area under the GAI curve (Agc). Da and Snr co-locating is unlikely to be significant, as it only appeared in separate years.

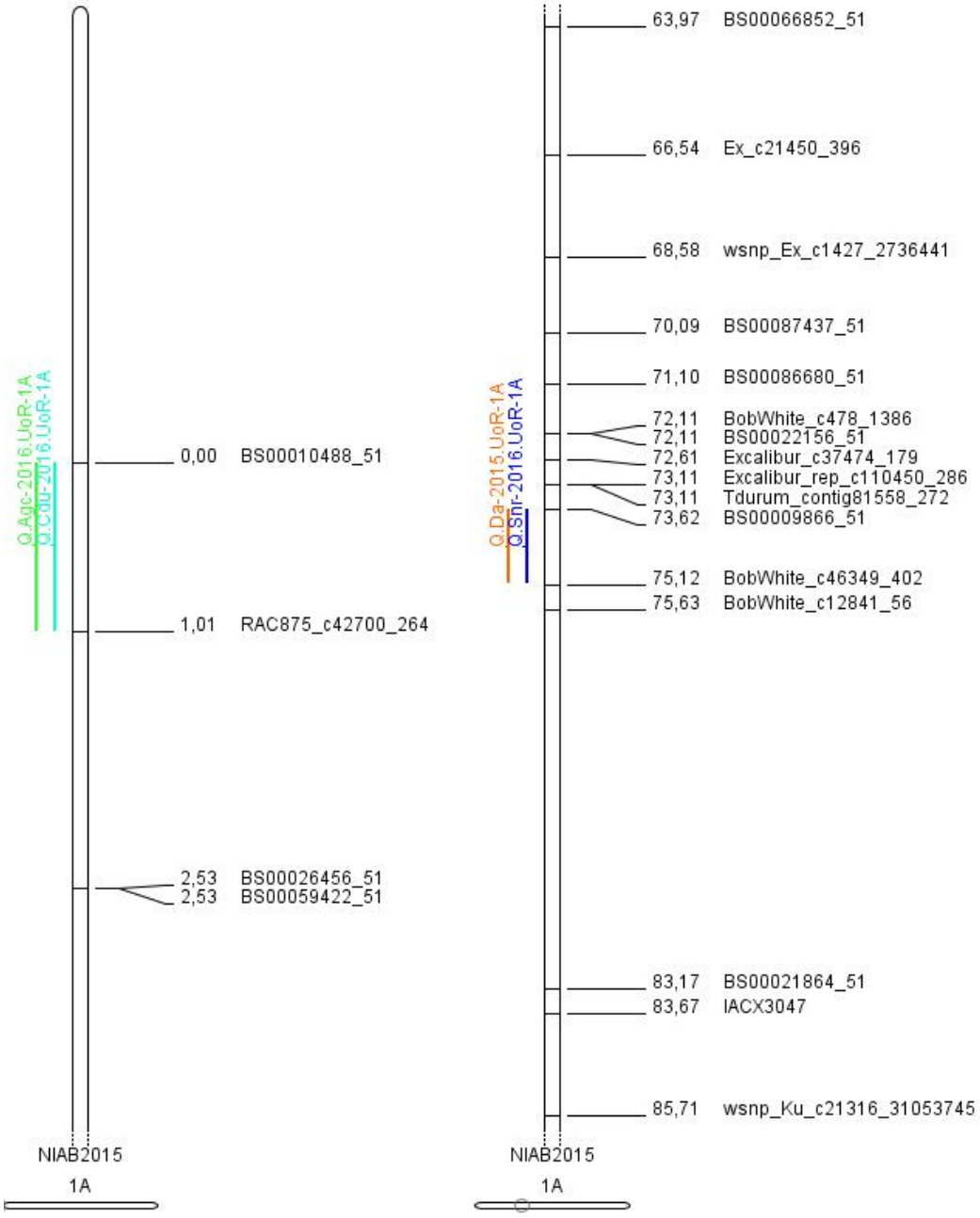

Figure 4-4 - Fragments of chromosome 1A showing co-locating QTL for Accumulated green cover (green bar), Canopy duration (light blue bar), Date of Anthesis (orange bar) and Senescence rate (dark blue bar).

4.2.4.2 Chromosome 2A

On chromosome 2A, two sets of co-locating QTL were observed for: Yield and date of anthesis; accumulated green cover and canopy duration (Figure 4.5). *Q.Yld-2016.UoR-*

2A and *Q.Da-2016.UoR-2A* are co-located between markers *Kukri_rep_c90581_382* and *BobWhite_c12252_476* (102.4 – 106.9cM), explaining 1.83 and 3.02% of the total phenotypic variation respectively. *Q.Agc-2016.UoR-2A* and *Q.Cdu-2016.UoR-2A* also co-locate on 2A, between markers *wsnp_Ex_c28204_37349164* and *BobWhite_c28819_733* (129.13 – 135.19cM), explaining 7.03 and 6.51% of the total phenotypic variation respectively.

The two QTL are likely to be pleiotropic, as the correlation between Yld and Da in 2016 was -0.19, and the same subsets of parents had opposite increasing and decreasing alleles for the QTL. Agc and Cdu in 2016 had a correlation of 0.73, and the same subsets of parents had increasing and decreasing alleles for the QTL and biologically at this location as well.

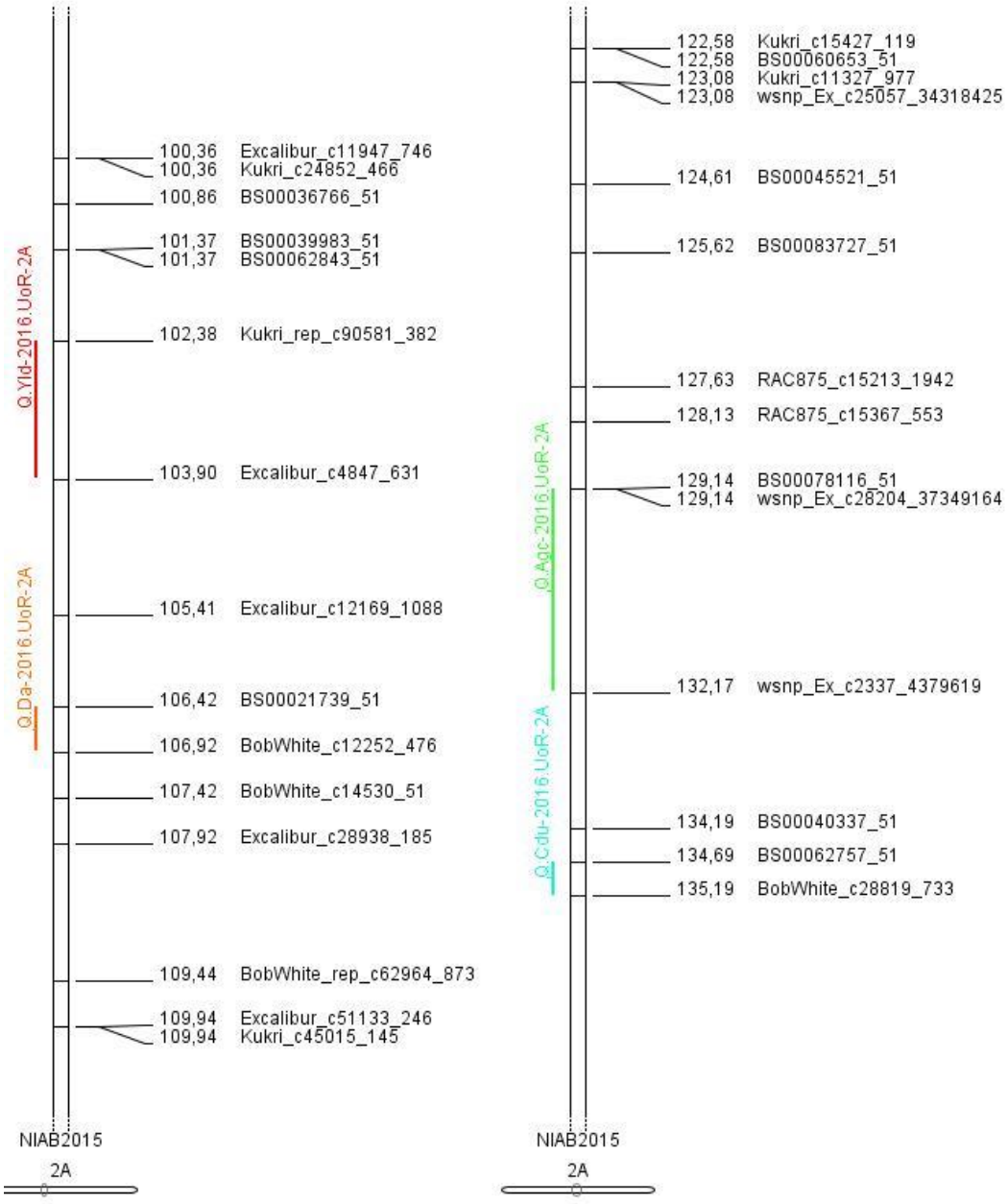

Figure 4-5 - Fragments of chromosome 2A showing co-locating QTL for Accumulated green cover (green bar), Canopy duration (light blue bar), Date of Anthesis (orange bar) and Grain Yield (red bar).

4.2.4.3 Chromosome 2B

On chromosome 2B, two sets of co-locating QTL were observed for: accumulated green cover and maximum green value; early height, accumulated green cover and canopy duration (Figure 4.6). *Q.Agc-2015.UoR-2B* and *Q.Mgv-2015.UoR-2B.1* were co-locating

between markers *Excalibur_c14396_1629* and *Excalibur_c1787_1199* (27.82 - 28.32cM), explaining 5.25 and 5.05% of the total phenotypic variation respectively. There is also a cluster for *Q.Agc-2016.UoR-2B.2, Q.Eht-2016.UoR-2B* and *Q.Cdu-2016.UoR-2B* between markers *Ex_c16948_754* and *BobWhite_c38001_528* (241.07 - 243.11cM) explaining 2.61, 2.89 and 4.29% of the total phenotypic variation respectively.

The two QTL are likely to be pleiotropic as: the correlation between Agc and Mgv in 2015 was 0.88, and the same subsets of parents had increasing and decreasing alleles for the QTL with the exception of Hereward. In the 2015 environment, the Agc was significantly shorter, so it is plausible that the Mgv would have played a much larger part in the Agc.

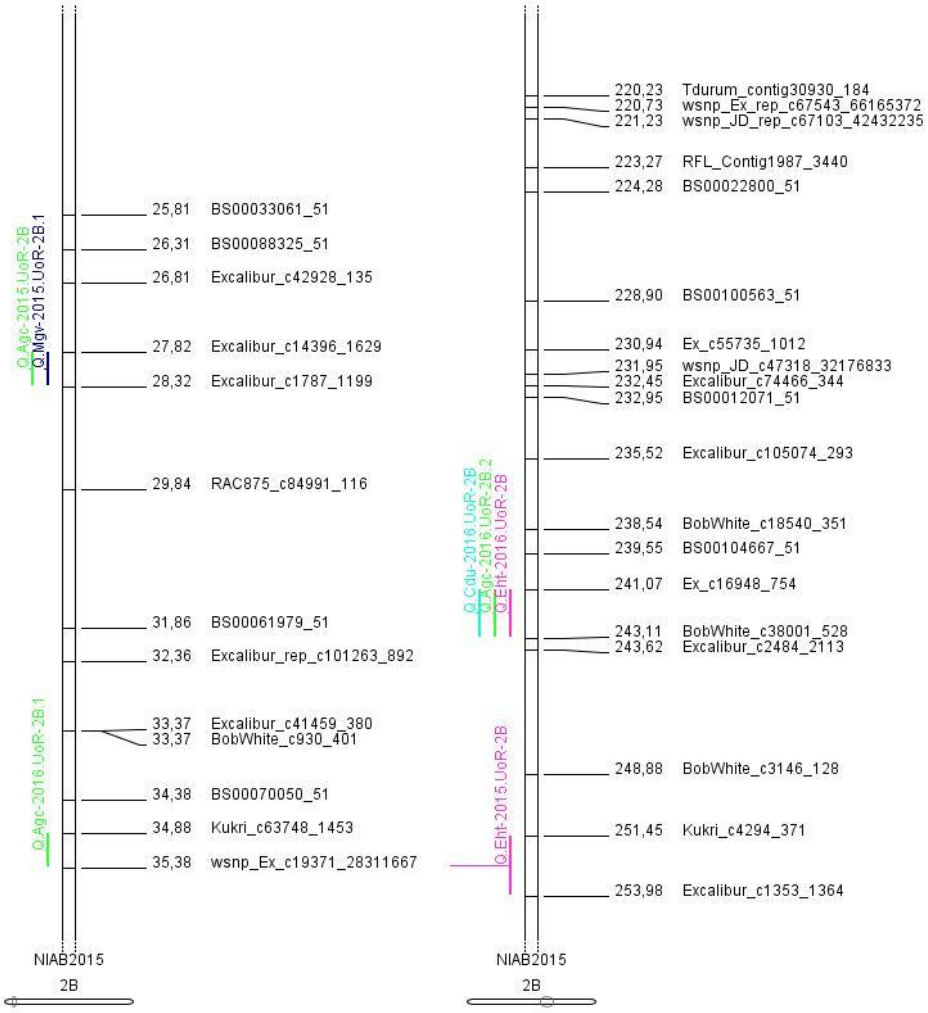

Figure 4-6 - Fragments of chromosome 2B showing co-locating QTL for Accumulated green cover (green bar), Canopy duration (light blue bar), Maximum green value (black bar) and Early height (pink bar)

4.2.4.4 Chromosome 2D

On chromosome 2D, two sets of co-locating QTL were observed (Figure 4.7). Maximum green value and senescence rate; *Q.Mgv-2016.UoR-2D* and *Q.Snr-2015.UoR-2D* were co-locating between markers *BS00010043_51* and *D_contig17313_245* (18.84 - 21.94cM), representing 4.06 and 3.62% of the total phenotypic variation explained. There is a second cluster of QTL controlling Days to Anthesis, Canopy Duration and Maximum Green Value involving *Q.Da-2015.UoR-2D, Q.Da-2016.UoR-2D, Q.Cdu-2016.UoR-2D* and *Q.Mgv-2015.UoR-2D* between markers *Kukri_c27309_590* and

snp_CAP12_c1503_764765 (55.40 – 62.71cM), explaining 10.78, 6.98, 1.35 and 4.48% of the total phenotypic variation respectively. The Soissons alleles of *Q.Da-2015.UoR-2D* and *Q.Da-2016.UoR-2D* cause flowering 4 days earlier than the average of the other founders and can therefore be identified as the *Ppd-D1a* photoperiod insensitivity allele, known to be located in this region and known to be carried only by Soissons amongst the eight-elite wheat MAGIC population. We can conclude that the effects on Canopy Duration in 2016 and Maximum Green Area in 2015 are pleiotropic effects of *Ppd-D1* allelic status, due to the similar size and the direction of the parental effects.

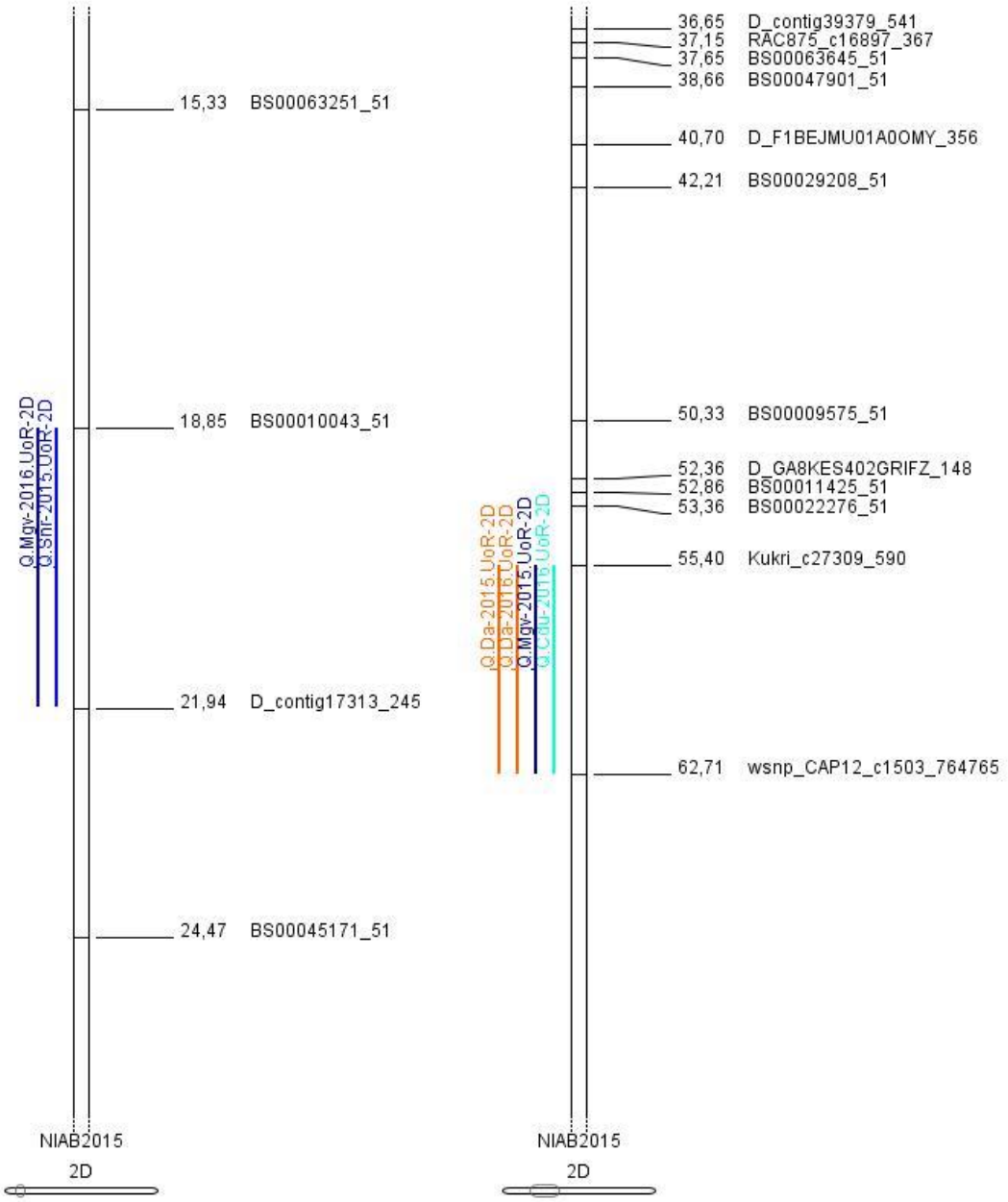

Figure 4-7- Fragments of chromosome 2D showing co-locating QTL for Senescence rate (dark blue bar), Canopy duration (light blue bar), Maximum green value (black bar) and Canopy duration (light blue bar).

4.2.4.5 Chromosome 4B

On chromosome 4B, there was one cluster of co-locating yield and height QTL (Figure 4.8). *Q.Eht-2016.UoR-4B, Q.Eht-2015.UoR-4B, Q.Fht-2015.UoR-4B, Q.Fht-2016.UoR-4B* and *Q.Yld-2016.UoR-4B* are co-locating between markers *BS00100839_51* and

BS00033614_51 (47.13 - 51.16cM), explaining 0.43, 1.89, 2.69, 4.45 and 1.62% of the total phenotypic variation respectively. Founder effects for *Q.Fht-2016.UoR-4B* and *Q.Yld-2016.UoR-4B* mirror each other with inheritance of Robigus or Soissons alleles decreasing height and increasing yield, whilst alleles inherited from the remaining six parents increase height and decrease yield, this is likely to be a pleiotropic effect of height reduction controlled by *Rht-B1b*, a dwarfing gene carried by two of the eight parents - Robigus and Soissons - altering the harvest index and decreasing lodging risk, both of which directly impact yield. It is notable that the *Rht-B1b* effect only explained yield in the high-yielding 2015-16 season.

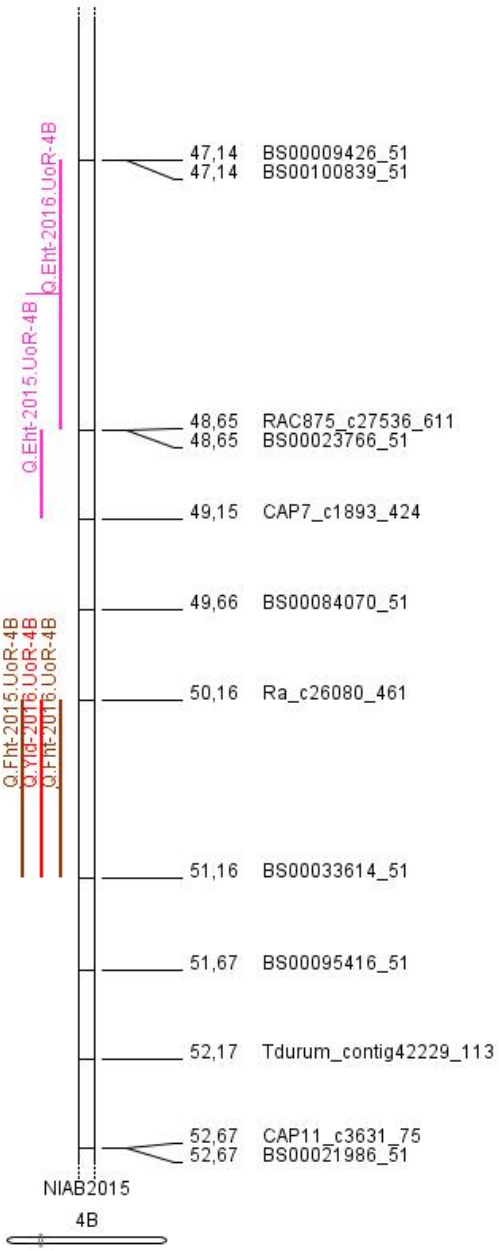

Figure 4-8 - Sections of chromosome 4B with co-locating markers Fragments of chromosome 2A showing co-locating QTL for Early height (pink bar), final (brown bar) and Grain yield (red bar).

4.2.4.6 Chromosome 4D

On chromosome 4D, there was one cluster of co-locating QTL observed for: early height, final height and grain number m^{-2} (Figure 4.9). *Q.Eht-2015.UoR-4D, Q.Eht-2016.UoR-4D, Q.Fht-2015.UoR-4D, Q.Fht-2016.UoR-4D, Q.GNO-2015.UoR-4D* and *Q.GNO-2016.UoR-*

4D are co-locating between *Kukri_rep_c68594_530* and *RAC875_rep_c70284_235* (24.93 – 49.47cM), explaining 12.32, 8.38, 21.2, 8.48, 6.11 and 3.51% of the total phenotypic variation respectively. These are likely to be the *Rht-D1b* gene, inherited from six of the eight parents - although the "perfect" marker (wMAS000002_Rht-D1) was not included in the genetic map for the MAGIC population. The differences in the variation explained and the strength of the QTL indicate that *Rht-D1b* is a stronger determinant of final height than early height and has more of a role in determining final height in unfavourable conditions (explaining 21.2% of final variation in 2014-15, as opposed to only 8.48% in 2015-16). *Rht-D1b* is known to affect the number of grain by altering the harvest index, however the low amount of variation explained here shows that this is only a small part of the overall process.

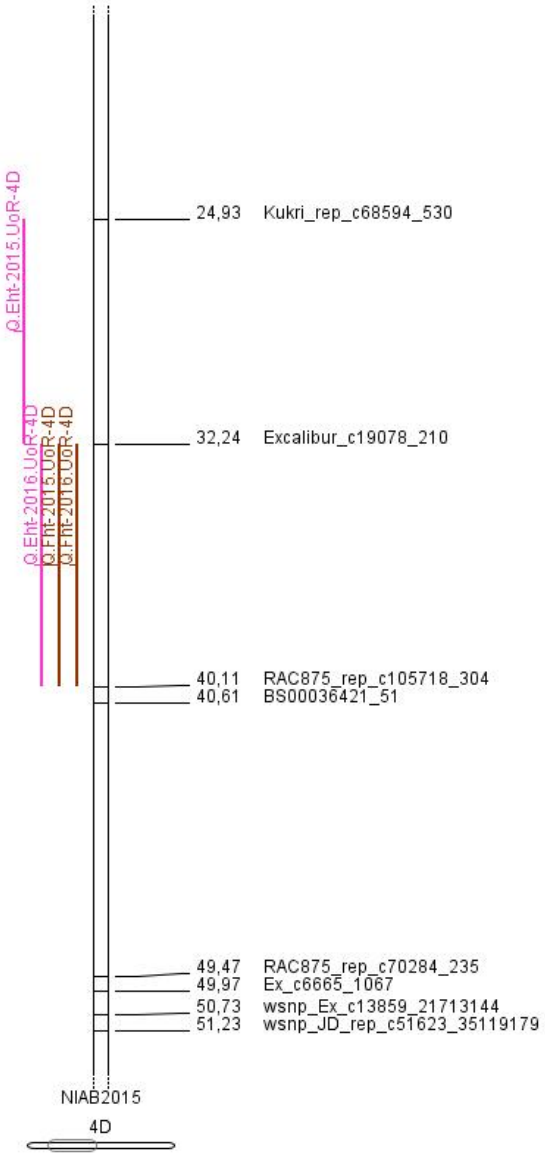

Figure 4-9 - Fragment of chromosome 4D showing co-locating QTL for Early height (Pink bar) and Final height(Brown bar).

4.2.4.7 Chromosome 5A

On chromosome 5A, there was one cluster of co-locating QTL observed for: early height and date of anthesis (Figure 4.11). *Q.Eht-2016.UoR-5A* and *Q.Da-2015.UoR-5A* are co-locating between markers *Tdurum_contig43844_1266* and *Excalibur_c1208_72* (139.95 – 141.98cM), explaining 3.47 and 1.51% of the total phenotypic variation respectively.

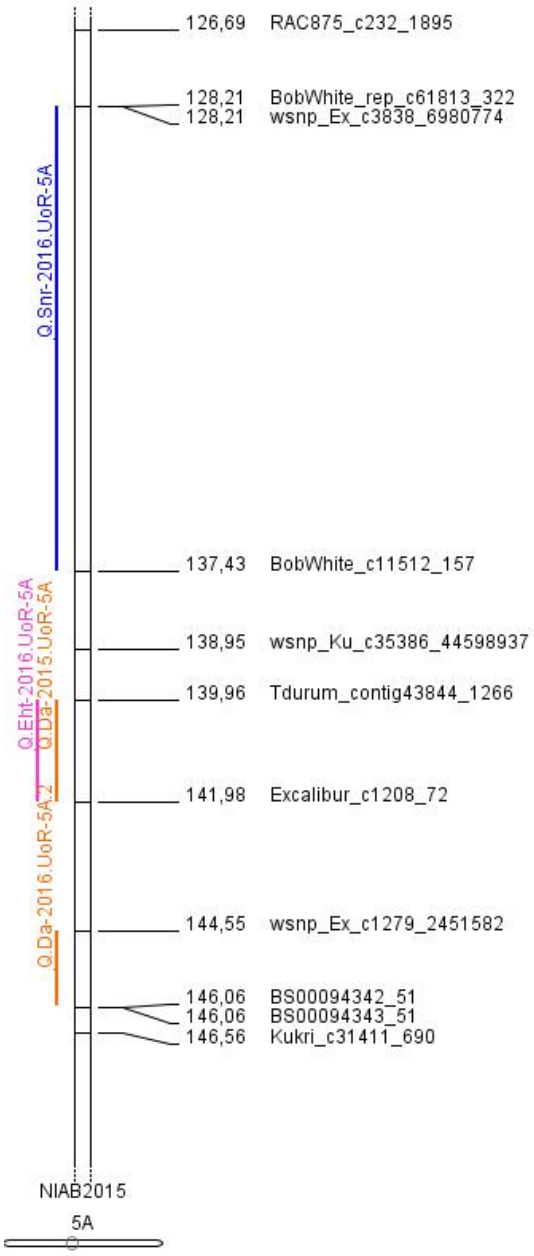

Figure 4-10 - Fragment of chromosome 5A showing co-locating QTL for Early height (Pink bar), Senescence rate (dark blue bar) and Date of Anthesis (orange bar).

4.2.4.8 Chromosome 6A

On chromosome 6A, there was one cluster of co-locating QTL observed for: early height and final height (Figure 4.11). *Q.Eht-2016.UoR-6A* and *Q.Fht-2016.UoR-6A* are co-locating between markers *Kukri_c77911_260* and *BS00022605_51* (131.44 – 132.95), explaining 2.58 and 2.92% of the total phenotypic variation respectively. Despite a high

correlation between these traits in 2016 (PCC= 0.55), it is unlikely these QTL are pleiotropic, as there were no consistencies on increasing and decreasing allelic affects from the parents.

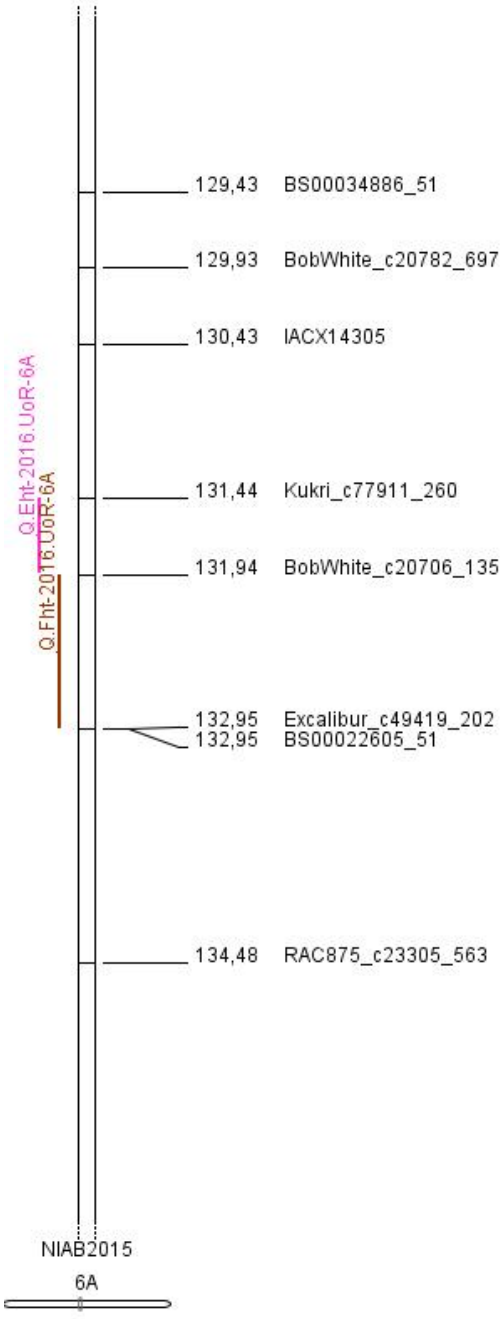

Figure 4-11 - Fragment of chromosome 6A showing co-locating QTL for Early height (Pink bar) and Final height (orange bar).

4.2.4.9 Chromosome 7B

On chromosome 7B, there was one cluster of co-locating yield QTL (Figure 4.12). Q.Yld-2015.UoR-7B and Q.Yld-2016.UoR-7B.1 are co-locating between RFL_Contig6075_1128 and Tdurum_contig5352_556 (0.00 - 6.39cM), explaining 1.55 and 1.68% of the total phenotypic variation respectively. Despite the relatively low variation explained, this is significant as one of the few QTL that are consistent across both years, and intriguingly appears to be independent of the source and sink (Chapter 3) traits that have been measured.

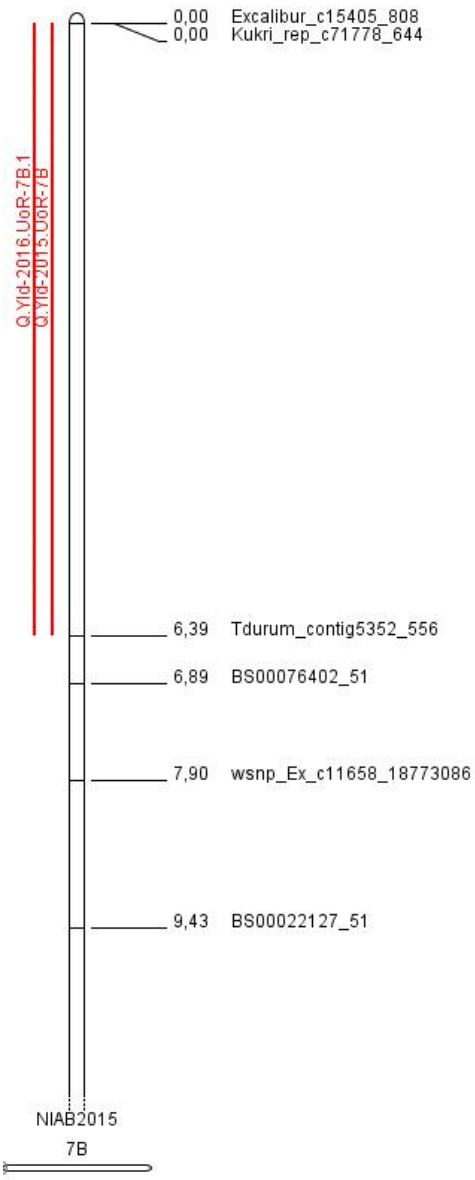

Figure 4-12- Fragment of chromosome 7B showing co-locating QTL for Grain Yield (Red bar)

4.3 Discussion

4.3.1 Phenotypic variation in yield trials in the MAGIC population

The nine traits measured in this chapter - Early Height, Final Height, Canopy Duration, Maximum Green Value, Accumulated Green Area, Anthesis, Yield, Senescence and Grain

number m^{-2} were measured over two years of field trials conducted in 2014-15 and 2015-16. The repetition over multiple years afforded the opportunity to assess in two quite contrasting seasons the extent of overlap (or lack thereof) in genetic architecture of source traits that underpin photosynthesis and biomass accumulation. Over the two years of the field trials, only 10.75 - 18.16% of the phenotypic variation in yield was explained by this analysis. For the source traits, significant QTL could explain anywhere between 3 – 36% of the total phenotypic variation for any given trait in a year, with height and anthesis predictably explaining the highest proportions of variation.

In 2014-15, crop height was on average around 4.6 - 5.8cm (8.4 – 10.7%) shorter than 2015-16 at any comparable time point. The significantly lower rainfall in spring and summer of 2015 (Figure 4.3) is likely to be the main driver of lower plant height in this season. This is in line with the reductions in Plant Height (PH) between 17 and 33% (depending on duration and intensity of drought) observed in a meta-analysis of 60 wheat drought response studies (Zhang *et al*., 2018). There are clear differences in phenology between the years, which can be seen in Figure 4.1. Anthesis occurs three days earlier on average in 2014-15, this would be due to environmental stresses, as it is well established that abiotic stresses such as water limitation can induce early flowering in wheat. An increase in the development rate of leaves can be seen in the differences between the timing of the maximum green values, which were on average up to 40 days earlier in 2014-15 than 2015-16. Because of this accelerated development rate, the maximum green cover is significantly lower in 2014-15, with the average cover being 25% lower. In the stressed, accelerated development scenario (2014-15), it is likely that the plants were utilising most of their resources on the flag leaf, leaving a lower density

of leaves overall, and reducing the total green area covered at any given time. Looking at the canopy duration, there is an increase of over 50% from 2014-15 to 2015-16, due to the higher canopy duration over a much longer period in the second year. Advancement of anthesis and earlier peaking of canopy under water limitation in turn affects senescence, with Bogard *et al* (2011) concluding that leaf senescence is mainly driven by the timing of anthesis. In addition to this, it has been commonly observed that stress induces premature senescence (Buchanan-Wollaston, 1997; Noodén *et al*., 1997; Verma *et al*., 2004).

4.3.2 Trait Heritability

Heritability of phenotypes is key to plant breeding as the extent to which the trait value reflects genetically-programmed 'merit' rather than environmentally-influenced 'response' determines the rate of gain in selection. Highly heritable traits are also consistently expressed over a range of growing conditions, providing reliability for growers.

As seen in Table 4.1, traits like height, date of anthesis and grain number m^{-2} are such attributes. Many of the source traits measured in this analysis however have relatively low heritability (H^2 = 0.12 - 0.27), which appears to be a common feature of source-related growth parameters. Camargo *et al* (2018) conducted growth parameter measurements on a subset 208 lines from the MAGIC population in controlled glasshouse conditions. The study also found low heritability in most growth parameters including modelled senescence curves, the minimum asymptote and value at the inflection point of the calculated plant area and height curves, concluding that any correlations between parameters were largely environmental. However, Pennacchi *et*

al (2018) showed a higher heritability (H^2 = 0.5 - 0.78) for Early Vigour, Accumulated Green Area, Maximum Cover and Stay Green – all derived from image analysis methods. However, this was based on a single year's experiment with conditions consistent across all replications.

Beyond the well-studied plant height and anthesis, the rate of senescence and grain number m^{-2} were the most heritable traits measured (H^2 = 0.54 and 0.38) over the two years. This high heritability makes it a potentially attractive target for breeding programs, as a slower rate of senescence should have a 'stay green' effect - potentially extending the grain filling period and increasing yields, and increases in grain number have a direct impact on yield. Delayed senescence has been linked to higher yields by Verma *et al* (2004), Bogard *et al* (2011) and Pennacchi *et al* (2018).

4.3.3 Correlation

The majority of traits had poor correlations between years and were inconsistent between traits. However, some remain agreeable with previous research. Anthesis and senescence are consistently negatively correlated across years (PCC= -0.1 and -0.36 respectively), which is consistent with Bogard *et al* (2011), where of the six environments studied that showed significant correlations between these traits, five of them were negative associations.

Yield is consistently correlated with canopy duration (PPC= 0.21 and 0.32 in respective years), compared to a slightly more inconsistent correlation with accumulated green area (PCC= 0.16 and 0.38) and no significant correlation between the maximum value and yield (PCC= 0.08 and -0.05). This lends weight to the theory that a longer canopy duration can have a significant effect on the yield. As expected, yield is also strongly

correlated with grain number m^{-2} (PCC= 0.62 and 0.57). This reflects previous breeding efforts where increases in grain number were responsible for the corresponding increases in yield.

Environmental effects and trait interactions can be seen throughout the correlations through the inconsistencies between years. The maximum green value and accumulated green area are positively correlated in both years (PCC= 0.88 and 0.17 respectively), with the higher correlation in 2014-15 reflecting the lower total time due to early senescence, meaning a short period of high green cover has significant impact on the accumulated biomass, whereas, in 'ideal' conditions, the maximum value doesn't appear to be as important as the time the plant spends near its maximum value. Indeed, the negative correlation (PCC=-0.45) between the maximum green value and the canopy duration observed in 2015-16 supports the idea that, in unstressed conditions, a higher maximum value comes at the expense of maintaining a high level of cover over time.

4.3.4 Co-locating QTL

Across ten chromosomes, QTL for two or more traits were detected, either co-locating between two markers, spanning adjacent marker intervals or having a shared flanking marker. As many of the traits analysed here are correlated with each other, it is expected that major QTL will either be pleiotropic and affect several phenotypic traits simultaneously, or that variability in one trait will affect another trait directly. QTL that are co-locating for the yield growth parameters suggest that some of the variability in yield can be explained by variations in plant growth affecting source capacity. The chromosomes of interest to this analysis are 1A, 1D, 2A, 2B, 2D, 3A, 4B, 4D, 5A, 6A and 7B. Previous studies have identified QTL for numerous growth parameters and biomass

measurements on all these chromosomes, using both bi-parental and association panels (Bogard *et al*., 2011; Camargo *et al*., 2018, 2016; El-Feki *et al*., 2018; Kulwal *et al*., 2003; Li *et al*., 2010; Pushpendra *et al*., 2007; Simmonds *et al*., 2014; Snape *et al*., 2007; Verma *et al*., 2004).

4.3.5 Major effect QTL

Within the analysed QTL, only 12 had a -log10p value greater than 10. Of these, 10 were related to anthesis (*Ppd*, 2D), height (*Rht-B1b,* 4B and *Rht-D1b*, 4D). The remaining two are *Q.Agc-2016.UoR-2A* and *Q.Yld-2016.UoR-5B* (-log10p= 11.13 and 11.69 respectively). Both of these appear in a single year, with *Q.Agc-2016.UoR-2A* co-locating with *Q.Cdu-2016.UoR-2A.*

Of the major effect QTL, *Ppd* is co-locating with the smaller QTL *Q.Cdu-2016.UoR-2D* and *Q.Mgv-2015.UoR-2D*, *Rht-B1b* co-locates with the yield QTL *Q.Yld-2016.UoR-4B*, and *Rht-D1b* does not co-locate with any of the other source traits.

4.4 Conclusions

The results of this chapter clearly show that the traits used for measuring growth parameters and biomass accumulation are highly variable with a significant environmental component.

There were few consistent correlations in the context of yield, however canopy duration was moderately correlated with yield in both years. Looking at the data from unstressed conditions in 2015-16, the vast majority of lines had maximum values above 90% cover. This supports the theory that a canopy will expand into the available space to the best of its resources. However, it may not reflect the level of light intercepted through

varying canopy densities, which still have potential to be targeted in breeding for attributes such as the size, number, and display of leaves to increase light interception (Long *et al*., 2006). The differences in the accumulated green area and the canopy duration would have been controlled by the rate of biomass accumulation, the onset of senescence and the rate of senescence, rather than the maximum cover for any line.

The correlations with yield were not generally reflected in the QTL analysis. QTL for yield and date of anthesis were co-located at 2A (102.37 - 103.89cM), and QTL for yield and height on 4B (50.15 - 51.16cM); these did follow correlations between these traits and yield, however they only appeared in the 2015-16 analysis. The only stable yield QTL was *Q.Yld-2015.UoR-7B,* located on 7B between markers *RFL_Contig6075_1128* and *Tdurum_contig5352_556* (0.00 - 6.39cM), explaining on average 1.6% of the total phenotypic variation.

To the best of our knowledge, this is the only study that attempts to look at the full growing season of wheat using large-scale image analysis to assess growth parameters for genetic analysis in field conditions. Other studies have utilised extensive image analysis on individual plants to examine canopy architecture and calculate growth, usually in using automated systems in a controlled environment (Camargo *et al*., 2018; Chen *et al*., 2014; Knecht *et al*., 2016). However, measurements in the field are more likely to be of use in the selection of genotypes that will perform well in farming practice, particularly in cases where large plots are used to simulate real farming conditions (Rebetzke *et al*., 2014). Both Pennacchi *et al* (2018) and Elsayed *et al* (2018) used image analysis to assess growth parameters in field settings. Elsayed *et al* (2018) looked directly at the percentage of green pixels and used destructive harvest to assess the

links between images and wet/dry biomass, nitrogen content and nitrogen uptake. These were taken at specific dates, with results showing significant relations between green area using imagery and biomass parameters. Pennacchi *et al* (2018) used similar methodology and growth parameters to those examined in this chapter and found broadly comparable results at a canopy level that accumulated cover and 'stay green' have positive correlations with yield, however statistically significant correlations between growth parameters and yield were not remarkably high, with the correlation coefficients being below 0.5. However, this study did not include a reported genetic component beyond trait heritability.

From this multi-year analysis, a combined total of 102 QTL were identified in all analyses, refined to 95 when identical QTL over multiple years are consolidated. Of these, 12 loci were associated with two or more traits. None of the co-locating QTL appeared to be stable across years.

Of the QTL identified in this chapter, there are several that may warrant further study. Many single environment QTL explain significant amounts of the total phenotypic variation, and therefore need to be understood as variants that enable the crop to respond flexibly to its environment.

5 Final Discussion

5.1 Thesis Overview

The aim of this thesis was to conduct an in-depth study of the genetic underpinnings of a suit of traits spanning both source and sink potential in wheat. Further objectives of the research included identifying alleles with positive or negative effects on the biomass accumulation and grain yield components; observing potential trade-offs between traits and the effects this has on the final yield. To this end, the eight-parent NIAB MAGIC population was studied in field conditions over two years (2014-16), with measurements taken from emergence through to final yield. Throughout the experiments, high resolution imagery was taken in order to derive biomass accumulation proxies, along with development assessments and final yield. Post-harvest, the grain yield was broken down into individual components - grain morphology, weight and quality, to assess the sink potential. This discussion will focus around the hypotheses stated at the beginning of this thesis, which are:

1. There will be a significant heritable difference in the components of sink capacity between MAGIC genotypes which will cause heritable differences in the final yield.
2. There will be significant genetic interactions between QTL for sink related traits.
3. There will be a significant heritable difference in varying aspects of biomass accumulation between MAGIC genotypes which will cause heritable differences in the final yield.
4. There will be significant genetic interactions between QTL for source related traits.

5. There will be significant genetic interactions between QTL for combinations of all measured traits.

5.2 Assessing the sink potential

The research documented in Chapter 3 was focused on breaking down yield into individual components, assessing their individual contributions and genetically mapping their traits. For all traits analysed, there were significant differences between genotypes, with the range of the progeny greatly exceeding that of the parental lines. These differences for the main driving traits of thousand grain weight (grain length, width and area) are highly heritable (PCC = 0.54 – 0.74). Yield itself has a relatively low heritability (H^2 = 0.26) and can be highly variable between years. In the case of this experiment, average yields differed by 2.2t/ha between years.

Many experiments have shown that the final yield is unstable and subject to environmental influences throughout the entire growing season (Snape *et al*., 2007; Tyagi *et al*., 2015; Wu *et al*., 2012). The low heritability in yield across all of these studies reflects the polygenic nature of the trait and the complexity of a trait that is essentially the sum of all other traits.

Of the sink components analysed, all except yield and nitrogen concentration were strongly correlated between years (PCC = 0.49 – 0.78). This followed the established patterns, with previous research having established that grain morphology and weight are more stable across environments than yield itself. In respect to yield, grain length is the most stably correlated with yield. Grain width, grain area, FFD and thousand grain weight had significantly higher correlations with yield in 2015-16 than in 2014-15. This shows that they are more susceptible to environmental stresses than grain length, but

under favourable conditions they can be expected to have a significant impact on yields. The inconsistent correlations between thousand grain weight and yield might reflect the conclusions of Fischer (2008), stating that increasing grain yield potential has been achieved by increasing the numbers of grain per unit land, rather than the size of individual seed.

Evidence in this thesis shows that grain length and width are controlled independently with minimal interaction. Across both years, there is low correlation between traits (PCC= -0.11 and 0.09), and there were no co-locating QTL found in any analyses. Although, Brinton *et al.* (2017) suggested that increasing grain length should allow for further enhancements of grain width as well.

In total, 85 unique QTL locations were identified over multiple analyses. Of these, 16 QTL locations involved two or more traits. Individually, these QTL explained anywhere between 0.13 and 11.91% of the total phenotypic variation explained for any given trait in a year. As expected, QTL were discovered on multiple chromosomes. Previous research has identified QTL for sink-related traits on almost every chromosome, with major QTL on 2A, 2D, 4A, 5A and 6A (Breseghello and Sorrells, 2007; Brinton *et al*., 2017; Echeverry-Solarte *et al*., 2015; Simmonds *et al*., 2014; Wu *et al*., 2015; Zhang *et al*., 2013).

Among our QTL, there were five major effect (-log10p > 10) QTL locations. These were located on chromosomes 1B, 4B, 4D, 5A and 6A. The QTL on 4B and 4D co-locate with the *Rht* genes (*Rht-B1b* and *Rht-D1b* respectively); 5A corresponds to fine mapping for grain length done by Brinton *et al* (2017); and 6A corresponds to Simmonds *et al* (2014)

likely to represent the *TaGW2* gene. The major QTL on chromosome 1B for grain length appears to be novel, explaining up to 5.7% of the total phenotypic variation.

5.3 Source Strength

The experiment conducted in Chapter 4 of this thesis aimed to observe differences in biomass accumulation and duration to discern how this impacts final yield. As with sink traits, the phenotypic range of the progeny greatly surpassed that of the founder varieties.

Many of the source-related traits in this analysis have relatively low heritability (H^2 = 0.12 - 0.29). This has been shown previously in experiments by Camargo *et al* (2018). Beyond the well-studied plant height and date of anthesis, the rate of senescence had the highest heritability (H^2 = 0.54). This is comparable to results seen in experiments by Pennacchi *et al* (2018), where of the canopy traits measured, stay green (delayed\slower senescence) had the highest heritability.

The majority of traits in Chapter 4 are poorly correlated between years, and correlations between traits are inconsistent with few exceptions. Date of anthesis and senescence rate are consistently negatively correlated, with earlier flowering producing a slower rate of senescence to maximise grain filling time. This was also shown by Bogard *et al* (2011), where of the six environments studied that showed significant correlations between these traits, five of them were negative associations. In respect to yield, canopy duration is the most consistently correlated (PCC = 0.21 and 0.32), followed by a more variable accumulated green area (PCC = 0.16 and 0.38). Maximum green cover has no significant correlation with yield (PCC = 0.08 and -0.05). From this, it can be

deduced that canopy duration can have a significant effect on the final yield, as has been suggested by Verma *et al* (2004) and Bogard *et al* (2011).

In total, 95 unique QTL were discovered over multiple analyses. Of these, 80 were single-environment QTL, and there were 12 loci associated with two or more traits. Individually, these QTL explained anywhere between 0.43 and 21.2% of the total phenotypic variation for any given trait in a year. In total, only 10.75 – 18.16% of the phenotypic variation in yield was explained in the analyses, with only one stable QTL across years on chromosome 7B. Of the 12 major effect QTL identified in the source analysis, 10 were related to anthesis (*Ppd*, 2D) or height (*Rht-B1b,* 4B and *Rht-D1b*, 4D). The remaining two are single environment QTL, *Q.Agc-2016.UoR-2A* and *Q.Yld-2016.UoR-5B.*

5.4 Source-sink interactions

Looking at the phenotypic relationships between the source and sink traits measured, the effects of plant height (*Rht*) on yield components are the most obvious (Correlation matrix of all data can be found in the appendix). This is due to the effect of semi-dwarfing genes introduced to increase the harvest index. Although harvest index was generally improved by increasing the numbers of grain per unit area, there would also have been an effect on the size of the individual grains. Grain morphology traits have been shown to be associated with chromosomes 4B and 4D in multiple previous studies (Flintham *et al*., 1997; Gegas *et al*., 2010; Giura and Saulescu, 1996). In this thesis, the only examples of traits that are QTL co-locating that are unambiguously appearing in both source and sink traits are the *Rht* genes. *Rht* is one of the biggest effects on grain morphology and has the most far reaching effects in respect to the number of

associated traits. Both *Rht-B1b* and *Rht-D1b* are consistently linked with grain width, thousand grain weight and FFD (Table 5.1).

QTL	Chr	LeftMrk	RightMrk	Pos	LeftMrk	RightMrk	pvalue	-log10p
Q.FFD-2015.UoR-4B	4B	*BS00084070_51*	*Ra_c26080_461*	49.66	49.66	50.16	3.90E-10	9.41
Q.FFD-ME.UoR-4B	4B	*BS00084070_51*	*Ra_c26080_461*	49.66	49.66	50.16	4.53E-06	5.34
Q.Fht-2015.UoR-4B	4B	*Ra_c26080_461*	*BS00033614_51*	50.16	50.16	51.16	2.61E-14	13.58
Q.Fht-2016.UoR-4B	4B	*Ra_c26080_461*	*BS00033614_51*	50.16	50.16	51.16	1.23E-13	12.91
Q.Yld-2016.UoR-4B	4B	*Ra_c26080_461*	*BS00033614_51*	50.16	50.16	51.16	2.56E-04	3.59
Q.GA-2015.UoR-4B	4B	*Ra_c26080_461*	*BS00033614_51*	51.16	50.16	51.16	2.81E-07	6.55
Q.GA-2016.UoR-4B.1	4B	*Ra_c26080_461*	*BS00033614_51*	51.16	50.16	51.16	2.54E-08	7.60
Q.GW-2015.UoR-4B	4B	*Ra_c26080_461*	*BS00033614_51*	51.16	50.16	51.16	1.00E-10	10.00
Q.GW-2016.UoR-4B	4B	*Ra_c26080_461*	*BS00033614_51*	51.16	50.16	51.16	2.47E-11	10.61
Q.GW-ME.UoR-4B	4B	*Ra_c26080_461*	*BS00033614_51*	51.16	50.16	51.16	1.44E-14	13.84
Q.TGW-ME.UoR-4B	4B	*Ra_c26080_461*	*BS00033614_51*	51.16	50.16	51.16	0.00E+00	17.5*
Q.TGW-2015.UoR-4B	4B	*Tdurum_contig42229_113*	*BobWhite_c44691_648*	52.17	52.17	52.67	6.66E-16	15.18
Q.GA-ME.UoR-4B	4B	*BS00011851_51*	*BS00084904_51*	54.7	54.70	55.20	1.81E-08	7.74
Q.TGW-2016.UoR-4B	4B	*BS00011851_51*	*BS00084904_51*	54.7	54.70	55.20	7.03E-11	10.15
Q.FFD-2016.UoR-4B	4B	*BS00084904_51*	*BS00022988_51*	55.7	55.20	55.70	1.14E-06	5.94
Q.Eht-2015.UoR-4D	4D	*Kukri_rep_c68594_530*	*Excalibur_c19078_210*	24.93	24.93	32.24	0.00E+00	35*
Q.GA-2016.UoR-4D	4D	*Kukri_rep_c68594_530*	*Excalibur_c19078_210*	24.93	24.93	32.24	3.53E-06	5.45
Q.GA-ME.UoR-4D	4D	*Kukri_rep_c68594_530*	*Excalibur_c19078_210*	24.93	24.93	32.24	5.44E-08	7.26
Q.Eht-2016.UoR-4D	4D	*Excalibur_c19078_210*	*RAC875_rep_c105718_304*	32.24	32.24	40.11	2.22E-11	10.65
Q.FFD-2015.UoR-4D	4D	*Excalibur_c19078_210*	*RAC875_rep_c105718_304*	32.24	32.24	40.11	2.66E-15	14.58
Q.FFD-2016.UoR-4D	4D	*Excalibur_c19078_210*	*RAC875_rep_c105718_304*	32.24	32.24	40.11	6.89E-06	5.16
Q.FFD-ME.UoR-4D	4D	*Excalibur_c19078_210*	*RAC875_rep_c105718_304*	32.24	32.24	40.11	6.66E-14	13.18
Q.Fht-2015.UoR-4D	4D	*Excalibur_c19078_210*	*RAC875_rep_c105718_304*	32.24	32.24	40.11	0.00E+00	68*
Q.Fht-2016.UoR-4D	4D	*Excalibur_c19078_210*	*RAC875_rep_c105718_304*	32.24	32.24	40.11	0.00E+00	25*
Q.GA-2015.UoR-4D	4D	*Excalibur_c19078_210*	*RAC875_rep_c105718_304*	32.24	32.24	40.11	9.99E-08	7.00
Q.GNO-2015.UoR-4D	4D	Excalibur_c19078_210	RAC875_rep_c105718_304	32.24	32.24	40.11	2.10E-08	7.68
Q.GW-2015.UoR-4D	4D	*Excalibur_c19078_210*	*RAC875_rep_c105718_304*	32.24	32.24	40.11	5.33E-14	13.27
Q.GW-2016.UoR-4D	4D	*Excalibur_c19078_210*	*RAC875_rep_c105718_304*	32.24	32.24	40.11	0.00E+00	29*
Q.GW-ME.UoR-4D	4D	*Excalibur_c19078_210*	*RAC875_rep_c105718_304*	32.24	32.24	40.11	0.00E+00	23*
Q.TGW-2015.UoR-4D	4D	*Excalibur_c19078_210*	*RAC875_rep_c105718_304*	32.24	32.24	40.11	0.00E+00	21*
Q.TGW-2016.UoR-4D	4D	*Excalibur_c19078_210*	*RAC875_rep_c105718_304*	32.24	32.24	40.11	1.23E-11	10.91
Q.TGW-ME.UoR-4D	4D	*Excalibur_c19078_210*	*RAC875_rep_c105718_304*	32.24	32.24	40.11	0.00E+00	21*
Q.GNO-2016.UoR-4D	4D	BS00036421_51	RAC875_rep_c70284_235	40.61	40.61	49.47	1.19E-05	4.92

Table 5.1 – Co-locating QTL with *Rht* on 4B and 4D, QTL names follow standard format as described in Chapter 2. Left and Right Marker Positions are the location of the markers in cM, p-value is the significance of the QTL and -log10p is the strength of the QTL

Looking at grain number m^{-2}, it is moderately correlated between years (PCC= 0.34), with a corresponding heritability of 0.38. As expected, grain number m^{-2} is highly correlated with yield (PCC= 0.57 - 0.62) but is poorly and inconsistently correlated with all measured source traits, despite being the culmination of the source capacity up to grain filling. Intuitively, grain number m^{-2} has strong negative correlations with most of the grain morphology traits; the strongest of these being thousand grain weight and grain width (average of PCC= -0.6 and 0.52 respectively). Given that grain width is a major contributor to thousand grain weight, and is established during grain filling, it is

unsurprising that these two traits are similarly correlated with grain number m^{-2}. The consistent negative correlation with grain morphology traits suggests a lack of source capacity during grain filling, with a higher number of grains requiring a more assimilates from the source at grain filling to reach its full potential. This may seem to be an insurmountable trade-off, as increasing the source capacity overall may increase may the number of tillers and fertile grain set, decreasing the available assimilates for individual grain. However, there is potential to increase the source capacity specifically during grain filling by delaying or slowing down senescence. The negative correlation between the rate of senescence and thousand grain weight (PCC= -0.15) shows that a reduced rate of senescence can increase grain filling, potentially compensating for a higher number of grains. This can be seen to a degree in the small but significant correlation between the rate of senescence and yield (PCC= -0.07 and -0.08).

Interestingly, accumulated green cover has moderate positive correlation with grain length, where grain width has a weak negative correlation. Biologically, this makes sense as the majority of the accumulated green cover occurs during the construction stage, when grain length is being set and will reach its maximum. In contrast grain width reaches in maximum after anthesis, where the green cover begins to decline. These indicate that there is a potential trade-off between grain length and width. However, there is no significant correlation between accumulated green cover and grain area or thousand grain weight, suggesting that any potential trade off because of this is negligible in the wider context of yield. The lack of genetic linkage between accumulated green cover and grain morphology suggests that these traits may be impacted green cover but are independently controlled.

Of the six co-locating QTL locations between source and sink traits, 5 involved QTL associated with plant height, two of which are *Rht* genes. Only QTL identified on 2A were independent of height, involving canopy duration, accumulated green cover, grain length and thousand grain weight. These co-locations between source and sink traits have the same direction of effect from each parent, suggesting that the QTLs are pleiotropic.

5.5 Implications for Plant Breeding

The findings of this thesis have several implications for plant breeding. Firstly, there is no single 'magic bullet'- there is still variation between years in the expression of QTL that are nonetheless important overall. This lends weight to the practice of using combinable yield as the main phenotype on which selection is based. Secondly, MAGIC populations have vast potential as a breeding resource. The range in variation for all phenotypes in this thesis, combined with the novel QTLs found on chromosomes 1B, 5B and 7B, show that there is untapped potential in existing elite germplasm. The number of single environment QTL suggests that with further study, these may help produce plants that are tailored to individual environments. Thirdly, some traits that are negatively correlated aren't necessarily in a trade-off. Grain width and length have shown a degree of independent control here and in previous studies (Brinton *et al*., 2017), as have thousand grain weight and grain number m^{-2}. These traits could be individually targeted in breeding programmes to improve both yield and economic quality of the crop.

5.6 Study limitations

In the first-year field trail, the crop was affected by drought stress, which was exacerbated by a free draining soil. This significantly affected the green crop cover

throughout the season, as well as reducing canopy duration and the timing of senescence.

Despite having developed Phenocart, phenotyping was still the largest bottleneck of this study. Limitations on manpower and the expense of advanced equipment limited the level of phenotyping possible, while the time needed to take complex measurements made it impractical on a large scale.

5.6 Future work

This research has identified some interesting possibilities in the genetics of source strength. Further work is needed to broaden the understanding of the genetic controls of photosynthetic capacity. While impractical on such a large scale, this study can be used to identify a subset of the magic population with the most variability in in relation to source traits for further studies. More direct measurements of photosynthetic capacity from both physiological (such as chlorophyll concentrations and CO_2 assimilation) and biochemical (stem carbohydrate stores and soluble sugars in flag leaf) perspectives would allow further detailed analysis of the full source capability.

There were some indications of connections between source and sink traits. These could be a potential area of further study utilising NILs to identify if these links are coincidental due to the large number of QTL identified in this study, due to tight linkage between genes or if it is the action of the same gene.

To complement this work, further analysis could take place examining in more detail the trade-offs and connection between source and sink traits. This could be accomplished using bayesian techniques such as those described by Scutari *et al* (2014).

References

Acreche, M.M., Slafer, G.A., 2006. Grain weight response to increases in number of grains in wheat in a Mediterranean area. F. Crop. Res. 98, 52–59. https://doi.org/10.1016/j.fcr.2005.12.005

Aranjuelo, I., Cabrera-Bosquet, L., Morcuende, R., Avice, J.-C., Nogués, S., Araus, J.L., Martínez-Carrasco, R., Pérez, P., 2011. Does ear C sink strength contribute to overcoming photosynthetic acclimation of wheat plants exposed to elevated CO_2? J. Exp. Bot. 62, 3957–3969. https://doi.org/10.1093/jxb/err095

Bandillo, N., Raghavan, C., Muyco, P.A., Sevilla, M.A.L., Lobina, I.T., Dilla-Ermita, C.J., Tung, C.W., McCouch, S., Thomson, M., Mauleon, R., Singh, R.K., Gregorio, G., Redoña, E., Leung, H., 2013. Multi-parent advanced generation inter-cross (MAGIC) populations in rice: Progress and potential for genetics research and breeding. Rice 6, 1–5. https://doi.org/10.1186/1939-8433-6-1

Bariana, H.S., Parry, N., Barclay, I.R., Loughman, R., McLean, R.J., Shankar, M., Wilson, R.E., Willey, N.J., Francki, M., 2006. Identification and characterization of stripe rust resistance gene *Yr34* in common wheat. Theor. Appl. Genet. 112, 1143–1148. https://doi.org/10.1007/s00122-006-0216-3

Beales, J., Turner, A., Griffiths, S., Snape, J.W., Laurie, D.A., 2007. A *Pseudo-Response Regulator* is misexpressed in the photoperiod insensitive *Ppd-D1a* mutant of wheat (*Triticum aestivum* L.). Theor. Appl. Genet. 115, 721–733. https://doi.org/10.1007/s00122-007-0603-4

Bednarek, J., Boulaflous, A., Girousse, C., Ravel, C., Tassy, C., Barret, P., Bouzidi, M.F., Mouzeyar, S., 2012. Down-regulation of the *TaGW2* gene by RNA interference results in decreased grain size and weight in wheat. J. Exp. Bot. 63, 5945–5955. https://doi.org/10.1093/jxb/ers249

Benbow, H., 2016. “Dissecting the Genetic Control of Grain Weight in Wheat”, PhD Thesis, University of Bristol.

Bennett, D., Reynolds, M., Mullan, D., Izanloo, A., Kuchel, H., Langridge, P., Schnurbusch,

T., 2012. Detection of two major grain yield QTL in bread wheat (*Triticum aestivum*) under heat, drought and high yield potential environments. Theor. Appl. Genet. 125, 1473–1485. https://doi.org/10.1007/s00122-012-1927-2

Bentley, A.R., Horsnell, R., Werner, C.P., Turner, A.S., Rose, G.A., Bedard, C., Howell, P., Wilhelm, E.P., Mackay, I.J., Howells, R.M., Greenland, A., Laurie, D.A., Gosman, N., 2013. Short, natural, and extended photoperiod response in BC_2F_4 lines of bread wheat with different *Photoperiod-1 (Ppd-1)* alleles. J. Exp. Bot. 64, 1783–1793. https://doi.org/10.1093/jxb/ert038

Blake, N.K., Lehfeldt, B.R., Lavin, M., Talbert, L.E., 1999. Phylogenetic reconstruction based on low copy DNA sequence data in an allopolyploid: the B genome of wheat. Genome 42, 351–360. https://doi.org/10.1139/g98-136

Bogard, M., Jourdan, M., Allard, V., Martre, P., Perretant, M.R., Ravel, C., Heumez, E., Orford, S., Snape, J., Griffiths, S., Gaju, O., Foulkes, J., Le Gouis, J., 2011. Anthesis date mainly explained correlations between post-anthesis leaf senescence, grain yield, and grain protein concentration in a winter wheat population segregating for flowering time QTLs. J. Exp. Bot. 62, 3621–3636. https://doi.org/10.1093/jxb/err061

Bonneau, J., Taylor, J., Parent, B., Bennett, D., Reynolds, M., Feuillet, C., Langridge, P., Mather, D., 2013. Multi-environment analysis and improved mapping of a yield-related QTL on chromosome 3B of wheat. Theor. Appl. Genet. 126, 747–761. https://doi.org/10.1007/s00122-012-2015-3

Borlaug, N.E., 1983. Contributions of conventional plant breeding to food production. Science. 219, 689–693. https://doi.org/10.1126/science.219.4585.689

Botstein, D., Lander, E.S., 1989. Mapping mendelian factors underlying quantitative traits using RFLP linkage maps. Genetics 121, 185–199. https://doi.org/10.1038/hdy.2014.4

Bradbury, P., Parker, T., Hamblin, M.T., Jannink, J.L., 2011. Assessment of power and false discovery rate in genome-wide association studies using the barleyCAP

germplasm. Crop Sci. 51, 52–59. https://doi.org/10.2135/cropsci2010.02.0064

Breseghello, F., Sorrells, M.E., 2007. QTL analysis of kernel size and shape in two hexaploid wheat mapping populations. F. Crop. Res. 101, 172–179. https://doi.org/10.1016/j.fcr.2006.11.008

Brinton, J., Simmonds, J., Minter, F., Leverington-waite, M., Snape, J., Uauy, C., 2017. Increased pericarp cell length underlies a major QTL for grain weight in hexaploid wheat. New Phytol. 215, 1026–1038. https://doi.org/10.1111/nph.14624

Broman, K.W., Wu, H., Sen, Ś., Churchill, G.A., 2003. R/qtl: QTL mapping in experimental crosses. Bioinformatics 19, 889–890. https://doi.org/10.1093/bioinformatics/btg112

Brown, T.A., Jones, M.K., Powell, W., Allaby, R.G., 2009. The complex origins of domesticated crops in the Fertile Crescent. Trends Ecol. Evol. 24, 103–109. https://doi.org/10.1016/j.tree.2008.09.008

Buchanan-Wollaston, V., 1997. The molecular biology of leaf senescence. J. Exp. Bot. 48, 181–199. https://doi.org/10.1093/jxb/48.2.181

Bushuk, W., Rasper, V.F., 1994. Wheat Production, Properties and Quality. Springer 239, 1–30. https://doi.org/10.1007/978-1-4615-2672-8

Cabral, A.L., Jordan, M.C., Larson, G., Somers, D.J., Humphreys, D.G., McCartney, C.A., 2018. Relationship between QTL for grain shape, grain weight, test weight, milling yield, and plant height in the spring wheat cross RL4452/ 'AC Domain,' PLoS ONE. https://doi.org/10.1371/journal.pone.0190681

Camargo, A. V., Mackay, I., Mott, R., Han, J., Doonan, J.H., Askew, K., Corke, F., Williams, K., Bentley, A.R., 2018. Functional mapping of quantitative trait loci (QTLs) associated with plant performance in a wheat MAGIC mapping population. Front. Plant Sci. 9. https://doi.org/10.3389/fpls.2018.00887

Camargo, A. V., Mott, R., Gardner, K.A., Mackay, I.J., Corke, F., Doonan, J.H., Kim, J.T., Bentley, A.R., 2016. Determining phenological patterns associated with the onset

of senescence in a wheat MAGIC mapping population. Front. Plant Sci. 7. https://doi.org/10.3389/fpls.2016.01540

Carver, B.F., 2009. Wheat Science and Trade. Wheat Sci. Trade 1–569. https://doi.org/10.1002/9780813818832

Casadesús, J., Villegas, D., 2014. Conventional digital cameras as a tool for assessing leaf area index and biomass for cereal breeding. J. Integr. Plant Biol. 56, 7–14. https://doi.org/10.1111/jipb.12117

Casebow, R., Hadley, C., Uppal, R., Addisu, M., Loddo, S., Kowalski, A., Griffiths, S., Gooding, M., 2016. Reduced height (*Rht*) alleles affect wheat grain quality. PLoS One 11. https://doi.org/10.1371/journal.pone.0156056

Chen, D., Neumann, K., Friedel, S., Kilian, B., Chen, M., Altmann, T., Klukas, C., 2014. Dissecting the phenotypic components of crop plant growth and drought responses based on high-throughput image analysis. Plant Cell Online 26, 4636–4655. https://doi.org/10.1105/tpc.114.129601

Churchill, G.A., Doerge, R.W., 1994. Empirical threshold values for quantitative trait mapping. Genetics 138, 963–971. https://doi.org/10.1534/genetics.107.080101

Cockram, J., Scuderi, A., Barber, T., Furuki, E., Gardner, K.A., Gosman, N., Kowalczyk, R., Phan, H.P., Rose, G.A., Tan, K.-C., Oliver, R.P., Mackay, I.J., 2015. Fine-mapping the wheat Snn1 locus conferring sensitivity to the *Parastagonospora nodorum necrotrophic* effector SnTox1 using an eight founder multiparent advanced generation inter-cross population. G3; Genes|Genomes|Genetics 5, 2257–2266. https://doi.org/10.1534/g3.115.021584

Colin, C., Matthew, M., Ian, M., Wayne, P., 2008. From mutations to MAGIC: resources for gene discovery, validation and delivery in crop plants. Curr. Opin. Plant Biol. 11, 215–221. https://doi.org/10.1016/j.pbi.2008.01.002

CPVO, 2009. Protocol for Distinctness, Uniformity and Stability Tests in *Triticum aestivum* 1–35.

Darvasi, A., Soller, M., 1995. Advanced intercross lines, an experimental population for fine genetic mapping. Genetics 141, 1199–1207.

Deery, D., Jimenez-Berni, J., Jones, H., Sirault, X., Furbank, R., 2014. Proximal remote sensing buggies and potential applications for field-based phenotyping. Agronomy 4, 349–379. https://doi.org/10.3390/agronomy4030349

Dell'Acqua, M., Gatti, D.M., Pea, G., Cattonaro, F., Coppens, F., Magris, G., Hlaing, A.L., Aung, H.H., Nelissen, H., Baute, J., Frascaroli, E., Churchill, G.A., Inzé, D., Morgante, M., Pè, M.E., 2015. Genetic properties of the MAGIC maize population: A new platform for high definition QTL mapping in *Zea mays*. Genome Biol. 16, 1–23. https://doi.org/10.1186/s13059-015-0716-z

Dixon, J., Braun, H., Kosina, P., Crouch, J., 2009. Wheat facts and futures 2009.

Dohleman, F.G., Heaton, E.A., Leakey, A.D.B., Long, S.P., 2009. Does greater leaf-level photosynthesis explain the larger solar energy conversion efficiency of Miscanthus relative to switchgrass? Plant, Cell Environ. 32, 1525–1537. https://doi.org/10.1111/j.1365-3040.2009.02017.x

Dohleman, F.G., Long, S.P., 2009. More productive than maize in the midwest: how does Miscanthus do it? Plant Physiol. 150, 2104–2115. https://doi.org/10.1104/pp.109.139162

Driever, S.M., Lawson, T., Andralojc, P.J., Raines, C.A., Parry, M.A.J., 2014. Natural variation in photosynthetic capacity, growth, and yield in 64 field-grown wheat genotypes. J. Exp. Bot. 65, 4959–4973. https://doi.org/10.1093/jxb/eru253

Dubcovsky, J., Dvorak, J., 2007. Genome plasticity a key factor in the success of polyploid wheat under domestication. Science. 316, 1862–1866. https://doi.org/10.1126/science.1143986

Dvořák, J., Terlizzi, P. di, Zhang, H.-B., Resta, P., 1993. The evolution of polyploid wheats: identification of the A genome donor species. Genome 36, 21–31. https://doi.org/10.1139/g93-004

Echeverry-Solarte, M., Kumar, A., Kianian, S., Mantovani, E.E., McClean, P.E., Deckard, E.L., Elias, E., Simsek, S., Alamri, M.S., Hegstad, J., Schatz, B., Mergoum, M., 2015. Genome-wide mapping of spike-related and agronomic traits in a common wheat population derived from a supernumerary spikelet parent and an elite parent. Plant Genome 8, 0. https://doi.org/10.3835/plantgenome2014.12.0089

El-Feki, W., Byrne, P., Reid, S., Haley, S., 2018. Mapping quantitative trait loci for agronomic traits in winter wheat under different soil moisture levels. Agronomy 8, 133. https://doi.org/10.3390/agronomy8080133

Ellis, M.H., Spielmeyer, W., Gale, K.R., Rebetzke, G.J., Richards, R.A., 2002. "Perfect" markers for the *Rht-B1b* and *Rht-D1b* dwarfing genes in wheat. Theor. Appl. Genet. 105, 1038–1042. https://doi.org/10.1007/s00122-002-1048-4

Elsayed, S., Barmeier, G., Schmidhalter, U., 2018. Passive reflectance sensing and digital image analysis allows for assessing the biomass and nitrogen status of wheat in early and late tillering stages. Front. Plant Sci. 9, 1–15. https://doi.org/10.3389/fpls.2018.01478

Evans, L.T., Fisher, R.A., 1999. Yield potential: Its definition, measurement, and significance. Crop Sci. 39, 1544–1551. https://doi.org/10.2135/cropsci1999.3961544x

FAO, 2016. FAO World Food Situation [WWW Document]. URL http://www.fao.org/worldfoodsituation/en/

FAOSTAT, 2018. Production Wheat [WWW Document].

Farré, A., Sayers, L., Leverington-Waite, M., Goram, R., Orford, S., Wingen, L., Mumford, C., Griffiths, S., 2016. Application of a library of near isogenic lines to understand context dependent expression of QTL for grain yield and adaptive traits in bread wheat. BMC Plant Biol. 16, 1–13. https://doi.org/10.1186/s12870-016-0849-6

Fischer, R., Byerlee, D., Edmeades, G., 2009. Can technology deliver on the yield challenge to 2050, in: Expert Meeting on How to Feed the World. pp. 24–26.

Fischer, R., Stockman, Y., 1986. Increased kernel number in Norin 10-derived dwarf wheat: evaluation of the cause. Aust. J. Plant Physiol. 13, 767–784. https://doi.org/10.1071/PP9860767

Fischer, R.A., 2008. The importance of grain or kernel number in wheat: A reply to Sinclair and Jamieson. F. Crop. Res. 105, 15–21. https://doi.org/10.1016/j.fcr.2007.04.002

Flintham, J.E., Börner, A., Worland, A.J., Gale, M.D., 1997. Optimizing wheat grain yield: Effects of *Rht* (gibberellin-insensitive) dwarfing genes. J. Agric. Sci. 128, 11–25. https://doi.org/10.1017/S0021859696003942

Foulkes, M.J., Scott, R.K., Sylvester-Bradley, R., 2002. The ability of wheat cultivars to withstand drought in UK conditions: Formation of grain yield. J. Agric. Sci. 138, 153–169. https://doi.org/10.1017/S0021859601001836

Friend, D.J.C., 1965. Ear length and spikelet number of wheat grown at different temperatures and light intensities. Can. J. Bot. 43, 345–353. https://doi.org/10.1139/b65-037

Gale, M.D.., Youssefian, S., 1985. Dwarfing genes in wheat I. p. 1–35. In: G.E. Russell (Ed). Progress in Plant Breeding. Butterworths and Co., London. https://doi.org/10.1016/B978-0-407-00780-2.50005-9.

Gardner, K.A., Wittern, L.M., Mackay, I.J., 2016. A highly recombined, high-density, eight-founder wheat MAGIC map reveals extensive segregation distortion and genomic locations of introgression segments. Plant Biotechnol. J. 14, 1406–1417. https://doi.org/10.1111/pbi.12504

Gaur, P.M., Thudi, M., Samineni, S., Varshney, R.K., 2014. Advances in chickpea genomics, Legumes in the Omic Era. https://doi.org/10.1007/978-1-4614-8370-0_4

Gebbing, T., Schnyder, H., 1999. Pre-anthesis reserve utilization for protein and carbohydrate synthesis in grains of wheat. Plant Physiol. 121, 871–878. https://doi.org/10.1104/pp.121.3.871

Gegas, V.C., Nazari, A., Griffiths, S., Simmonds, J., Fish, L., Orford, S., Sayers, L., Doonan, J.H., Snape, J.W., 2010. A genetic framework for grain size and shape variation in wheat. Plant Cell 22, 1046–1056. https://doi.org/10.1105/tpc.110.074153

Giura, A., Saulescu, N.N., 1996. Chromosomal location of genes controlling grain size in a large grained selection of wheat (*Triticum aestivum* L.). Euphytica 89, 77–80. https://doi.org/10.1007/BF00015722

Godfray, H.C.J., Beddington, J.R., Crute, I.R., Haddad, L., Lawrence, D., Muir, J.F., Pretty, J., Robinson, S., Thomas, S.M., Toulmin, C., 2010. Food Security: The challenge of feeding 9 billion people. Science. 327, 812–818. https://doi.org/10.1126/science.1185383

Grassini, P., Eskridge, K.M., Cassman, K.G., 2013. Distinguishing between yield advances and yield plateaus in historical crop production trends. Nat. Commun. 4, 1–11. https://doi.org/10.1038/ncomms3918

Griffiths, S., Wingen, L., Pietragalla, J., Garcia, G., Hasan, A., Miralles, D., Calderini, D.F., Ankleshwaria, J.B., Waite, M.L., Simmonds, J., Snape, J., Reynolds, M., 2015. Genetic dissection of grain size and grain number trade-offs in CIMMYT wheat germplasm. PLoS One 10. https://doi.org/10.1371/journal.pone.0118847

Hardin, L.S., 2008. Bellagio 1969: The green revolution. Nature 455, 470–471. https://doi.org/10.1038/455470a

Harlan, J.R., 1967. Wild Wheat Harvest in Turkey. Archaeology 20, 197–201.

Haudry, A., Cenci, A., Ravel, C., Bataillon, T., Brunel, D., Poncet, C., Hochu, I., Poirier, S., Santoni, S., Glémin, S., David, J., 2007. Grinding up wheat: A massive loss of nucleotide diversity since domestication. Mol. Biol. Evol. 24, 1506–1517. https://doi.org/10.1093/molbev/msm077

Hay, R.K.M., Porter, J.R., 2006. The Physiology of Crop Yield. Second edition. Oxford: Blackwell Publishing (2006), pp. 314

Heun, M., Schäfer-Pregl, R., Klawan, D., Castagna, R., Accerbi, M., Borghi, B., Salamini, F., 1997. Site of einkorn wheat domestication identified by DNA fingerprinting. Science. 278, 1312–1314. https://doi.org/10.1126/science.278.5341.1312

Holland, J.B., 2007. Genetic architecture of complex traits in plants. Curr. Opin. Plant Biol. 10, 156–161. https://doi.org/10.1016/j.pbi.2007.01.003

Horton, P., 2000. Prospects for crop improvement through the genetic manipulation of photosynthesis: morphological and biochemical aspects of light capture. J. Exp. Bot. 51, 475–485. https://doi.org/10.1093/jexbot/51.suppl_1.475

Hu, L., Li, Y., Xu, W., Zhang, Q., Zhang, L., Qi, X., Dong, H., 2012. Improvement of the photosynthetic characteristics of transgenic wheat plants by transformation with the maize C_4 phosphoenolpyruvate carboxylase gene. Plant Breed. 131, 385–391. https://doi.org/10.1111/j.1439-0523.2012.01960.x

Huang, B.E., George, A.W., 2011. R/mpMap: A computational platform for the genetic analysis of multiparent recombinant inbred lines. Bioinformatics 27, 727–729. https://doi.org/10.1093/bioinformatics/btq719

Huang, B.E., George, A.W., Forrest, K.L., Kilian, A., Hayden, M.J., Morell, M.K., Cavanagh, C.R., 2012. A multiparent advanced generation inter-cross population for genetic analysis in wheat. Plant Biotechnol. J. 10, 826–839. https://doi.org/10.1111/j.1467-7652.2012.00702.x

Huang, S., Sirikhachornkit, A., Su, X., Faris, J., Gill, B., Haselkorn, R., Gornicki, P., 2002. Genes encoding plastid acetyl-CoA carboxylase and 3-phosphoglycerate kinase of the *Triticum*/*Aegilops* complex and the evolutionary history of polyploid wheat. Proc. Natl. Acad. Sci. 99, 8133–8138. https://doi.org/10.1073/pnas.072223799

Jannink, J.L., 2007. Identifying quantitative trait locus by genetic background interactions in association studies. Genetics 176, 553–561. https://doi.org/10.1534/genetics.106.062992

Kato, K., Yokoyama, H., 1992. Geographical variation in heading characters among wheat landraces, *Triticum aestivum* L., and its implication for their adaptability.

Theor. Appl. Genet. 84, 259–265. https://doi.org/10.1007/BF00229480

Kellogg, E., 2001. Update on evolution, Evolutionary history of the grasses. Plant Physiol. 125, 1198–1205. https://doi.org/10.1104/pp.125.3.1198

Kersting, H.J., Lindhauer, M.G., Bergthaller, W., 1994. Application of wheat gluten in non-food industry - wheat gluten as a natural cobinder in paper coating. Ind. Crops Prod. 3, 121–128. https://doi.org/10.1016/0926-6690(94)90085-X

Knecht, A.C., Campbell, M.T., Caprez, A., Swanson, D.R., Walia, H., 2016. Image Harvest: An open-source platform for high-throughput plant image processing and analysis. J. Exp. Bot. 67, 3587–3599. https://doi.org/10.1093/jxb/erw176

Kover, P.X., Valdar, W., Trakalo, J., Scarcelli, N., Ehrenreich, I.M., Purugganan, M.D., Durrant, C., Mott, R., 2009. A multiparent advanced generation inter-cross to fine-map quantitative traits in *Arabidopsis thaliana*. PLoS Genet. 5. https://doi.org/10.1371/journal.pgen.1000551

Kuchel, H., Williams, K.J., Langridge, P., Eagles, H.A., Jefferies, S.P., 2007. Genetic dissection of grain yield in bread wheat. I. QTL analysis. Theor. Appl. Genet. 115, 1029–1041. https://doi.org/10.1007/s00122-007-0629-7

Kulwal, P.L., Roy, J.K., Balyan, H.S., Gupta, P.K., 2003. QTL mapping for growth and leaf characters in bread wheat. Plant Sci. 164, 267–277. https://doi.org/10.1016/S0168-9452(02)00409-0

Kumar, A., Li, C., Portis, A.R., 2009. *Arabidopsis thaliana* expressing a thermostable chimeric Rubisco activase exhibits enhanced growth and higher rates of photosynthesis at moderately high temperatures. Photosynth. Res. 100, 143–153. https://doi.org/10.1007/s11120-009-9438-y

Kumar, A., Mantovani, E.E., Seetan, R., Soltani, A., Echeverry-Solarte, M., Jain, S., Simsek, S., Doehlert, D., Alamri, M.S., Elias, E.M., Kianian, S.F., Mergoum, M., 2016. Dissection of genetic factors underlying wheat kernel shape and size in an elite × nonadapted cross using a high density SNP linkage map. Plant Genome 9, 0. https://doi.org/10.3835/plantgenome2015.09.0081

Lewis, C.M., 2002. Genetic association studies: design, analysis and interpretation. Brief. Bioinform. 3, 146–153. https://doi.org/10.1093/bib/3.2.146

Li, C., Bai, G., Carver, B.F., Chao, S., Wang, Z., 2015. Single nucleotide polymorphism markers linked to QTL for wheat yield traits. Euphytica 206, 89–101. https://doi.org/10.1007/s10681-015-1475-3

Li, X., Wang, H., Li, H., Zhang, L., Teng, N., Lin, Q., Wang, J., Kuang, T., Li, Z., Li, B., Zhang, A., Lin, J., 2006. Awns play a dominant role in carbohydrate production during the grain-filling stages in wheat (*Triticum aestivum*). Physiol. Plant. 127, 701–709. https://doi.org/10.1111/j.1399-3054.2006.00679.x

Li, Z., Peng, T., Xie, Q., Han, S., Tian, J., 2010. Mapping of QTL for tiller number at different stages of growth in wheat using double haploid and immortalized F_2 populations. J. Genet. 89, 409–415. https://doi.org/10.1007/s12041-010-0059-1

Lobell B., D., Field B., C., 2007. Global scale climate–crop yield relationships and the impacts of recent warming. Environ. Res. Lett. 2.

Long, S.P., Zhu, X.G., Naidu, S.L., Ort, D.R., 2006. Can improvement in photosynthesis increase crop yields? Plant, Cell Environ. 29, 315–330. https://doi.org/10.1111/j.1365-3040.2005.01493.x

López-Castañeda, C., Richards, R.A., 1994. Variation in temperate cereals in rainfed environments II. Phasic development and growth. F. Crop. Res. 37, 63–75. https://doi.org/10.1016/0378-4290(94)90082-5

Lynch, M., Walsh, B., 2004. Genetics and Analysis of Quantitative Traits, J Anim Breed Genet. https://doi.org/10.1046/j.1439-0388.2002.00356.x

Ma, J., Wingen, L.U., Orford, S., Fenwick, P., Wang, J., Griffiths, S., 2015. Using the UK reference population Avalon × Cadenza as a platform to compare breeding strategies in elite Western European bread wheat. Mol. Breed. 35. https://doi.org/10.1007/s11032-015-0268-7

Mackay, I., Powell, W., 2007. Methods for linkage disequilibrium mapping in crops.

Trends Plant Sci. 12, 57–63. https://doi.org/10.1016/j.tplants.2006.12.001

Mackay, I.J., Bansept-Basler, P., Barber, T., Bentley, A.R., Cockram, J., Gosman, N., Greenland, A.J., Horsnell, R., Howells, R., O'Sullivan, D.M., Rose, G.A., Howell, P.J., 2014. An eight-parent multiparent advanced generation inter-cross population for winter-sown wheat: creation, properties, and validation. G3; Genes|Genomes|Genetics 4, 1603–1610. https://doi.org/10.1534/g3.114.012963

Maestra, B., Naranjo, T., 1998. Homoeologous relationships of *Aegilops speltoides* chromosomes to bread wheat. Theor. Appl. Genet. 97, 181–186. https://doi.org/10.1007/s001220050883

McMullen, M.D., Kresovich, S., Villeda, H.S., Bradbury, P., Li, H., Sun, Q., Flint-Garcia, S., Thornsberry, J., Acharya, C., Bottoms, C., Brown, P., Browne, C., Eller, M., Guill, K., Harjes, C., Kroon, D., Lepak, N., Mitchell, S.E., Peterson, B., Pressoir, G., Romero, S., Rosas, M.O., Salvo, S., Yates, H., Hanson, M., Jones, E., Smith, S., Glaubitz, J.C., Goodman, M., Ware, D., Holland, J.B., Buckler, E.S., 2009. Genetic properties of the maize nested association mapping population. Science. 325, 737–740. https://doi.org/10.1126/science.1174320

Milne, I., Shaw, P., Stephen, G., Bayer, M., Cardle, L., Thomas, W.T.B., Flavell, A.J., Marshall, D., 2010. Flapjack-graphical genotype visualization. Bioinformatics 26, 3133–3134. https://doi.org/10.1093/bioinformatics/btq580

Milner, S., Maccaferri, M., Huang, B.., Mantovani, P., Massi, A., Frascaroli, E., Tuberosa, R., Salvi, S., 2016. A multiparental cross population for mapping QTL for agronomic traits in durum wheat (*Triticum turgidum*). Plant Biotechnol. J. https://doi.org/10.1111/pbi.12424

Miyao, M., 2003. Molecular evolution and genetic engineering of C_4 photosynthetic enzymes. J. Exp. Bot. 54, 179–189. https://doi.org/10.1093/jxb/erg026

Molero, G., Sukumaran, S., Reynolds, M.P., 2014. Spike photosynthesis contribution to grain yield and identification of molecular markers: A potential trait for breeding programs? Proc. 4th Int. Work. Wheat Yield Consort. 175–186.

Mott, R., Talbot, C.J., Turri, M.G., Collins, A.C., Flint, J., 2000. A method for fine mapping quantitative trait loci in outbred animal stocks. Proc. Natl. Acad. Sci. 97, 12649–12654. https://doi.org/10.1073/pnas.230304397

Nalam, V.J., Vales, M.I., Watson, C.J.W., Kianian, S.F., Riera-Lizarazu, O., 2006. Map-based analysis of genes affecting the brittle rachis character in tetraploid wheat (*Triticum turgidum* L.). Theor. Appl. Genet. 112, 373–381. https://doi.org/10.1007/s00122-005-0140-y

Noodén, L.D., Guiamét, J.J., John, I., 1997. Senescence mechanisms. Physiol. Plant. 101, 746–753. https://doi.org/10.1034/j.1399-3054.1997.1010410.x

Öztuna, D., Elhan, A.H., Tüccar, E., 2006. Investigation of four different normality tests in terms of type 1 error rate and power under different distributions. Turkish J. Med. Sci. 36, 171–176.

Parry, M.A.J., Madgwick, P.J., Carvalho, J.F.C., Andralojc, P.J., 2007. Prospects for increasing photosynthesis by overcoming the limitations of Rubisco. J. Agric. Sci. 145, 31–43. https://doi.org/10.1017/S0021859606006666

Parry, M.A.J., Reynolds, M., Salvucci, M.E., Raines, C., Andralojc, P.J., Zhu, X.G., Price, G.D., Condon, A.G., Furbank, R.T., 2011. Raising yield potential of wheat. II. Increasing photosynthetic capacity and efficiency. J. Exp. Bot. 62, 453–467. https://doi.org/10.1093/jxb/erq304

Pask, A., Pietragalla, J., Mullan, D., 2012. Physiological Breeding II: A Field Guide to Wheat Phenotyping., Communications in Soil Science and Plant Analysis. https://doi.org/10.1017/CBO9781107415324.004

Peng, J., Richards, D.E., Hartley, N.M., Murphy, G.P., Devos, K.M., Flintham, J.E., Beales, J., Fish, L.J., Worland, A.J., Pelica, F., Sudhakar, D., Christou, P., Snape, J.W., Gale, M.D., Harberd, N.P., 1999. “Green revolution” genes encode mutant gibberellin response modulators. Nature 400, 256–261. https://doi.org/10.1038/22307

Peng, J.H., Sun, D., Nevo, E., 2011. Domestication evolution, genetics and genomics in wheat. Mol. Breed. 28, 281–301. https://doi.org/10.1007/s11032-011-9608-4

Pennacchi, P., Carmo-silva, E., Andralojc, P.J., Feuerhelm, D., Powers, S.J., Parry, M.A.J., 2018. Dissecting wheat grain yield drivers in a mapping population in the UK. Agronomy 8. https://doi.org/10.3390/agronomy8060094

Peter, H., 2003. The genes of the Green Revolution. Trends Genet. 19, 5–9.

Pingali, P.L., 2012. Green Revolution: Impacts, limits, and the path ahead. Proc. Natl. Acad. Sci. 109, 12302–12308. https://doi.org/10.1073/pnas.0912953109

Pinto, R.S., Reynolds, M.P., Mathews, K.L., McIntyre, C.L., Olivares-Villegas, J.J., Chapman, S.C., 2010. Heat and drought adaptive QTL in a wheat population designed to minimize confounding agronomic effects. Theor. Appl. Genet. 121, 1001–1021. https://doi.org/10.1007/s00122-010-1351-4

Preece, C., Livarda, A., Wallace, M., Martin, G., Charles, M., Christin, P.A., Jones, G., Rees, M., Osborne, C.P., 2015. Were Fertile Crescent crop progenitors higher yielding than other wild species that were never domesticated? New Phytol. 207, 905–913. https://doi.org/10.1111/nph.13353

Pushpendra, K.G., Harindra, S.B., Pawan, L.K., Neeraj, K., Ajay, K., Reyazul, R.M., Amita, M., Jitendra, K., 2007. QTL analysis for some quantitative traits in bread wheat. J. Zhejiang Univ. Sci. B 8, 807–814. https://doi.org/10.1631/jzus.2007.B0807

Qi, X., Xu, W., Zhang, J., Guo, R., Zhao, M., Hu, L., Wang, H., Dong, H., Li, Y., 2017. Physiological characteristics and metabolomics of transgenic wheat containing the maize C_4 phosphoenolpyruvate carboxylase (PEPC) gene under high temperature stress. Protoplasma 254, 1017–1030. https://doi.org/10.1007/s00709-016-1010-y

R Core Team, 2017. R: A Language and Environment for Statistical Computing. R Found. Stat. Comput. https://doi.org/10.1007/978-3-540-74686-7

Raines, C.A., 2006. Transgenic approaches to manipulate the environmental responses of the C_3 carbon fixation cycle. Plant, Cell Environ. 29, 331–339. https://doi.org/10.1111/j.1365-3040.2005.01488.x

Rebetzke, G.J., Fischer, R.A., Van Herwaarden, A.F., Bonnett, D.G., Chenu, K., Rattey,

A.R., Fettell, N.A., 2014. Plot size matters: Interference from intergenotypic competition in plant phenotyping studies. Funct. Plant Biol. 41, 107–118. https://doi.org/10.1071/FP13177

Reynolds, M., Foulkes, M.J., Slafer, G.A., Berry, P., Parry, M.A.J., Snape, J.W., Angus, W.J., 2009. Raising yield potential in wheat. J. Exp. Bot. 60, 1899–1918. https://doi.org/10.1093/jxb/erp016

Rosegrant, M.W., Agcaoili, M., 2010. Global food demand, supply, and price prospects to 2010. Washington, DC Int. Food Policy Res. Inst.

Sallam, A., Martsch, R., 2015. Association mapping for frost tolerance using multi-parent advanced generation inter-cross (MAGIC) population in faba bean (*Vicia faba* L.). Genetica 143, 501–514. https://doi.org/10.1007/s10709-015-9848-z

Sanchez-Bragado, R., Molero, G., Reynolds, M.P., Araus, J.L., 2014. Relative contribution of shoot and ear photosynthesis to grain filling in wheat under good agronomical conditions assessed by differential organ $\delta^{13}C$. J. Exp. Bot. 65, 5401–5413. https://doi.org/10.1093/jxb/eru298

Scutari, M., Howell, P., Balding, D.J., Mackay, I., 2014. Multiple quantitative trait analysis using bayesian networks. Genetics 198, 129–137. https://doi.org/10.1534/genetics.114.165704

Sharrow, S.H., 1984. A simple disc meter for measurement of pasture height and forage bulk. J. Range Manag. 37, 94. https://doi.org/10.2307/3898833

Shewry, P.R., 2009. Wheat. J. Exp. Bot. 60, 1537–1553. https://doi.org/10.1093/jxb/erp058

Shiferaw, B., Smale, M., Braun, H.J., Duveiller, E., Reynolds, M., Muricho, G., 2013. Crops that feed the world 10. Past successes and future challenges to the role played by wheat in global food security. Food Secur. 5, 291–317. https://doi.org/10.1007/s12571-013-0263-y

Simmonds, J., Scott, P., Leverington-Waite, M., Turner, A.S., Brinton, J., Korzun, V.,

Snape, J., Uauy, C., 2014. Identification and independent validation of a stable yield and thousand grain weight QTL on chromosome 6A of hexaploid wheat (*Triticum aestivum* L.). BMC Plant Biol. 14, 1–13. https://doi.org/10.1186/s12870-014-0191-9

Simons, K.J., Fellers, J.P., Trick, H.N., Zhang, Z., Tai, Y.S., Gill, B.S., Faris, J.D., 2006. Molecular characterization of the major wheat domestication gene *Q*. Genetics 172, 547–555. https://doi.org/10.1534/genetics.105.044727

Slafer, G.A., 2003. Genetic basis of yield as viewed from a crop physiologist's perspective. Ann. Appl. Biol. 142, 117–128. https://doi.org/10.1111/j.1744-7348.2003.tb00237.x

Snape, J.W., Butterworth, K., Whitechurch, E., Worland, A.J., 2001. Waiting for fine times: Genetics of flowering time in wheat, Euphytica. https://doi.org/10.1023/A:1017594422176

Snape, J.W., Foulkes, M.J., Simmonds, J., Leverington, M., Fish, L.J., Wang, Y., Ciavarrella, M., 2007. Dissecting gene x environmental effects on wheat yields via QTL and physiological analysis. Euphytica 154, 401–408. https://doi.org/10.1007/s10681-006-9208-2

Song, X.J., Huang, W., Shi, M., Zhu, M.Z., Lin, H.X., 2007. A QTL for rice grain width and weight encodes a previously unknown RING-type E3 ubiquitin ligase. Nat. Genet. 39, 623–630. https://doi.org/10.1038/ng2014

Sosnowski, O., Charcosset, A., Joets, J., 2012. Biomercator V3: An upgrade of genetic map compilation and quantitative trait loci meta-analysis algorithms. Bioinformatics 28, 2082–2083. https://doi.org/10.1093/bioinformatics/bts313

Tambussi, E.A., Bort, J., Guiamet, J.J., Nogués, S., Araus, J.L., 2007. The photosynthetic role of ears in C_3 cereals: Metabolism, water use efficiency and contribution to grain yield. CRC. Crit. Rev. Plant Sci. 26, 1–16. https://doi.org/10.1080/07352680601147901

Trethowan, R.M., Reynolds, M., Sayre, K., Ortiz-Monasterio, I., 2005. Adapting wheat

cultivars to resource conserving farming practices and human nutritional needs. Ann. Appl. Biol. 146, 405–413. https://doi.org/10.1111/j.1744-7348.2005.040137.x

Tyagi, S., Mir, R.R., Balyan, H.S., Gupta, P.K., 2015. Interval mapping and meta-QTL analysis of grain traits in common wheat (*Triticum aestivum* L.). Euphytica 201, 367–380. https://doi.org/10.1007/s10681-014-1217-y

Verma, V., Foulkes, M.J., Worland, A.J., Sylvester-Bradley, R., Caligari, P.D.S., Snape, J.W., 2004. Mapping quantitative trait loci for flag leaf senescence as a yield determinant in winter wheat under optimal and drought-stressed environments. Euphytica 135, 255–263. https://doi.org/10.1023/B:EUPH.0000013255.31618.14

Wang, S., Basten, C.J., Zeng, Z.B., 2011. Windows QTL Cartographer 2.5. J. Infect. Dis. 204 Suppl, 198–199. https://doi.org/10.1002/tcr.201090006

Wang, S., Wong, D., Forrest, K., Allen, A., Chao, S., Huang, B.E., Maccaferri, M., Salvi, S., Milner, S.G., Cattivelli, L., Mastrangelo, A.M., Whan, A., Stephen, S., Barker, G., Wieseke, R., Plieske, J., Lillemo, M., Mather, D., Appels, R., Dolferus, R., Brown-Guedira, G., Korol, A., Akhunova, A.R., Feuillet, C., Salse, J., Morgante, M., Pozniak, C., Luo, M.C., Dvorak, J., Morell, M., Dubcovsky, J., Ganal, M., Tuberosa, R., Lawley, C., Mikoulitch, I., Cavanagh, C., Edwards, K.J., Hayden, M., Akhunov, E., 2014. Characterization of polyploid wheat genomic diversity using a high-density 90 000 single nucleotide polymorphism array. Plant Biotechnol. J. 12, 787–796. https://doi.org/10.1111/pbi.12183

Whan, A.P., Smith, A.B., Cavanagh, C.R., Ral, J.P.F., Shaw, L.M., Howitt, C.A., Bischof, L., 2014. GrainScan: A low cost, fast method for grain size and colour measurements. Plant Methods 10, 1–10. https://doi.org/10.1186/1746-4811-10-23

White, J.W., Conley, M.M., 2013. A flexible, low-cost cart for proximal sensing. Crop Sci. 53, 1646–1649. https://doi.org/10.2135/cropsci2013.01.0054

Whittle, A.W.R., Cummings, V., 2007. Going over: the Mesolithic-Neolithic transition in north-west Europe. Oxford University Press for the British Academy, Oxford.

Williams, K., Sorrells, M.E., 2014. Three-dimensional seed size and shape QTL in hexaploid wheat (*Triticum aestivum* L.) populations. Crop Sci. 54, 98–110. https://doi.org/10.2135/cropsci2012.10.0609

Winfield, M., 2011. Wheat Genomics: Wheat BP...the big picture [WWW Document]. URL http://www.cerealsdb.uk.net

Wu, Q.H., Chen, Y.X., Zhou, S.H., Fu, L., Chen, J.J., Xiao, Y., Zhang, D., Ouyang, S.H., Zhao, X.J., Cui, Y., Zhang, D.Y., Liang, Y., Wang, Z.Z., Xie, J.Z., Qin, J.X., Wang, G.X., Li, D.L., Huang, Y.L., Yu, M.H., Lu, P., Wang, L.L., Wang, L., Wang, H., Dang, C., Li, J., Zhang, Y., Peng, H.R., Yuan, C.G., You, M.S., Sun, Q.X., Wang, J.R., Wang, L.X., Luo, M.C., Han, J., Liu, Z.Y., 2015. High-density genetic linkage map construction and QTL mapping of grain shape and size in the wheat population Yanda1817 x Beinong6. PLoS One 10, 1–17. https://doi.org/10.1027/0269-8803/a000168

Wu, X., Chang, X., Jing, R., 2012. Genetic insight into yield-associated traits of wheat grown in multiple rain-fed environments. PLoS One 7. https://doi.org/10.1371/journal.pone.0031249

Xie, Q., Mayes, S., Sparkes, D.L., 2015. Carpel size, grain filling, and morphology determine individual grain weight in wheat. J. Exp. Bot. 66, 6715–6730. https://doi.org/10.1093/jxb/erv378

Yang, Z., Bai, Z., Li, Xiaolin, Wang, P., Wu, Q., Yang, L., Li, L., Li, Xuejun, 2012. SNP identification and allelic-specific PCR markers development for *TaGW2*, a gene linked to wheat kernel weight. Theor. Appl. Genet. 125, 1057–1068. https://doi.org/10.1007/s00122-012-1895-6

Youssefian, S., Kirby, E.J.M., Gale, M.D., 1992. Pleiotropic effects of the GA-insensitive *Rht* dwarfing genes in wheat. 2. Effects on leaf, stem, ear and floret growth. F. Crop. Res. 28, 191–210. https://doi.org/10.1016/0378-4290(92)90040-G

Yu, J., Holland, J.B., McMullen, M.D., Buckler, E.S., 2008. Genetic design and statistical power of nested association mapping in maize. Genetics 178, 539–551. https://doi.org/10.1534/genetics.107.074245

Zadoks, J.C., Chang, T.T., Konzak, C.F., 1974. A decimal code for the growth stages of cereals. Weed Res. 14, 415–421. https://doi.org/10.1111/j.1365-3180.1974.tb01084.x

Zhang, J., Dell, B., Biddulph, B., Drake-Brockman, F., Walker, E., Khan, N., Wong, D., Hayden, M., Appels, R., 2013. Wild-type alleles of *Rht-B1* and *Rht-D1* as independent determinants of thousand-grain weight and kernel number per spike in wheat. Mol. Breed. 32, 771–783. https://doi.org/10.1007/s11032-013-9905-1

Zhang, J., Zhang, S., Cheng, M., Jiang, H., Zhang, X., Peng, C., Lu, X., Zhang, M., Jin, J., 2018. Effect of drought on agronomic traits of rice and wheat: A meta-analysis. Int. J. Environ. Res. Public Health 15, 839. https://doi.org/10.3390/ijerph15050839

Zhang, Z., Ersoz, E., Lai, C.Q., Todhunter, R.J., Tiwari, H.K., Gore, M.A., Bradbury, P.J., Yu, J., Arnett, D.K., Ordovas, J.M., Buckler, E.S., 2010. Mixed linear model approach adapted for genome-wide association studies. Nat. Genet. 42, 355–360. https://doi.org/10.1038/ng.546

Zhao, K., Aranzana, M.J., Kim, S., Lister, C., Shindo, C., Tang, C., Toomajian, C., Zheng, H., Dean, C., Marjoram, P., Nordborg, M., 2007. An *Arabidopsis* example of association mapping in structured samples. PLoS Genet. 3, 71–82. https://doi.org/10.1371/journal.pgen.0030004

Zohary, D., Hopf, M., Weiss, E., 2015. Domestication of Plants in the Old World. https://doi.org/10.1093/acprof:osobl/9780199549061.001.0001

Appendix

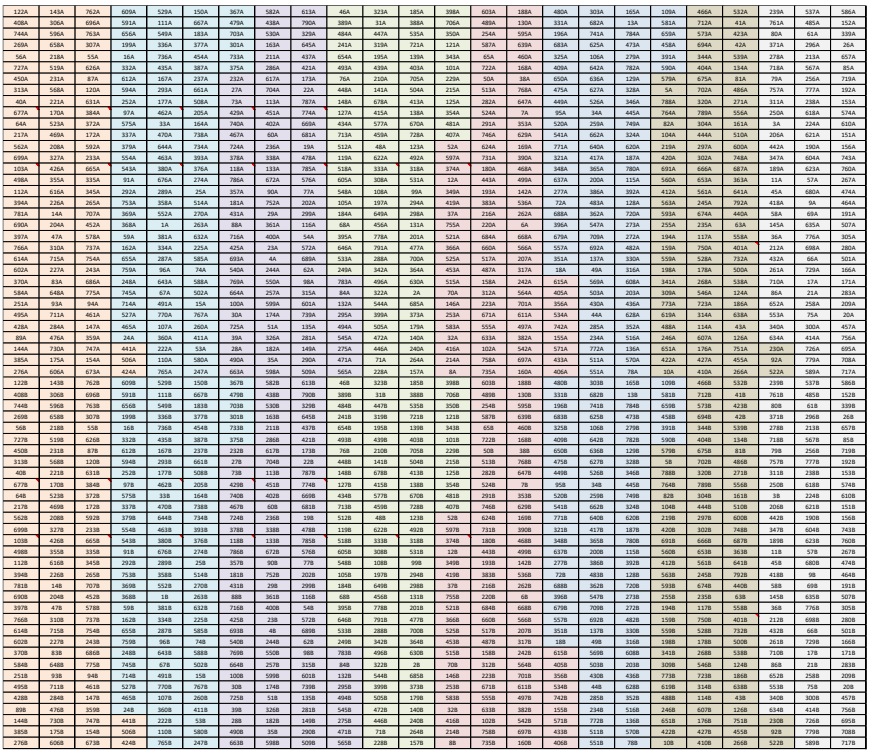

Field plan 2014-15 (Gravelpit), each colour represents a different block

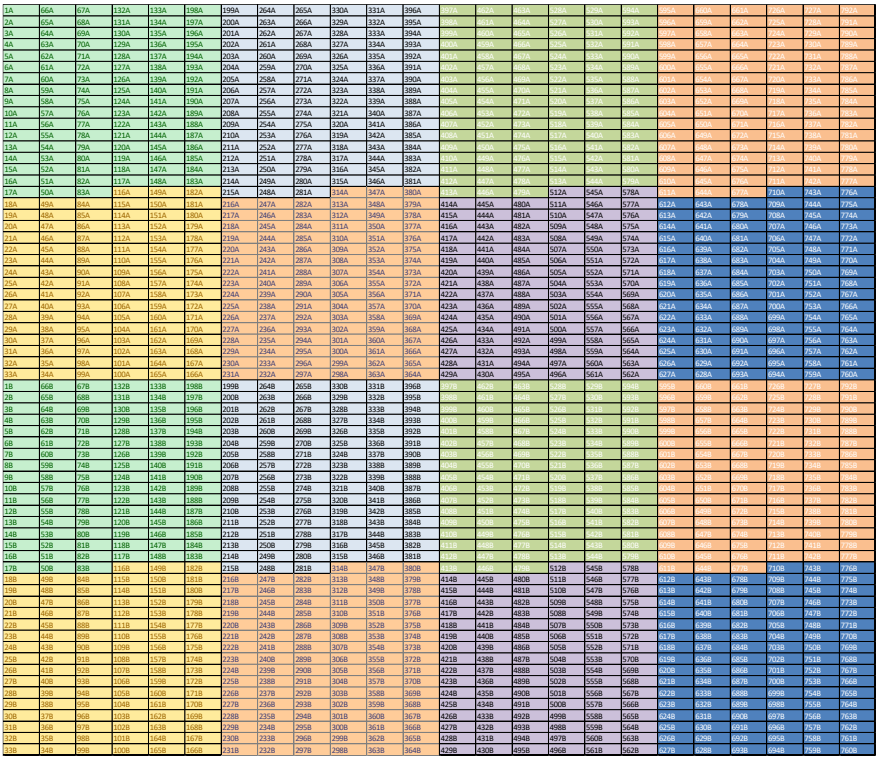

Field plan 2015-16 (Lamyard) each colour represents a different block

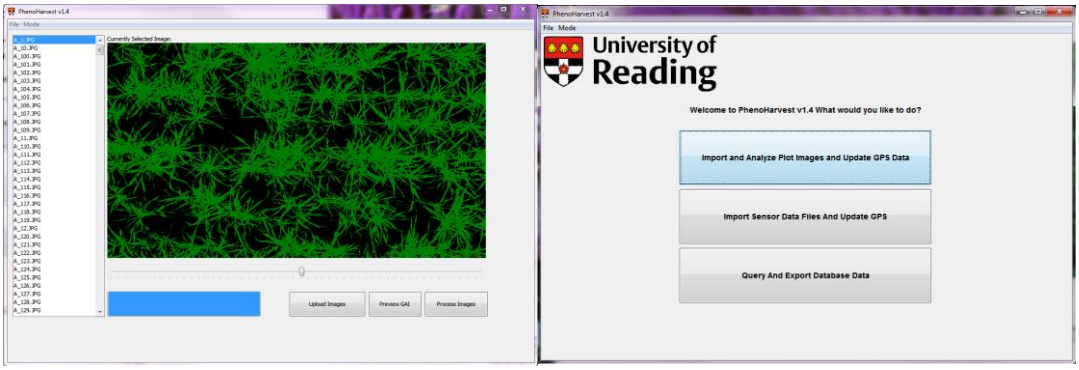

Representation of the PhenoHarvest software

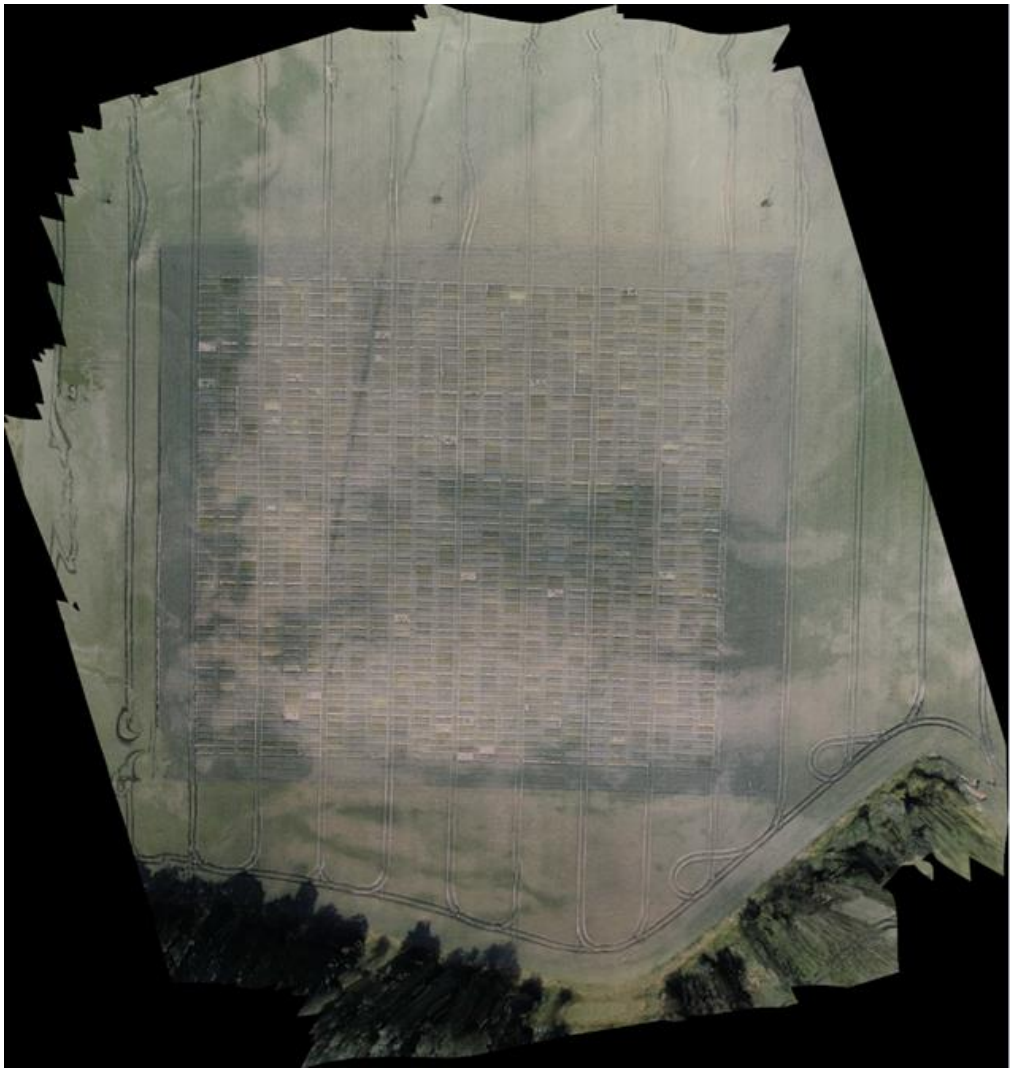

Composite image of approximately 200 drone images from Gravelpit (2014-15) (original imagery by Richard Casebow)

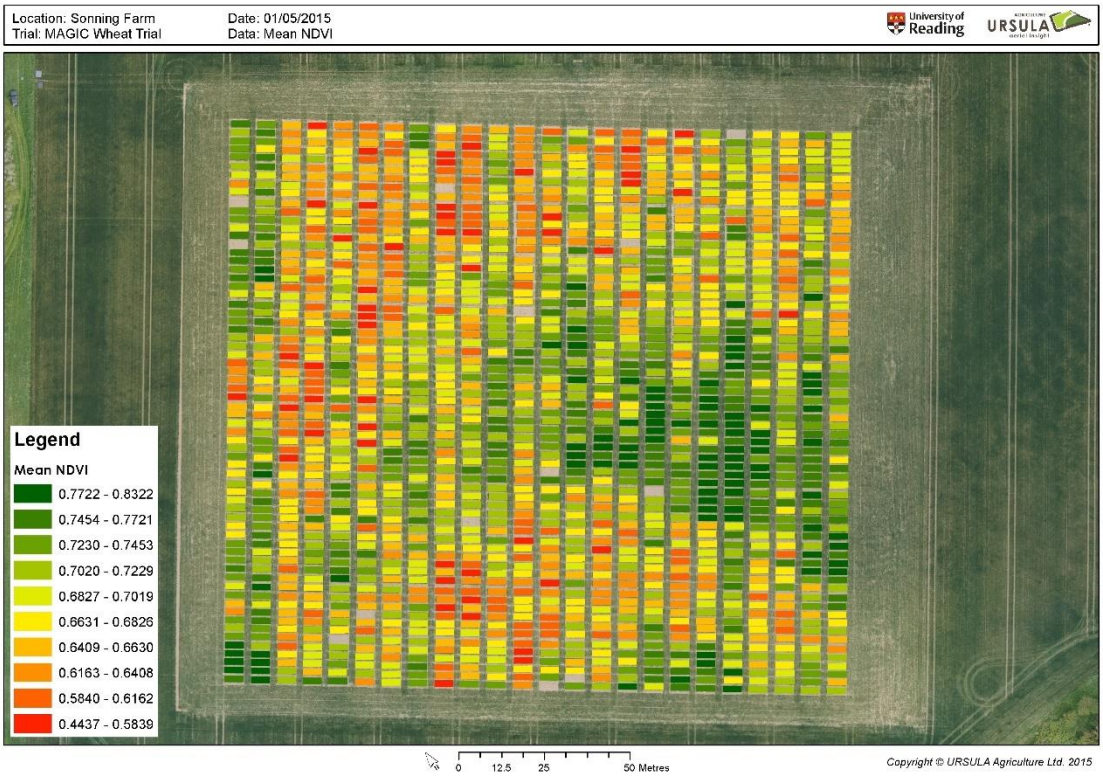

Panel A: Composite RGB image of RGB aerial imagery on 1/5/2015. Panel B: Composite false-colour NDVI image of aerial imagery on 1/5/2015.

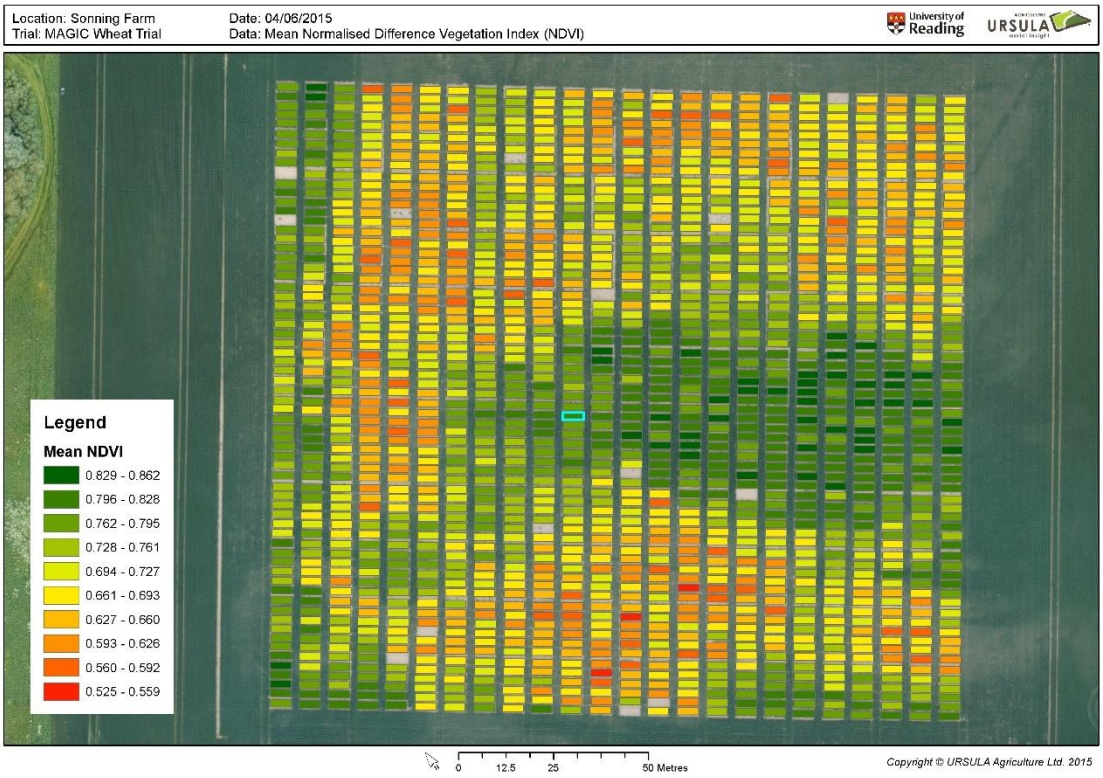

Panel A: Composite RGB image of RGB aerial imagery on 4/6/2015. Panel B: Composite false-colour NDVI image of aerial imagery on 4/6/2015.

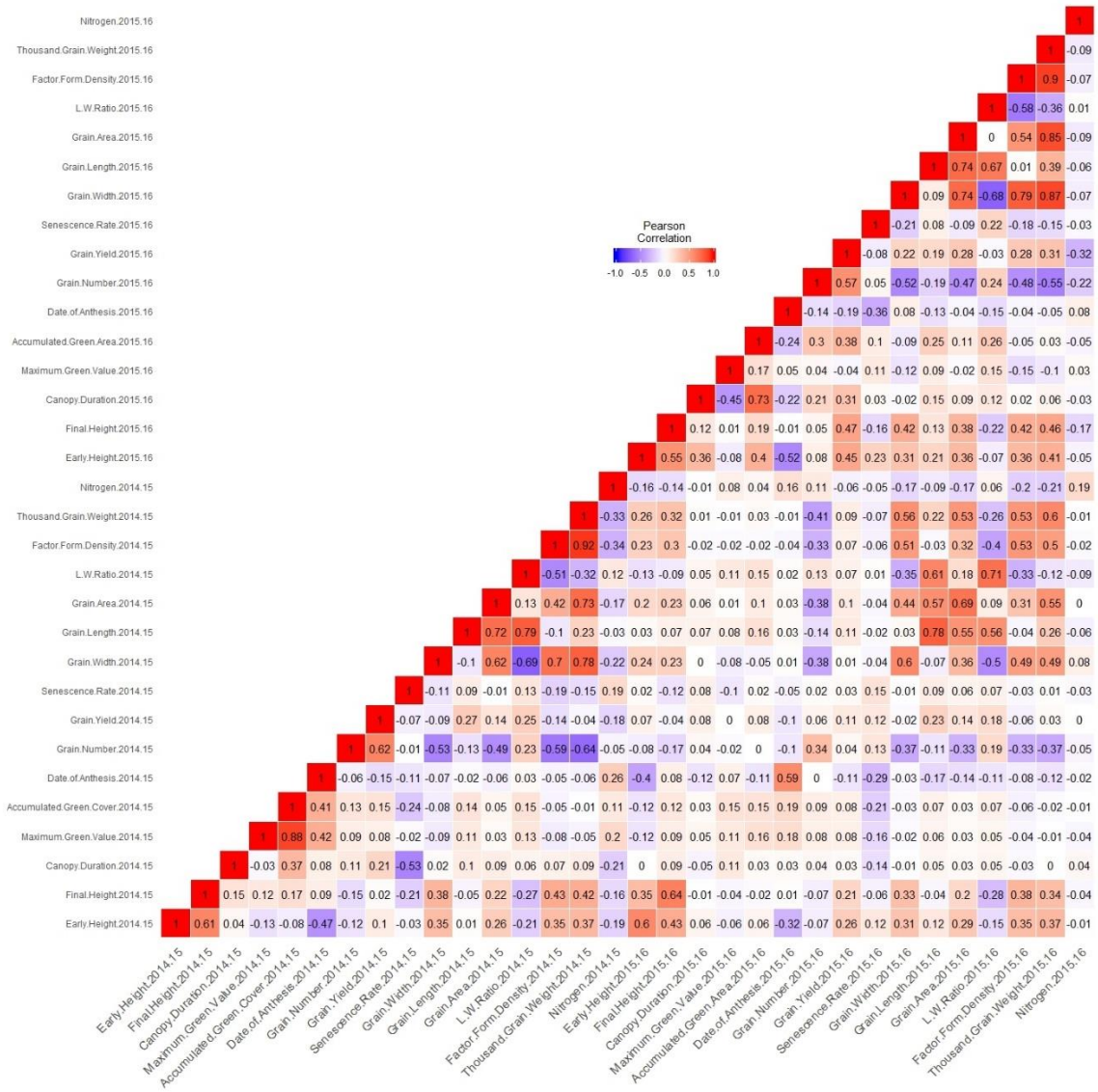

Full correlation matrix of all data